

## Aberystwyth University

### *Approaches and challenges to the study of loess—Introduction to the LoessFest Special Issue*

Schaetzl, Randall J.; Bettis, E. Arthur; Crouvi, Onn; Fitzsimmons, Kathryn E.; Grimley, David A.; Hambach, Ulrich; Lehmkuhl, Frank; Markovi, Slobodan B.; Mason, Joseph A.; Owczarek, Piotr; Roberts, Helen M.; Rousseau, Denis-Didier; Stevens, Thomas; Vandenberghe, Jef; Zárate, Marcelo; Veres, Daniel; Yang, Shiling; Zech, Michael; Conroy, Jessica L.; Dave, Aditi K.

*Published in:*

Quaternary Research

*DOI:*

[10.1017/qua.2018.15](https://doi.org/10.1017/qua.2018.15)

*Publication date:*

2018

*Citation for published version (APA):*

Schaetzl, R. J., Bettis, E. A., Crouvi, O., Fitzsimmons, K. E., Grimley, D. A., Hambach, U., Lehmkuhl, F., Markovi, S. B., Mason, J. A., Owczarek, P., Roberts, H. M., Rousseau, D-D., Stevens, T., Vandenberghe, J., Zárate, M., Veres, D., Yang, S., Zech, M., Conroy, J. L., ... Zech, R. (2018). Approaches and challenges to the study of loess—Introduction to the LoessFest Special Issue. *Quaternary Research*, 89(03), 563-618. <https://doi.org/10.1017/qua.2018.15>

#### **Document License** CC BY-NC-ND

#### **General rights**

Copyright and moral rights for the publications made accessible in the Aberystwyth Research Portal (the Institutional Repository) are retained by the authors and/or other copyright owners and it is a condition of accessing publications that users recognise and abide by the legal requirements associated with these rights.

- Users may download and print one copy of any publication from the Aberystwyth Research Portal for the purpose of private study or research.
- You may not further distribute the material or use it for any profit-making activity or commercial gain
- You may freely distribute the URL identifying the publication in the Aberystwyth Research Portal

#### **Take down policy**

If you believe that this document breaches copyright please contact us providing details, and we will remove access to the work immediately and investigate your claim.

tel: +44 1970 62 2400  
email: [is@aber.ac.uk](mailto:is@aber.ac.uk)

## Approaches and Challenges to the Study of Loess

- 1
- 2
- 3 **Randall J. Schaetzl** Department of Geography, Environment, and Spatial Sciences  
4 673 Auditorium Rd, Michigan State University, East Lansing, MI USA 48824-1117 [soils@msu.edu](mailto:soils@msu.edu)
- 5 **E. Arthur Bettis III** Department of Earth and Environmental Sciences, Institute for Hydraulic Research  
6 IHR-Hydroscience and Engineering, University of Iowa, Iowa City, Iowa USA 52242 [art-](mailto:art-bettis@uiowa.edu)  
7 [bettis@uiowa.edu](mailto:bettis@uiowa.edu)
- 8 **Onn Crouvi** Geological Survey of Israel, Jerusalem 9550161, Israel [onn.crouvi@mail.huji.ac.il](mailto:onn.crouvi@mail.huji.ac.il)
- 9 **Kathryn E. Fitzsimmons** Research Group for Terrestrial Palaeoclimates, Max Planck Institute for  
10 Chemistry, Hahn-Meitner-Weg 1, 55128 Mainz, Germany [k.fitzsimmons@mpic.de](mailto:k.fitzsimmons@mpic.de)
- 11 **David A. Grimley** Illinois State Geological Survey, University of Illinois, Urbana-Champaign, Illinois, USA  
12 61820 [dgrimley@illinois.edu](mailto:dgrimley@illinois.edu)
- 13 **Ulrich Hambach** BayCEER and Chair of Geomorphology, University of Bayreuth, Germany  
14 [ulrich.hambach@uni-bayreuth.de](mailto:ulrich.hambach@uni-bayreuth.de)
- 15 **Frank Lehmkuhl** Department of Geography, RWTH Aachen University, Templergraben 55, 52066  
16 Aachen, Germany [FLehmkuhl@geo.rwth-aachen.de](mailto:FLehmkuhl@geo.rwth-aachen.de)
- 17 **Slobodan B. Marković** Faculty of Sciences, University of Novi Sad, Trg Dositeja Obradovića 3, 21000 Novi  
18 Sad, Serbia; Serbian Academy of Sciences and Arts Knez Mihajlova 35, 11000 Belgrade, Serbia  
19 [baca.markovic@gmail.com](mailto:baca.markovic@gmail.com)
- 20 **Joseph A. Mason** Department of Geography, University of Wisconsin-Madison, 550 N. Park St., Madison,  
21 Wisconsin, 53706 USA [mason@geography.wisc.edu](mailto:mason@geography.wisc.edu)
- 22 **Piotr Owczarek**, Institute of Geography and Regional Development, Faculty of Earth Sciences and  
23 Environmental Management, University of Wrocław, Pl. Uniwersytecki 1, 50-137 Wrocław, Poland  
24 [piotr.owczarek@uwr.edu.pl](mailto:piotr.owczarek@uwr.edu.pl)
- 25 **Helen M. Roberts** Department of Geography and Earth Sciences, Aberystwyth University, Aberystwyth,  
26 Wales, SY23 3DB, United Kingdom [hmr@aber.ac.uk](mailto:hmr@aber.ac.uk)
- 27 **Denis-Didier Rousseau** Ecole Normale Supérieure, UMR CNRS 8539, Laboratoire de Météorologie  
28 Dynamique, and CERES-ERTI, 24 rue Lhomond, 75231 Paris CEDEX 5, France; Lamont-Doherty Earth  
29 Observatory of Columbia University, Palisades, New York, 10964 USA [denis.rousseau@lmd.ens.fr](mailto:denis.rousseau@lmd.ens.fr)
- 30 **Thomas Stevens** Department of Earth Sciences, Program for Air, Water and Landscape Sciences; Physical  
31 Geography, Uppsala University, Villav. 16, Uppsala, Sweden [thomas.stevens@geo.uu.se](mailto:thomas.stevens@geo.uu.se)

- 32 **Jef Vandenberghe** Department of Earth Sciences, De Boelelaan 1085, Vrije Universiteit, Amsterdam,  
33 1081 HV Amsterdam, The Netherlands [jef.vandenberghe@vu.nl](mailto:jef.vandenberghe@vu.nl)
- 34 **Daniel Veres** Institute of Speleology, Romanian Academy, Romania, and Interdisciplinary Research  
35 Institute on Bio-Nano-Science of Babes-Bolyai University, Cluj-Napoca, Romania [daniel.veres@ubbcluj.ro](mailto:daniel.veres@ubbcluj.ro)
- 36 **Shiling Yang** Institute of Geology and Geophysics, Chinese Academy of Sciences, 19 BeiTuChengXi Road,  
37 Beijing 100029, China [yangsl@mail.iggcas.ac.cn](mailto:yangsl@mail.iggcas.ac.cn)
- 38 **Michael Zech** Institute of Geography, Technical University of Dresden, Helmholtzstrasse 10, D-01062  
39 Dresden, Germany, and Department of Terrestrial Biogeochemistry, Martin-Luther University Halle-  
40 Wittenberg, Weidenplan 14, D-06120 Halle, Germany [michael\\_zech@gmx.de](mailto:michael_zech@gmx.de)
- 41 **Jessica L. Conroy** Departments of Geology and Plant Biology, University of Illinois, Urbana-Champaign,  
42 Illinois, USA 61820 [jconro@illinois.edu](mailto:jconro@illinois.edu)
- 43 **Aditi K. Dave** Research Group for Terrestrial Palaeoclimates, Max Planck Institute for Chemistry, Hahn-  
44 Meitner-Weg 1, 55128 Mainz, Germany [a.dave@mpic.de](mailto:a.dave@mpic.de)
- 45 **Dominik Faust** Institute of Geography, Dresden University of Technology, 01062 Dresden, Germany  
46 [dominik.faust@tu-dresden.de](mailto:dominik.faust@tu-dresden.de)
- 47 **Qingzhen Hao** Key Laboratory of Cenozoic Geology and Environment, Institute of Geology and  
48 Geophysics, Chinese Academy of Sciences, and College of Earth Science, University of Chinese Academy  
49 of Sciences, Beijing, China [haoqz@mail.iggcas.ac.cn](mailto:haoqz@mail.iggcas.ac.cn)
- 50 **Igor Obreht** Department of Geography, RWTH Aachen University, Germany; Organic Geochemistry  
51 Group, MARUM-Center for Marine Environmental Sciences and Department of Geosciences, University  
52 of Bremen, 28359 Bremen, Germany [igor.obreht@geo.rwth-aachen.de](mailto:igor.obreht@geo.rwth-aachen.de)
- 53 **Charlotte Prud'homme** Research Group for Terrestrial Palaeoclimates, Max Planck Institute for  
54 Chemistry, Hahn-Meitner-Weg 1, 55128 Mainz, Germany [c.prudhomme@mpic.de](mailto:c.prudhomme@mpic.de)
- 55 **Ian Smalley** School of Geology, Geography and the Environment, University of Leicester, Leicester, LE1  
56 7RH, United Kingdom [ijsmalley@googlemail.com](mailto:ijsmalley@googlemail.com)
- 57 **Alfonsina Tripaldi** IGEBa-CONICET-Universidad de Buenos Aires Pabellón 2, Primer piso, Oficina 3 Ciudad  
58 Universitaria C1428EHA, Buenos Aires, Argentina [alfo@gl.fcen.uba.ar](mailto:alfo@gl.fcen.uba.ar)
- 59 **Christian Zeeden** Department of Geography, RWTH Aachen University, Germany; IMCCE, Observatoire  
60 de Paris, PSL Research Université, CNRS, Sorbonne Universités, UPMC Université Paris 06, Université  
61 Lille, 75014 Paris, France [c.zeeden@geo.rwth-aachen.de](mailto:c.zeeden@geo.rwth-aachen.de)
- 62 **Roland Zech** Institute of Geography, Friedrich-Schiller University Jena, Löbdergraben 32, D-07743 Jena,  
63 Germany [roland.zech@uni-jena.de](mailto:roland.zech@uni-jena.de)
- 64

65 **Introduction**

66           In September, 2016, the annual meeting of INQUA’s Loess and Pedostratigraphy Focus Group  
67 met in western Wisconsin, USA. This focus group is part of the International Union for Quaternary  
68 Research’s (INQUA) commission on Stratigraphy and Chronology  
69 (<http://www.inqua.org/aboutCommissions.html>). Meetings of this group have traditionally been  
70 referred to as LoessFests. The 2016 LoessFest focused on “thin” loess deposits and loess transportation  
71 surfaces. Held in Eau Claire, Wisconsin from Sep. 22-25, this LoessFest included 75 registered  
72 participants from 10 countries. Almost half of the participants were from outside the US, and 18 of the  
73 participants were students. In all, 29 oral papers and 14 posters were presented during the first two  
74 days. Kathleen Goff (University of Iowa) won the award for the best student poster, and Rastko  
75 Marković (University of Novi Sad, Serbia) won the award for the best student oral paper. The last two  
76 days of the conference involved field trips to sites in western Wisconsin. The trips included 13 stops,  
77 most of which were exposures or backhoe pits in loess or related sediments (Fig. 1).

78           After the meeting, the conference organizers were approached by *Quaternary Research* and  
79 *Aeolian Research* about developing special issues for these journals, dedicated to topics focusing on  
80 loess. This paper represents the Introduction to the special issue for *Quaternary Research*. The goals of  
81 this paper are (1) to provide brief summaries of some of the current approaches/strategies used to  
82 study loess deposits, and (2) in so doing, highlight some of the ongoing work on loess in various regions  
83 of the world. Numerous examples from, and reviews of, some of the world’s major loess deposits are  
84 discussed first, to provide context. We hope that these summaries, written by a selection of the world’s  
85 most prominent loess researchers, will not only highlight the fascinating world of loess research, but  
86 also draw attention to loess-related questions, approaches and methods that may form the basis of  
87 future research.

88           We wish to thank the many people who helped to make the Eau Claire LoessFest a success,  
89 especially Doug Faulkner, Garry Running, and Kent Syverson of the University of Wisconsin-Eau Claire,  
90 John Attig of the Wisconsin Geological and Natural History Survey, and Kristine Gruley and Joseph  
91 Mason of the University of Wisconsin-Madison. Chase Kasmerchak of Michigan State University was a  
92 key support person for field trip and conference planning. We thank Michigan State University and the

93 University of Wisconsin-Eau Claire for financial and logistical support, and acknowledge receipt of grants  
94 in support of the LoessFest from INQUA and the National Science Foundation.

95 This special issue was the idea of Nick Lancaster, editor of *Quaternary Research*. Nick brought in  
96 Art Bettis and Randall Schaetzl as guest editors. The authorship order for this paper is, after the two  
97 editors, alphabetical order by last name of the primary authors, and then again in alphabetical order by  
98 last name of the secondary authors.

99 The editors also wish to thank the many reviewers of the papers that follow, for their  
100 constructive input and expertise. We would especially like to thank Dan Muhs and Peter Jacobs for their  
101 thorough reviews of the final “assembled” manuscript. Dan Muhs deserves a special commendation for  
102 his thorough and insightful comments and suggestions on the sections entitled “Loess in Alaska” and  
103 “Geochemical Approaches to the Study of Loess”. We believe that the 20 contributions in this  
104 Introduction, and the 20 papers in this LoessFest issue proper, nicely represent the diversity of loess  
105 research being done today worldwide, and exemplify some of the best that this discipline has to offer.  
106 Enjoy.

107

## 108 **(Most of) The World’s Major Loess Deposits**

### 109 **Loess in China**

110 Shiling Yang

111 Loess deposits in China are widely distributed across the Chinese Loess Plateau (Fig. 2), where  
112 they attain thicknesses ranging from several tens to >300 meters, across an area of ca. 273,000 km<sup>2</sup> (Liu,  
113 1985). The thickest and most complete loess sequences occur mainly in the central and southern parts  
114 of the Plateau, where they range from 130 to 200 m thick and consist of as many as 34 loess-paleosol  
115 couplets (Fig. 3; Yang and Ding, 2010). As per standard nomenclature, loess horizons are labeled L<sub>i</sub> and  
116 the intercalated paleosols S<sub>i</sub>. Several loess and paleosol units are usually used as stratigraphic markers  
117 across the Loess Plateau, including thick and coarse grained loess units L<sub>9</sub>, L<sub>15</sub>, L<sub>24</sub>, L<sub>27</sub> and L<sub>32</sub>, and  
118 strongly developed paleosols S<sub>5</sub> and S<sub>26</sub> (Ding et al., 1993, 2002). The alternation of loess and paleosols

119 reflects large-scale oscillations between glacial conditions, when loess accumulates, and interglacial  
120 conditions, when loess deposition wanes and soils form.

121           The modern climate of the Chinese Loess Plateau is characterized by the seasonal alternation of  
122 summer and winter monsoons. During winter, the northwesterly monsoonal winds driven by the  
123 Siberian High dominate the Chinese Loess Plateau, and lead to cold and dry weather, whereas in  
124 summer, the southeasterly monsoonal winds bring heat and moisture from the low-latitude oceans,  
125 leading to warm and humid weather. Meteorological data indicate that ~60-80% of annual precipitation  
126 is concentrated in the summer season (Yang et al., 2012, 2015).

127           Loess material in northern China is likely to have first formed through glacial abrasion and  
128 erosion by other geomorphic processes in mountainous areas (Sun, 2002a; Smalley et al., 2014), then  
129 was transported by fluvial and eolian processes into deserts which act as silt and clay storage regions,  
130 rather than places where particles are formed. The eolian dust that constitutes the loess is mainly  
131 transported from these deserts by the winter monsoon, whereas the post-depositional alteration of  
132 dust deposits is closely related to the precipitation provided by the summer monsoon (Liu, 1985; Liu and  
133 Ding, 1998). Therefore, Chinese loess deposits provide a unique opportunity to investigate the evolution  
134 of the East Asian monsoon over the past 2.8 Ma (Yang and Ding, 2010) and the complex interactions of  
135 Earth surface-climate systems (Sun, 2002b; Smalley et al., 2014).

136           Studies of Chinese loess have shown that various proxy records in the loess column can reveal  
137 abundant information on regional climatic and environmental changes. The most common  
138 paleoenvironmental proxies used here are magnetic susceptibility (Kukla et al., 1988; An et al., 1991a),  
139 grain size (An et al., 1991b; Ding et al., 1994), chemical weathering indexes (Gallet et al., 1996; Chen et  
140 al., 1999; Yang et al., 2006), isotopic ratios (Liu et al., 2011; Yang et al., 2012), soil micromorphology  
141 (Bronger and Heinkele, 1989; Rutter and Ding, 1993), biomarkers (Peterse et al., 2014; Thomas et al.,  
142 2016; Li et al., 2016a), and pollen, snail and opal phytolith assemblages (Lu et al., 2007; Rousseau et al.,  
143 2009; Jiang et al., 2013, 2014). In the last few decades, many studies have focused on the evolution of  
144 the East Asian monsoon and regional tectonic uplift (e.g., Liu and Ding, 1998 and references therein;  
145 Maher, 2016 and references therein), using mainly proxy data from loess deposits. The East Asian  
146 monsoon varies over tectonic to millennial time scales, but is mostly driven by Northern Hemisphere  
147 glacial cyclicity (Ding et al., 2002, 2005; Yang and Ding, 2014). On tectonic, i.e., the longest, timescales,

148 since the mid-Pliocene there appears to have been a stepwise weakening of the East Asian summer  
149 monsoon at 2.6, 1.2, 0.7 and 0.2 Ma (Ding et al., 2005). On orbital timescales, the East Asian summer  
150 (winter) monsoon weakened (strengthened) during glacials, and vice versa during interglacials, leading  
151 to a 200- to 300-km advance-retreat of the desert boundary (Yang and Ding, 2008), and its associated  
152 vegetation changes (Jiang et al., 2013, 2014; Yang et al., 2015) in northern China. As for the millennial-  
153 scale climate variability, high-resolution grain-size data from the Chinese loess deposits show that  
154 millennial-scale climatic events are superimposed onto a prominent long-term cooling trend, during  
155 both the last and penultimate glaciations (Yang and Ding, 2014). However, millennial-scale ecological  
156 reconstructions of the Loess Plateau remain to be investigated.

157         Although the foundational work on Chinese loess, such as the major stratigraphic, chronological,  
158 sedimentological and paleoclimatic frameworks, has already been established (Liu and Ding, 1998; Ding  
159 et al., 2002), there remains a great deal of work to be done. First, accurate quantitative reconstructions  
160 of temperature and precipitation are needed to improve existing ones, and there is a need to develop  
161 new methods and approaches for quantitative paleoenvironmental and paleoclimatic reconstructions.  
162 These reconstructions are challenging. Second, it is crucial to investigate whether the exceptionally  
163 coarse-grained units (e.g., L<sub>9</sub>, L<sub>15</sub> and L<sub>33</sub>) in the Chinese loess deposits are the products of enhanced  
164 erosion produced by tectonic uplift of mountains in Asia (Sun and Liu, 2000; Wu and Wu, 2011) or of  
165 extreme regional climatic events (Ding et al., 2002). Third, the provenance of Chinese loess remains a  
166 highly debated topic (Sun, 2002b; Pullen et al., 2011; Che and Li, 2013; Stevens et al., 2013a; Nie et al.,  
167 2015), mainly due to varying interpretations of geochemical proxies used for determining the main  
168 source areas. The controversy centers on whether the loess deposits come from the deserts to the west  
169 or to the north of the Loess Plateau. A possible solution in this regard would be to combine geochemical  
170 data with the data on the spatiotemporal changes in sedimentological characteristics of Chinese loess to  
171 gain a better insight into past loess source areas (Liu, 1966; Yang and Ding, 2008). Finally, modeling  
172 studies of dust production, transport, and deposition are required to fully understand the processes  
173 responsible for the formation of the loess deposits across the Chinese Loess Plateau.

174

175

176 **Loess in Central Asia**

177 Kathryn E. Fitzsimmons, Charlotte Prud'homme and Aditi K. Dave

178 Central Asia is characterized by comparatively patchy piedmont deposits of loess of varying  
179 thickness, in contrast to other regions of the world. The widespread riverine loess steppe of the Russian  
180 Plain has a distinctly different character and is therefore not included in our definition. We define the  
181 Central Asian piedmont deposits as extending from the foothills of the north Iranian Alborz/Elbruz  
182 Mountains at their westernmost extent (Kehl et al., 2005; Vlamincx et al., 2016), eastward to the Pamir  
183 and Alai ranges (Dodonov, 2002; Dodonov and Baiguzina, 1995), the Tien Shan (Fitzsimmons et al., 2017;  
184 Fitzsimmons et al., in press; Youn et al., 2014), and north along the Altai (Zykin and Zykina, 2015; Zykina  
185 and Zykin, 2012) and Mongolian Hangay (Lehmkuhl and Haselein, 2000; Lehmkuhl et al., 2011) mountain  
186 margins. The loess deposits around the Tarim Basin rim may also be considered part of the Central Asian  
187 piedmont loess due to their geographical similarities (Zheng et al., 2002; Zheng et al., 2003). Figure 4  
188 shows the general distribution of loess deposits across the core of this region (after Dodonov, 1991).

189 The active uplift of the Central Asian high mountains (Campbell et al., 2015; Grützner et al.,  
190 2017) results in steep, rugged terrain, effectively preventing wide-scale accumulation and development  
191 of loess plateaus. This Central Asian piedmont, set in the rain shadow of the Asian high mountains,  
192 generally experiences a semi-arid continental climate. Climatic parameters vary more specifically with  
193 altitude, latitude, orographic effects and the relative influences of the major northern hemisphere  
194 climate subsystems. The dominant climatic influences are the mid-latitude westerlies, northerly polar  
195 fronts, the Siberian high pressure system, and East Asian and Indian monsoon systems (Dettman et al.,  
196 2001; Machalett et al., 2008; Vandenberghe et al., 2006).

197 The thickest sections of Central Asian piedmont loess extend beyond the Brunhes-Matuyama  
198 paleomagnetic reversal (Ding et al., 2002; Dodonov and Baiguzina, 1995; Shackleton et al., 1995; Wang  
199 et al., 2016). As such, they represent long sediment archives that may provide a wealth of potential  
200 paleoclimatic information (Machalett et al., 2008; Vandenberghe et al., 2006; Yang and Ding, 2006).  
201 Despite the location of these deposits in a sensitive transitional climatic zone, however, relatively little is  
202 known about the past environmental history of this region, in part due to political history and logistical  
203 challenges.



204           Loess formation in Central Asia was generally assumed to be genetically linked to sediments  
205 generated by glaciers and rivers in the mountains which flow into the desert basins to the north, and  
206 from which fine-grained dust is transported back onto the piedmonts (Aubekerov, 1993; Smalley, 1995;  
207 Smalley et al., 2009; Smalley et al., 2006). Because numerical chronologies for loess and glaciation in this  
208 region were lacking until recently, scholars assumed that periods of peak loess flux corresponded to cold  
209 glacial phases, and pedogenesis corresponded with interglacials (Ding et al., 2002b; Machalett et al.,  
210 2008; Vandenberghe et al., 2006). This assumption implied an overwhelming and continuous influence  
211 of the North Atlantic westerlies on the region, and has been recently challenged. Direct dating of glacial  
212 moraines showed that some Central Asian glaciers expanded during warmer, wetter phases such as  
213 Marine Isotope Stage (MIS) 3 (Koppes et al., 2008), and that the timing of glacial expansion varied across  
214 the Asian high mountains (Owen and Dortch, 2014). Subsequent dating of piedmont loess deposits also  
215 showed variable timing and rates of accumulation (Fitzsimmons et al., 2017; Fitzsimmons et al., in press;  
216 Li et al., 2016b; Song et al., 2015). Proxy data relating to paleoenvironmental conditions relating to  
217 temperature, precipitation, influence of specific climate subsystems and geomorphic stability are so far  
218 limited. Data are limited either through lack of direct chronological information (Machalett et al., 2008;  
219 Vandenberghe et al., 2006; Yang et al., 2006; Yang and Ding, 2006), or because of insufficient  
220 chronological depth of the available paleoenvironmental proxies (Dodonov et al., 2006; Feng et al.,  
221 2011; Fitzsimmons et al., in press; Ghafarpour et al., 2016).

222           The current state of knowledge for the region indicates variable influence of the different  
223 climate subsystems over the region and through time. One recent hypothesis suggests that loess  
224 accumulation in the Central Asian piedmont peaks under two scenarios (Fitzsimmons et al., in press).  
225 Under the first scenario, loess flux increases due to the increased sediment availability facilitated by  
226 glacial expansion - resulting from increased mountain precipitation due to northward monsoon  
227 migration - combined with compression of the mid-latitude westerlies against the glaciated mountains  
228 and increasing wind strength (for example, during MIS 3). Under the second scenario, loess deposition  
229 increases under cold, dry glacial conditions with reduced but sustained ice volume and persistent  
230 westerly winds (for example the Last Glacial Maximum -- LGM). So far, the climate mechanisms driving  
231 this hypothesis remain unidentified.

232 Elucidating climatic patterns from loess across Central Asia through time will require targeted  
233 investigations covering the entire piedmont and applying methods that provide meaningful information  
234 addressing gaps in our understanding. Robust, long-term chronological frameworks, for example  
235 exploiting new luminescence dating protocols (e.g. Ankjærgaard et al., 2016; Liu et al., 2016; Pickering et  
236 al., 2013; Wintle and Adamiec, 2017), are required to place proxy paleoclimatic data in context.  
237 Meaningful proxies which quantify climatic parameters, such as temperature, precipitation, and  
238 seasonality (e.g. Peterse et al., 2014; Prud'Homme et al., 2015), are important future tools for clarifying  
239 the influence of climatic subsystems on the region through time. These should always be combined with  
240 classical measures of physical characteristics collected at high resolution (e.g. Vandenberghe et al.,  
241 2006; Zeeden et al., in press), and measures of loess sediment provenance facilitating wind regime  
242 reconstruction (e.g. Li et al., 2016b; Stevens et al., 2013a; Stevens et al., 2013b; Újvári et al., 2012).  
243 These approaches herald a new direction for loess research in this poorly understood region that may be  
244 the key to global paleoclimate reconstruction.

245

## 246 **Loess in Europe**

247 Frank Lehmkuhl, Dominik Faust, Ulrich Hambach, Slobodan B. Marković, Igor Obreth, Denis-Didier  
248 Rousseau, and Jef Vandenberghe

249 Loess is one of the most extensively distributed terrestrial Pleistocene deposits in Europe. The  
250 thickness of loess varies between a few decimeters to several tens of meters, depending on its proximity  
251 to the source area and the geomorphologic setting. Due to its wide distribution, loess is often studied in  
252 thick stratigraphic sequences interbedded with paleosols (loess-paleosol-sequences = LPS). LPS are the  
253 most intensively and extensively studied terrestrial archives for the reconstruction of environmental and  
254 climatic changes of glaciations in Europe, since the 1950's. This work has continued onward in the  
255 context of the 'INQUA Loess Commission' (e.g., Gullentops, 1954; Fink, 1956; Pécsi, 1966; Kukla, 1977;  
256 Fink and Kukla, 1977; Lautridou, 1981). Often these studies focused on stratigraphic subdivisions and  
257 correlations (e.g., Paepe, 1966) and were based on field data from sites that have given their name to  
258 classical lithostratigraphical horizons (e.g., Rocourt, Kesselt).

259 Maps of loess in Europe were first presented by Grahmann (1932) and later by Fink et al. (1977);  
260 the most recent compilations were published by Haase et al. (2007) and Bertan et al. (2016). In Europe,  
261 loess is distributed across several main regions (Fig. 5): (1) the northern European loess belt, south of  
262 the Weichselian (MIS 2) ice margin in the north, extending to the uplands in the south [e.g., Ardennes,  
263 Rhenish shield, Harz Mountains, Ore Mountains, Karkonosze Mountains and northern Carpathians  
264 (Tatra)]; (2) eastern Europe (east of the Carpathians), including eastern Romania, Moldova, southeastern  
265 Poland, Ukraine, western Kazakhstan, and Russia; (3) the Upper Rhine Valley and the basins of the  
266 mountainous areas in central and southwestern Germany, including Bohemia and Moravia in Česká; (4)  
267 along the Danube River, from Bavaria towards Austria, Hungary, Slovakia, Croatia, Serbia, Romania and  
268 northern Bulgaria. Small patches of loess also occur in southern and Mediterranean parts of Europe,  
269 mainly in Spain and along the Rhone River in southern France. Minor - although paleoclimatically  
270 important loess deposits – also occur in the Po plain of Italy and along the northern Adriatic coast  
271 (Cremaschi et al., 2015; Wacha et al., 2017).

272 According to various authors, the trapping of dust (loess) is mostly related to vegetation cover  
273 (e.g. Tsoar and Pye, 1987; Danin and Ganor, 1991; Hatté et al., 1998, 2013; Svirčev et al., 2013).  
274 Therefore, the northern border of the loess distribution probably coincides with the northern fringe of  
275 past vegetation systems. Almost no loess accumulated south of the northern timberline during the Last  
276 Glacial Maximum (LGM), as the accumulation of loess was mostly related to both tundra and steppe  
277 environments. Erosion, transport, deposition, and preservation/loessification of dust follows completely  
278 different flows of processes in the periglacial areas compared to the steppe regions.

279 The northern European loess belt, extending from France to Germany, Poland and northern  
280 Ukraine, was strongly influenced by periglacial environments, with its fluctuating boundaries of  
281 continuous and discontinuous permafrost (Vandenberghe et al., 2012; 2014). As a consequence, and  
282 because of the North Atlantic influence, loess in Northern Europe has a complex stratigraphy that is  
283 generally similar from Brittany through to Ukraine (Rousseau, 1987; Antoine et al., 2009, 2013; Buggle et  
284 al., 2009; Rousseau et al. 2017a; Lehmkuhl et al., 2016; Fig. 5). Loess in the northern European loess belt  
285 is situated mainly at the northern front of the Central European Mountains, in basins below 200 to 300  
286 m and partly below 400 to 500 m in southern Germany (Lehmkuhl et al., 2016). Environmental  
287 conditions during periods of loess deposition were likely highly variable, with erosive processes (slope

288 wash and deflation) playing important roles, implying that loess was not continuously deposited here or  
289 completely preserved during glacial periods. Thus, erosional unconformities are typical features of  
290 Central European LPS, which often make stratigraphic interpretations and correlations challenging  
291 (Zöller and Semmel, 2001). The distribution of eolian sediments was also influenced by sediment  
292 availability (e.g., proximity to larger river systems, and the ice sheet itself) and prevailing wind  
293 directions. As a result, the temporal resolution and thickness of LPS can vary locally as well as between  
294 different loess regions. Despite the growing focus on the impact of source areas and geomorphological  
295 position on loess deposits (Lehmkuhl et al. 2016), there is still a search for (litho-) stratigraphic  
296 correlations (e.g., Schirmer, 2016; Haesaerts et al., 2016). More recently, research has been focusing on  
297 the impact of rapid climatic oscillations on European continental environments, by comparing biological,  
298 geochemical and sedimentological proxy data from LPS with variations in Greenland ice core data (e.g.,  
299 Rousseau et al., 2002; 2007; 2013; 2014; 2017a,b; Antoine et al., 2003, 2009; 2013; Moine, 2014;  
300 Schirmer, 2016).

301           Loess in Southeastern Europe is mostly found on large, broad loess plateaus, mainly in the  
302 Danube Basin (Fitzsimmons et al., 2012), indicating the Danube River and its tributaries were important  
303 source areas (Smalley and Leach, 1978; Buggle et al., 2008; Újvári et al., 2008; Bokhorst et al., 2011). The  
304 Danube Basin represents the largest European loess region west of the Russian / Ukrainian Plain,  
305 preserving a paleoenvironmental record extending to the Early Pleistocene (Marković et al., 2011). Due  
306 to its plateau setting and the absence of periglacial influences (Fig. 5), Danube LPS are some of the most  
307 complete, representing one of the thickest (up to > 40 m), longest (since early / mid-Pleistocene) and  
308 most widespread terrestrial Quaternary paleoclimate archives in Europe (Fink and Kukla, 1977; Buggle et  
309 al., 2013; Marković et al., 2015). In the southern Pannonian / Carpathian Basin (Hungary and Serbia) and  
310 in the Lower Danube Basin (Romania and Bulgaria) core data point to loess thicknesses > 100 m  
311 (Pfannenstiel, 1950; Pécsi, 1985; Koloszar, 2010; Jipa, 2014). Unlike Central and Western Europe, loess  
312 here is characterized by a generally straightforward stratigraphy (Fig. 6), where stronger soil formation is  
313 related to warmer phases (usually associated with odd-numbered Marine Isotope Stages), and loess  
314 deposition occurs mainly during colder stages (Fig. 7) (Marković et al., 2015). Despite the wide  
315 distribution of the Danube loess, the southern limit of the European loess belt interior of the Balkan  
316 Peninsula is characterized by many isolated loess deposits that originate from local sources rather than

317 from the Danube proper. These smaller loess deposits exhibit unique geophysical and geochemical  
318 properties (Basarin et al., 2011; Obreht et al., 2014, 2016).

319           Loess in Eastern Europe forms a blanket that covers an area exceeding one million km<sup>2</sup>. This  
320 loess was derived from the alluvial and lacustrine plains that formed in front of the advancing and  
321 retreating Pleistocene ice sheets (Velichko, 1990). This huge loess belt covers different bioclimatic  
322 zones, from the boreal southern taiga to the sub-Mediterranean Black and Azov Sea coasts, and also  
323 farther east to the Caspian Sea. Loess thickness here generally increases to the south, indicating glacial  
324 sources but also including material from local and other origins within a mixed zone in the south. Most  
325 comprehensive studies of LPS in Eastern Europe have been performed in the southern part of the East  
326 European Plain (Tsatskin et al., 1998; Rousseau et al., 2001, 2013; Haesaerts et al. 2003; Velichko et al.,  
327 2009; Liang et al., 2016).

328           Loess in Southwestern Europe is almost entirely concentrated in the Ebro valley and Central  
329 Spain (e.g. Bertran et al., 2016). This loess does not reach the thicknesses of loess in Central and Eastern  
330 Europe, and is mostly preserved as relocated loess-derivates. Boixadera et al. (2015) reported about  
331 loess deposits that are generally 3 – 4 m thick and consist of well-sorted fine sands and silts, i.e., coarser  
332 than typical loess. Loess in Central Spain is distributed along the Tajo River, covering fluvial terraces and  
333 depressions nearby.

334

### 335 **Loess in Midcontinent North America**

336 Joseph A. Mason

337           Some of the most important issues that still challenge loess researchers in the Central Lowlands  
338 and Great Plains of North America were already apparent in the classic map of aeolian deposits of the  
339 United States, Alaska and parts of Canada by Thorp and Smith (1952). Drawing on extensive  
340 observations by soil surveyors as well as geologists, Thorp and Smith (1952) mapped thick loess  
341 bordering the Mississippi, Missouri, Illinois, Wabash, and Ohio rivers, all of which had drained the ice  
342 sheet of the last glaciation. Loess deposits exhibited well-defined thinning trends away from each river  
343 valley. A much broader swath of thick loess extended across the central Great Plains, from eastern

344 Colorado to the Missouri River, thinning toward the southeast but with no obvious relationship to  
345 possible river valley sources (for an updated map, see Bettis et al., 2003). Thorp and Smith (1952) also  
346 accurately mapped many areas of thin loess across the Central Lowlands and Great Plains, and provided  
347 a separate map of the Illinoian (MIS 6) Loveland Loess, but their work emphasized the great thickness  
348 and extensive distribution of Late Pleistocene (MIS 2) Peoria Loess.

349 Today, interpretations of Peoria Loess, its sources and their paleoenvironmental controls, and its  
350 episodic and often very rapid accumulation rates, remain a central issue in midcontinent loess research.  
351 Provenance studies have revealed that much of the Peoria Loess of the central Great Plains was derived  
352 from Cenozoic rocks cropping out in unglaciated landscapes to the northwest (Aleinikoff et al., 2008;  
353 Aleinikoff et al., 1999; Muhs et al., 2008a). The paleoenvironments and processes involved in this  
354 enormous amount of nonglacial dust production remain poorly understood. In contrast, much of the  
355 Peoria Loess farther east is closely linked to glacial sediments carried by the Mississippi and other rivers  
356 during MIS 2, with changing sediment availability linked to ice lobe advance and retreat (Bettis et al.,  
357 2003; Follmer, 1996; Grimley, 2000). Peoria Loess deposits record some of the highest mass  
358 accumulation rates known worldwide, and just as interesting, improved age control—most recently  
359 through <sup>14</sup>C dating of gastropod shells—has confirmed large changes in accumulation rate over time  
360 (Muhs et al., 2013; Nash et al., 2017; Pigati et al., 2013; Roberts et al., 2003). At present it appears that  
361 these changes were not synchronous across the Central Lowlands or Great Plains and thus may be  
362 related to local variations in sediment supply, or changing source areas (e.g., Nash et al., 2017) rather  
363 than broader climatic change, not surprising given the complexity of Peoria Loess sources. Geomorphic  
364 evidence also exists for large-scale deflation of coarse, source-proximal Peoria Loess, and experimental  
365 evidence suggests that there is a high potential for aeolian re-entrainment in the absence of vegetation  
366 cover or cohesive crusts (Sweeney and Mason, 2013). These processes could also be responsible for  
367 abrupt local changes in grain size or accumulation rate.

368 The stratigraphy of loess, both older and younger than the Peoria Loess, emphasizes the unique  
369 nature of the loess system during MIS 2 (Mason et al., 2007), but also raises many other questions. Parts  
370 of the White River (Late Eocene-Oligocene) and Arikaree (Oligocene-Miocene) groups in western  
371 Nebraska are interpreted as volcanoclastic loess (Hunt, 1990; LaGarry, 1998; Swinehart et al., 1985),  
372 helping to explain why large volumes of these rocks were later reworked into Peoria Loess (Aleinikoff et

373 al., 2008; Aleinikoff et al., 1999; Yang et al., 2017). Loess-like silt predating the Matuyama-Brunhes  
374 boundary at 780 ka has been identified in Illinois (Grimley and Oches, 2015); however, continuous loess  
375 sequences in the midcontinent apparently all postdate the M-B boundary and/or the Lava Creek B  
376 tephra (~630 ka, Matthews et al., 2015). The relative scarcity of Early Pleistocene loess must in part  
377 reflect poor preservation, but other factors should also be explored. For example, if Early Pleistocene ice  
378 sheets extended farther south but had lower profiles (Clark and Pollard, 1998), the resulting glacial  
379 atmospheric circulation might not have favored dryland dust production from potential sources on the  
380 Great Plains.

381         The loess sequence in eastern and central Nebraska (Fig. 8) is broadly representative of the  
382 stratigraphy of thick loess at localities across the midcontinent where preservation is high. The oldest  
383 part of this sequence includes multiple thin depositional units of the Middle Pleistocene Kennard  
384 Formation (Mason et al., 2007). The stratigraphy, chronology, provenance, and paleoenvironmental  
385 record of the Kennard Formation remain largely unstudied, as have possible correlations with pre-  
386 Loveland loess units reported from scattered localities along the Mississippi River valley (Grimley, 1996;  
387 Jacobs and Knox, 1994; Leigh and Knox, 1994; Markewich et al., 1998; Porter and Bishop, 1990; Rutledge  
388 et al., 1996). A variety of evidence indicates the overlying Loveland Loess was deposited during the MIS  
389 6 glacial, although luminescence ages at some sites suggest the uppermost part may be younger  
390 (Forman et al., 1992; Forman and Pierson, 2002; Grimley and Oches, 2015; Maat and Johnson, 1996;  
391 Markewich et al., 1998; Rodbell et al., 1997). An intriguing characteristic of thick Loveland Loess is the  
392 presence of a lower, darker-colored zone, which may contain multiple weak paleosols, suggestive of  
393 slow and/or intermittent deposition (Grimley, 1996; Mason et al., 2007). Above the prominent  
394 Sangamon Soil, which caps the Loveland Loess and developed through MIS 5 and 4, is a MIS 3 loess unit  
395 variously known as the Roxana Silt (Mississippi valley), Pisgah Loess (Iowa) or Gilman Canyon Formation  
396 (Great Plains). It has characteristics similar to the lower Loveland Loess; <sup>14</sup>C and luminescence dating  
397 confirms its slow accumulation rate (Bettis et al., 2003; Follmer, 1996; Johnson et al., 2007; Leigh, 1994;  
398 Markewich et al., 1998; Muhs et al., 2013a). This similarity suggests the lower zone of Loveland Loess on  
399 the Great Plains could preserve an isotopic record of shifting dominance by C<sub>3</sub> and C<sub>4</sub> grassland, as does  
400 the Gilman Canyon Formation (Johnson et al., 2007). Above the MIS 3 loess, Peoria Loess accumulated  
401 between about 28 ka and 13 ka (MIS 2) across the midcontinent, with the exact time span varying  
402 regionally and possibly locally (Bettis et al., 2003; Muhs et al., 2013; Nash et al., 2017; Pigati et al., 2013).



403 On the central Great Plains and along the Missouri River valley in North and South Dakota, the loess  
404 record continues into the Holocene. The Brady Soil, formed during a period of limited dust accumulation  
405 between about 14 and 10 ka, is sometimes found in the upper Peoria Loess, when Bignell Loess overlies  
406 it. Where the latter is thick it represents a high-resolution record of Holocene dust deposition (Johnson  
407 and Willey, 2000; Mason et al., 2003; Mason et al., 2008). The specific geomorphic mechanisms of  
408 Holocene dust production, downwind dispersal, and patchy retention in the landscape, and their  
409 connections to changing climate and vegetation, are worthy of additional study because of their  
410 potential relevance to the environmental changes associated with a warmer and drier future climate.

411

## 412 **Loess in Alaska**

413 E. Arthur Bettis III

414 Loess associated with glacial valley-train sources is extensive over much of Alaska and  
415 adjacent parts of Yukon Territory in Canada (Fig. 9). In some parts of central Alaska, loess can  
416 be as much as several tens of meters thick and, based on a combined tephra and paleomagnetic record,  
417 may date back as far as the onset of North American glaciation, ~3 Ma (Westgate et al., 1990). It was not  
418 until the mid-1950's that the extensive deposits of silt on the Alaskan landscape were properly  
419 recognized as loess. Prior to that time, some researchers regarded them as the result of frost shattering  
420 or other processes (Taber, 1943, 1953, 1958). It was Péwé (1955), however, who finally brought  
421 together several converging lines of evidence--geomorphic, stratigraphic, and mineralogic—that  
422 established that these silt bodies in Alaska are loess. Loess is now recognized over many parts of the  
423 region, including a broad area of the coastal plain north of the Brooks Range, over parts of the Seward  
424 Peninsula (Hopkins, 1963), in the Yukon River basin (Williams, 1962; Begét et al., 1991; Jensen et al.,  
425 2013), in the Tanana River valley and along the Delta River valley of central Alaska (Péwé, 1955, 1975,  
426 Muhs et al., 2003), in southern Alaska in the Matanuska Valley (Muhs et al., 2004, 2016), on the Kenai  
427 Peninsula (Reger et al., 1996), and along the Copper River Valley in Wrangell-St. Elias National Park  
428 (Muhs et al., 2013; Pigati et al., 2013).



429           Loess deposits in Alaska that have been securely dated to the last glacial period are elusive, or  
430 are very thin. On the Seward Peninsula, less than a meter of loess blankets a land surface with fossil  
431 tundra vegetation that dates to the last glacial period (Höfle and Ping, 1996; Höfle et al., 2000). In the  
432 Fox Permafrost Tunnel near Fairbanks, loess that is bracketed by a radiocarbon age of ~9.5 ka above and  
433 ~34 ka below could date to the last glacial period (Hamilton et al., 1988), as is the case for very thin loess  
434 dated between ~12 ka and ~36 ka nearby in an upland locality (Muhs et al., 2003). In neither of these  
435 two cases, however, is loess dated directly to the last glacial period. Attempts to date other last glacial  
436 central Alaskan loess deposits have been frustrated by a lack of materials suitable for radiocarbon  
437 analyses or uncertainties in luminescence geochronology (Oches et al., 1998; Berger, 2003; Muhs et al.,  
438 2003; Auclair et al., 2007). However, recent identification of the Dawson tephra (~30 ka) in the upper  
439 part of loess deposits near Fairbanks permits an interpretation of as much as ~3 m of accumulation since  
440 the time of tephra deposition (Jensen et al., 2016). Nevertheless, it is not known how much of this  
441 sediment is of last-glacial age and how much may be of Holocene age.

442           Older, pre-last glacial loesses are well documented in Alaska. The chronology of these older  
443 loesses has been aided immeasurably by detailed studies of tephras that are interbedded with the  
444 aeolian silts (Westgate et al., 1990; Begét et al., 1991; Preece et al., 1999; Jensen et al., 2013, 2016).  
445 Jensen et al. (2016) described evidence for significant pre-last glacial loess accumulation in central  
446 Alaska during Marine Isotope Stages 4 and 6, with accumulation rates greatest during transitions  
447 between isotope stages. Furthermore, these investigators noted that in the middle and early  
448 Pleistocene, glaciations were much more extensive in Alaska than during the last glacial period (Kaufman  
449 et al., 2004), which likely enhanced the supply of glaciogenic silt available for loess accumulation.

450           Whereas loess dated to the last glacial period has been elusive in Alaska, there are abundant  
451 loess bodies that date to the Holocene, and deposition continues today in many parts of the region. In  
452 the Delta Junction area of central Alaska, only Holocene loess has been documented (Péwé, 1975; Muhs  
453 et al., 2003). On the Kenai Peninsula of southern Alaska, the Lethe tephra dating to ~19 ka to ~15 ka is  
454 found below, or in the lower part of loess, but as on the Seward Peninsula, this eolian silt is less than a  
455 meter thick (Reger et al., 1996). Elsewhere in southern Alaska, near Anchorage, loess of the Matanuska  
456 Valley all dates to the Holocene (Muhs et al., 2004, 2016), as does loess of the Copper River Valley in  
457 Wrangell-St. Elias National Park, to the east (Muhs et al., 2013; Pigati et al., 2013).

458 Paleosols intercalated in loess sequences have long been the focus of study, for stratigraphy,  
459 geochronology, and paleoenvironmental interpretation in most loess regions. In Alaska, however, little  
460 mention of paleosols in the loess sequence was made by geologists until relatively recently. Indeed,  
461 some researchers even doubted their existence (Péwé et al., 1997). Begét and his colleagues at the  
462 University of Alaska were the first to bring the geological community's attention to the rich record of  
463 paleosols in Alaskan loess in a landmark series of papers (Begét, 1990; Begét and Hawkins, 1989; Begét  
464 et al., 1990). Paleosol research in Alaska and adjacent Yukon Territory since the time of these pioneering  
465 studies has provided new insights into the paleoenvironment during periods of reduced loess  
466 accumulation (Sanborn et al., 2006; Muhs et al., 2008b).

467

#### 468 **Loess in Argentina, South America**

469 Marcello Zárate

470 The loess deposits of southern South America cover broad areas of the eastern Pampean plain  
471 of Argentina, southern Brazil and Uruguay, as well as several areas of the Chaco region, and mountain  
472 valleys of the northwestern Pampean ranges (Figure 10). The focus of this overview is on the loess  
473 deposits in Argentina. In the Pampean region of Argentina, loess and loess-like deposits range in age  
474 from the late Miocene through the Quaternary; in some Pampean areas, loess accumulation even  
475 continued until the early-mid Holocene. Luminescence chronology carried out in the extensive apron of  
476 the last glacial loess suggests regional variation in depositional rates over this interval, with relatively  
477 high accumulation rates during the Last Glacial Maximum and the Late Glacial intervals. The average  
478 thickness of the last glacial Pampean loess is ca. 1.5-2 m, with up to 3-4 m in the mountains surrounding  
479 the Pampean plain, i.e., the Tandilia and Ventania ranges and the Pampean ranges of Córdoba-San Luis.  
480 Sandy eolian deposits (dune fields, sand sheets) dominate in the western-southwestern Pampean plain  
481 and grade into loess mantles downwind (Zárate and Tripaldi 2012). The loess deposits also show a  
482 gradual grain size decrease from silty fine sands to silty deposits in the eastern Pampean plain (González  
483 Bonorino, 1966). The mineralogical assemblage of the Pampean loess is dominantly composed of  
484 plagioclase, volcanic shards (both fresh and weathered), quartz, K-feldspars, and fragments of basalt,  
485 andesite and rhyolite. Magnetite, amphibole, and pyroxene, among others, are the most common heavy

486 minerals. The direct input of Andean volcanic eruptions in the loess deposits is documented by fresh  
487 volcanic shards, whereas most of the loess grains were derived from the erosion and fluvial  
488 transportation of extensive volcanoclastic units (*sensu* Fisher, 1961) exposed in the Andes Cordillera and  
489 its piedmont. These volcanoclastic units comprise late Miocene to Quaternary fine-grained pyroclastic  
490 deposits, and volcanic rocks (basalts, andesites), as well as lower Mesozoic acid volcanic rocks (González  
491 Bonorino, 1966). The origin of the volcanoclastic sedimentary sand and silt particles has been attributed  
492 to explosive volcanism (Zárate and Blasi, 1993) and physical weathering (Iriondo, 1990). Secondary loess  
493 sources, including the Brazilian plateau, the Tandilia and Ventania ranges and the Pampean ranges  
494 surrounding the Pampean plain, have also been documented and show variable contributions, according  
495 to the area considered (Zárate and Tripaldi 2012). The eolian sand and silt particles are thought to have  
496 been deflated by W-SW winds from the fluvial system of (1) the Bermejo-Desaguadero-Salado-Curacó  
497 (BDSC) River (Iriondo, 1990), a wide depositional system at the distal eastern piedmont of the Andes,  
498 and (2) the Colorado-Negro Rivers (Zárate and Blasi, 1993), where volcanoclastic sediments are  
499 abundant. NE-SE winds prevailed along the northern extent of the BDSC system, between the Diamante  
500 and San Juan Rivers, and the western Pampas near the San Luis ranges (Figure 10), where eolian sandy  
501 sediments document a mixed provenance, including volcanoclastic, metamorphic, and igneous rocks  
502 from the surrounding Pampean ranges (Zárate and Tripaldi, 2012). In order to improve our  
503 understanding of Quaternary eolian systems, most current research has focused on two main topics  
504 related to the loess here: 1) investigation of the sedimentary environments of the source area  
505 represented by the BDSC fluvial system and 2) Quaternary loess deposits of the northwestern mountain  
506 valleys.

507           Studies in progress suggest that the BDSC fluvial system is a complex sedimentary setting  
508 consisting of major alluvial fans generated by its main tributaries (*i.e.*, the San Juan, Mendoza, Tunuyán,  
509 Atuel, and Diamante Rivers), all of which drain eastward, out of the Andes Mountains. General  
510 paleoclimatological and paleoenvironmental reconstructions suggest that arid and arid-semiarid  
511 conditions dominated here during the accumulation of the alluvial deposits, *i.e.*, from the late  
512 Pleistocene to the present (Mancini *et al.*, 2005). The San Juan, Mendoza, Tunuyán, Atuel, and Diamante  
513 drainage basins have a seasonal precipitation regime, with winter snowfalls generated by the Pacific  
514 cyclones, in their upper basins. These areas were also glaciated (Espizúa, 2004), promoting increased  
515 seasonal discharges during the Pleistocene. Sedimentological analysis focused on the lower basins of the

516 Atuel and Diamante Rivers have documented a large alluvial fan (200 km long and 100 km wide)  
517 dominated by fine sand-coarse silt deposits. Diverse sedimentary settings, including numerous channels  
518 and their associated floodplains, as well as shallow saline lakes, are reported for this system, along with  
519 extensive eolian deposits (dunes and sand sheets) covering large parts of the alluvial deposits (Lorenzo  
520 et al., 2017; Tripaldi and Zárata, 2017). Farther north, in Catamarca Province, loess deposits have been  
521 recently explored in a valley situated ~100 km SW from the Tafí del Valle loess locality of Tucumán  
522 (Stiglitz et al., 2006). The loess deposits here are up to 40 m thick, and include interlayered fluvial  
523 sediments and paleosols. Loess has also been reported nearby, covering the planation surface of the  
524 Ancasti Pampean range (Sayago, 1983). Immediately west of the Catamarca valley are large  
525 intermountain tectonic basins (e.g., the Salar de Pipanaco, Campo del Arenal) that contain fine alluvial  
526 sands and silts from rivers that drain the Andes and the Puna region and their associated dune fields.

527           Although several areas still remain unexplored and/or poorly investigated, current studies  
528 allow for a reinterpretation of the BDSC fluvial system as a large bajada resulting from the north-south  
529 coalescence of several major alluvial fans generated by rivers with highly seasonal flow regimes from  
530 winter snowfalls and glaciers, under generally arid-semiarid conditions. This depositional environment  
531 has abundant sand and silt, derived from the erosion of late Cenozoic volcanic rocks and pyroclastic  
532 deposits, and older volcanic and volcanoclastic units exposed in the Andes and the eastern piedmont, as  
533 well as metamorphic and igneous rocks from the surrounding Pampean ranges. These sediments were  
534 subject to entrainment by prevailing W-SW winds in the southern part of the BDSC fluvial system, and  
535 NE-SE winds in the northern part.

536           Two important questions remain regarding the source area of the northwestern mountain  
537 valley loess of Catamarca: (1) What were the prevailing wind directions? and (2) Has this loess been  
538 deflated from the tectonic basins located to the west-northwest, or did it originate via high suspension  
539 from more distal environments (i.e., the Puna plateau)? Future research should include a more detailed  
540 analysis of the late Quaternary eolian deposits in the northern BDSC system that may show a mixed  
541 provenance, and which may have been derived from NE-SE winds, as well as the loess deposits of the  
542 NW mountain valleys. These studies may help discern the role played by regional and/or local factors  
543 during the aeolian accumulation phases in this region.

544

545 **Loess at Desert Margins**

546 Onn Crouvi

547 Loess at desert margins (termed here as ‘desert loess’) refers to eolian silt deposits generated  
548 in, and derived from, non-glaciated, low-latitude warm-arid or semi-arid regions. The documentation of  
549 loess at desert margins since the mid-20<sup>th</sup> century (e.g., Coude-Gaussen, 1987; McTainsh, 1987; Yaalon,  
550 1969) has confounded the traditional view of silt generation solely by glacial grinding (e.g., Smalley and  
551 Krinsley, 1978) that is widely attributed to most of the world’s well-known loess deposits. Thus, a  
552 number of non-glacial processes that produce silt grains in deserts have long been proposed and  
553 debated (e.g., Assallay et al., 1998; Muhs and Bettis, 2003; Smalley, 1995; Smith et al., 2002; Wright,  
554 2001), including salt weathering, frost weathering, deep weathering, fluvial comminution, and eolian  
555 abrasion.

556 Desert loess is known to exist at the margins of deserts in Africa (Tunisia, Libya, Algeria, Nigeria  
557 and Namibia), in the Middle East (Israel, Yemen, the UAE, Iran), in the western US, the Great Plains of  
558 North America, and in Australia (Figure 11a). With the exception of the thick non-glacial loess in the  
559 Great Plains of North America, loess of this kind is patchy and varies in thickness from few meters on  
560 uplands to few tens of meters in valleys. Importantly, desert loess is the parent material for some of the  
561 most fertile soils in these regions. A few characteristics are common to all reported desert loess sites in  
562 Africa and the Middle East (Crouvi et al., 2010): (1) loess sediments are dominantly coarse silt to very  
563 fine sand, with median grain sizes ranging from 50 to 80  $\mu\text{m}$ , and at some sites, the particle size  
564 distribution (PSD) is reported to be tri- or bi-modal; (2) loess mineralogy is mostly quartz and feldspars,  
565 with various amounts of carbonate, depending on the degree of soil development in the loess; (3) at  
566 most sites, the underlying lithologies are inconsistent with the presence of quartz in the loess,  
567 suggesting an external silt source; (4) the shapes of loess particles are reported as subangular to angular  
568 for most regions; and (5) most loess bodies were deposited during the last glacial period (~110-10 ka).  
569 Crouvi et al. (2010) noted that all these loess regions are located only few tens of km downwind from  
570 sand dunes (Figure 11), and based on the mineralogical, spatial and temporal associations between  
571 these two eolian bodies, suggested that the proximal source of the coarse silt in loess is the upwind  
572 dunes, via eolian abrasion of sand grains.

573           The Negev loess (Israel) is one of the world's best studied desert loess deposits, with scientific  
574 exploration that goes back to the early 20<sup>th</sup> century (Figure 11b; see Crouvi et al, 2017a). The carbonate  
575 bedrock lithology of the Negev and its physiography provide a unique opportunity to understand the  
576 sources of this silicate-rich loess, and to explore silt formative processes in deserts. Grain size data from  
577 the Negev loess have three main characteristics: 1) clear textural bimodality, with one mode in the  
578 coarse silt fraction (36-65  $\mu\text{m}$ ) and another in the fine silt to clay fraction (2.5-10  $\mu\text{m}$ ), 2) grain-size  
579 decreases to the north, east, and south, away from the sand dunes that border the loess deposit on the  
580 west, and 3) increasing grain-size upward in each individual primary sequence. Recognizing the  
581 bimodality of the loess, Dan Yaalon was the first to suggest that the Negev loess had two different  
582 sources that supplied sediments through two different transport pathways (Yaalon, 1969; Yaalon and  
583 Dan, 1974; Yaalon and Ganor, 1973, 1979): distal sources in the Sahara and Arabia deserts supplying fine  
584 silt and clays transported by cyclonic winds over thousands of kilometers, and proximal sources in Sinai,  
585 such as Wadi El-Arish in northern Sinai, supplying the coarser silts. However, recent studies have shown  
586 that the major source of the coarse silt grains are the adjacent, upwind sand dunes that advanced into  
587 Sinai and Negev during the late Pleistocene, concurrent with accumulation of the loess (Crouvi, 2009;  
588 Crouvi et al., 2008). This conclusion was based on the following observations: (1) increases of the  
589 quartzofeldspathic coarse mode upward in the loess deposits, (2) the spatio-temporal association of  
590 sand dune activities and dust mass accumulation rates (MARs) of the loess, (3) similarity in mineralogical  
591 composition and in isotopic composition of Sr and Nd between the sand dunes and the coarse fraction  
592 of the loess (Ben Israel et al., 2015; Muhs et al., 2013c), and (4) location – the loess was located  
593 downwind of sand dunes during the late Pleistocene, as evident by the linear orientation of the dunes.  
594 In addition, recent studies have shown that the quartz-rich silt fraction in soils in the Judean Mountains  
595 and their lowlands, north of the loess, can be regarded as the direct continuation of the dune – loess  
596 association (Amit et al., 2016; Crouvi et al., 2015). Due to the fact that these silt grains are farther away  
597 from their source than the Negev loess deposits, they are finer-grained and exhibit lower MAR's. Finally,  
598 because much of the Negev loess formed during the late Pleistocene, it has been undergoing erosion  
599 through most of the Holocene, and even more severely during the last 100 years due to agriculture  
600 practices. The erosion is both by water (e.g., Avni, 2005; Avni et al., 2006) and by wind (e.g., Crouvi et  
601 al., 2017b; Tanner et al., 2016), transferring the loess into a relatively young and new proximal dust  
602 source. Overall, the Negev loess can be regarded today as non-replenishable natural resource that is  
603 slowly disappearing.





630 glacial phases during the Quaternary Period. During these periods, complex natural processes related to  
631 the formation, production, and deposition of dust facilitated the formation of loess deposits.

632           Loess, which is a mixture of different minerals, represents an almost ideal substrate for soil  
633 formation. Even slight climate changes are able to initiate rapid soil formation in loess deposits. Thus,  
634 even slight shifts from periods of dust accumulation to pedogenesis can be recorded in loess; paleosols  
635 within these sequences are some of the most sensitive continental archives of environmental responses  
636 to Quaternary climate change. From this point of view, each typical loess deposit or strongly developed  
637 pedocomplex can be regarded as a basic climato-stratigraphic unit, representing full glacial or  
638 interglacial conditions. Other varieties of loess derivatives and weakly developed paleosols in loess are  
639 equivalent to stadial and interstadial environments, respectively.

640           Consequently, it is no surprise that climato-stratigraphic research in many loess regions has a  
641 long and distinguished history. Many such early loess stratigraphic models represented climato-  
642 stratigraphic approaches (e.g. Marković et al., 2016). Nonetheless, they had shortcomings. Developed at  
643 the beginning of the 20<sup>th</sup> century, many of these studies were highly speculative, and the nomenclatures  
644 used were usually derived from local place names. With the purpose of creating a common European  
645 loess stratigraphy, the Loess sub-commission (Currently Loess Focus Group) of the International Union  
646 for Quaternary Research (INQUA) promoted pedostratigraphic criteria as the primary basis for  
647 stratigraphic correlations (Fink, 1962; Smalley et al., 2010). This concept culminated in the studies of  
648 Bronger and co-workers, who presented their attempts at Eurasian continental loess correlation in a  
649 series of papers (Bronger, 1976, 2003; Bronger and Heinkele 1989; Bronger et al., 1998). Later,  
650 investigation of Czechian and Austrian loess exposures provided the background for correlation of  
651 terrestrial loess deposits with the oscillations recorded in deep-sea sediments, given that both likely  
652 reflect global paleoclimate drivers (Kukla, 1975, 1977; Fink and Kukla, 1977). The glacial cycle concept  
653 that Kukla applied to loess-paleosol sequences promoted loess as the most important terrestrial archive  
654 of Pleistocene climatic and environmental changes.

655           Further development of magnetostratigraphic techniques, as applied to loess in China,  
656 highlighted scientific interest in the multiple loess-paleosol couplets of the Chinese Loess Plateau (Heller  
657 and Liu, 1982, 1984; Liu, 1985). This new approach, based on paleomagnetic polarity zonation, allowed  
658 for direct correlations between profiles using loess-paleosol magnetic susceptibility variations and its



659 correspondence with Marine oxygen isotope stratigraphy. Eventually, this method became the basis for  
660 the famous so-called “L & S” (Loess & soil) Chinese loess stratigraphic model (Liu, 1985; Kukla, 1987;  
661 Kukla and An, 1989; Hao et al., 2012). Enhancement of the magnetic signal due to pedogenic processes  
662 appears to be valid for loess strata across the vast Eurasian semi-arid loess zone as well (Maher and  
663 Thompson, 1992), further extending its application (Figure 12). Data on loess magnetic susceptibility has  
664 since proven to be a rapid and consistent tool for inter-profile correlations, even over very long  
665 distances (Marković et al., 2015). Figure 13 shows the remarkable accordance between Serbian and  
666 Chinese loess stratigraphies. The loess magnetic record from Siberian and Alaskan loess provinces has  
667 the opposite trends, i.e., higher magnetic susceptibility values characterize loess deposits, with lower  
668 values in paleosols (e.g. Begét, 1990, 1996; Begét et al., 1990; Heller and Evans, 1995; Chlachula et al.  
669 1998). Additional quantitative chronological approaches, such as current improvements in amino acid  
670 racemization, relative geochronology, tephrochronology, <sup>14</sup>C and luminescence dating, have helped to  
671 significantly improve the accuracy of loess stratigraphic models, but still only at the level of correlation  
672 with the main Marine Isotope Stages. In the United States, most of the loess is younger than Middle  
673 Pleistocene in age and therefore, “classic” regional loess stratigraphic models supported by  
674 luminescence and radiocarbon dating are generally more useful for long-range correlations than are  
675 data on magnetic susceptibility or amino acid racemization (Bettis et al, 2003).

676           Loess stratigraphy in the Southern Hemisphere has been investigated less intensively in South  
677 America where there is a high diversity of loess and loess-like deposits as a consequence of quite diverse  
678 environmental responses to climate forcing (Zarate, 2003; Iriondo and Kröhling, 2007). An additional  
679 problem in some regions is similar to the examples mentioned previously for Siberian and Alaskan loess;  
680 in this case, the variation in magnetic susceptibility is because of contributions of volcanic material in  
681 the loess deposits (e.g. Ruocco, 1989; Heller and Evans, 1995). Similar conditions occur in New Zealand,  
682 although here the presence of many (dated) tephra layers became an important advantage for the  
683 establishment of loess stratigraphy (Palmer and Pillans, 1990; Roering et al., 2002).

684           Using the L&S stratigraphic nomenclature, already well accepted for Chinese and Danubean  
685 stratigraphic units, can be a useful global approach. The L&S stratigraphic scheme has led to  
686 standardized, regionally specific stratigraphies of European loess deposits. The L&S scheme also offers a  
687 potential for correlating the confusing diversity of European loess stratigraphic records across the

688 Eurasian loess belt and into Central Asia and China (Marković et al., 2015). In order for the L&S system to  
689 provide accurate correlations three conditions need to be met: 1) numerical ages or tie lines to  
690 numerical ages (e.g., volcanic ash dated elsewhere) need to be available and; 2) absence of  
691 unconformities in undated portions of the sections must be demonstrated; and 3) an assumption that  
692 global (or at least continental) geoenvironmental conditions fostering loess accumulation and  
693 subsequent soil development were more or less isochronous. The last assumption is the most  
694 problematic and can only be demonstrated with a much larger set of well-dated key localities than are  
695 currently available. Using this very simple labelling system is especially useful for geoscientists who may  
696 not be conversant in the region, or in loess research. Hence, a unified chronostratigraphic scheme like  
697 the L&S scheme makes synchronization between the loess stratigraphic units in different parts of world  
698 almost intuitive (Figure 14).

699           Contrary to successful attempts at correlations between the main loess stratigraphic models and  
700 their equivalent Marine Isotope Stages (e.g., Lisiecki and Raymo, 2005; Figure 13A), application of event  
701 stratigraphy in loess research is still problematic (*sensu* Björck et al., 1998). For example, direct  
702 correlations of the loess record with Greenland stadial-interstadial cycles (Rousseau et al., 2002, 2007;  
703 Antoine et al., 2009, 2013) or with Heinrich events (Porter and An, 1995; Stevens et al., 2008) are still  
704 under debate. The main problem lies in inadequate age control. Luminescence chronologies from loess  
705 sections are not sufficiently precise to make the proposed temporal correlations with the higher-  
706 resolution Greenland ice-core records. For example, one standard deviation uncertainties on a  
707 luminescence age are at best 5%, far too large to allow such fine correlations over this time interval  
708 (Roberts, 2008).

709           Due to the widespread distribution of loess and loess-like deposits, especially in the Northern  
710 Hemisphere, accurate loess climato-stratigraphic records supported with accurate age control can be  
711 regarded as an important first step toward appropriate correlation of sections from distant loess  
712 provinces. Nonetheless, they also provide a missing link for a better understanding of temporal and  
713 spatial environmental reconstructions during the Quaternary Period.

714

715 **Environmental Magnetism in Quaternary Loess Deposits**

716 Ulrich Hambach, Christian Zeeden, Qingzhen Hao, Igor Obreht, and Daniel Veres

717 Introduction and background

718 Iron is the fourth most common element in the Earth's crust and responsible for color in many  
719 geologic deposits. Because of its low energetic thresholds in redox processes, iron is involved in  
720 numerous bio-/geochemical process chains. It also belongs to the transition elements which exhibit  
721 para- and ferromagnetism (s. l.). The combination of these properties makes iron a key tracer and  
722 witness of environmental processes, and forms the base of rock, environmental, and paleomagnetism.

723 Since the seminal work of Friedrich Heller and Tungscheng Liu (Heller and Liu, 1982, 1984),  
724 environmental magnetic parameters have been recognized as fundamental paleoclimate proxies for  
725 Eurasian loess-paleosol sequences (LPS; see Marković, this paper). Later, George Kukla and Zhisheng An  
726 (Kukla et al., 1988; Kukla and An, 1989) further employed low field magnetic susceptibility (MS) as a  
727 stratigraphic tool, facilitating correlations between terrestrial deposits and the marine record; the latter  
728 is based on oxygen-isotope data for oceanic foraminifera, which in turn is a proxy for global ice volume  
729 (Lisiecki and Raymo, 2005). This early work demonstrated that MS, combined with magnetic polarity  
730 stratigraphy, provides a critical temporal framework for LPS. Later work confirmed that the MS record  
731 closely parallels the oxygen-isotope fluctuations in deep-sea sediments, suggesting a close  
732 interconnection between dust deposition on the Chinese Loess Plateau (CLP), global ice volume, and  
733 global climate (compare Figure 15, a&b). Since then, MS, a nondestructive and inexpensive  
734 measurement, has become a widely applied paleoclimatic proxy and correlation tool in the study of LPS  
735 worldwide (e.g., Guo et al., 2002, 2009; Hao et al., 2012; Heslop et al., 2000; Marković et al., 2011, 2015;  
736 Necula et al., 2015; Sun et al., 2006; Zeeden et al., 2016).

737 MS records from geochemically and mineralogically quite homogenous loess deposits provide a  
738 first order chronostratigraphic link between these terrestrial dust archives and the marine and lacustrine  
739 record, potentially resolving orbitally paced climatic variability since the Neogene (Guo et al., 2002; Hao  
740 and Guo, 2004; Heller and Liu, 1984). Precipitation controls soil moisture variations, which in turn are a  
741 first-order control for diagenesis and pedogenesis in terrestrial dust deposits. Moisture governs the  
742 geochemical process chains from silicate weathering of detrital eolian grains up to the neo-formation of  
743 magnetically highly effective Fe-oxide minerals, whose concentration and particle size in loess and

744 paleosols eventually reflect past climate variations (Bugge et al., 2014; Heller et al., 1991).  
745 Unweathered (primary) loess consists predominantly of silt-sized, silicate minerals, with variable  
746 amounts of detrital carbonate (e.g., Maher, 2016; Muhs, 2013a). Upon deposition, the loess undergoes  
747 “loessification”, a process involving initial silicate weathering, partial carbonate dissolution and re-  
748 precipitation, and neo-formation of clay minerals (Sprafke and Obrecht, 2016). Loessification also  
749 controls the geochemical dynamics of iron (Fe) and in so doing, influences the color and magnetic  
750 properties of the loess (Maher, 2011). Changes in moisture, accompanied by biological activity, both  
751 directly linked to global/regional climate conditions, lead to carbonate dissolution and silicate  
752 weathering; these pedogenic processes largely reflect global and regional variations in the hydroclimate  
753 regime (Maher, 2016).

754 In environmental magnetic studies, low-field or initial MS signal is usually determined at  
755 ambient temperatures, in low AC-fields of a few hundred A/m, and at different frequencies ranging from  
756 a few hundred to thousands of Hz (Evans and Heller, 2003). MS and its dependence on the frequency of  
757 the applied magnetic field ( $MS_{fd}$ ) provide highly sensitive proxies of climate conditions during loess  
758 accumulation (Bugge et al., 2014). This signal is first, based on the mineralogical homogeneity of the  
759 original dust/loess, and secondly, on the subsequent neo-formation of ferrimagnetic minerals during the  
760 course of silicate weathering and pedogenesis. Thus, intense pedogenesis leads to enhancement of the  
761 mineral magnetic signal (Figure 16). Ultimately though, the MS value of a given magnetic assemblage in  
762 a LPS depends on the concentration and composition of the mineral grains, as well as their particle size.  
763 Magnetic mineral particles reveal magnetic domain structures, with each domain being spontaneously  
764 magnetized to saturation. Particles may consist of a single domain (SD) or multiple domains (MD)  
765 depending on particle size, composition, and internal mineralogical structure. SD particles are either  
766 super-paramagnetic (SP) with high MS or stable SD (SSD) with low MS. The MS of MD-particles,  
767 however, is again higher without reaching the level of the SP-state (Evans and Heller, 2003; Zeeden et  
768 al., in press). Hence, it is not sedimentary particle size but the magnetically effective domain state of a  
769 particle which controls its magnetic properties (Bugge et al., 2014; Liu et al., 2012). The highest MS  
770 values occur in horizons containing higher concentrations of ultra-fine particles covering even the SP-  
771 SSD threshold. SP-particles mainly precipitate in situ, from soil moisture controlled weathering solutions;  
772 their abundance provides therefore a sensitive proxy for sediment and soil humidity (Gao et al., 2018;  
773 Heller et al., 1991; Maher, 2011; Song et al., 2014; Zeeden et al., in press).

774 Beside MS, the user can also utilize a range of mineral magnetic parameters and interparametric  
775 ratios. In addition to specific hysteresis parameters, laboratory induced remanences and their  
776 dependence on temperature can be employed. Although yielding valuable information, they are less  
777 frequently applied, as they are generally time-consuming to determine (Liu et al., 2012; Maher, 2011).

778

779 MS as the stratigraphic backbone in Eurasian loess deposits

780 In Eurasian loess deposits, MS is usually enhanced in paleosols, as compared to primary loess  
781 (Evans and Heller, 2003). This characteristic is explained by the neo-formation of ultrafine magnetic  
782 particles during pedogenesis (Chinese enhancement model; Heller et al., 1991). Figure 16 illustrates the  
783 magnetic enhancement trend for the Semail LPS (recent to  $\approx 400$  ka; SE Pannonian Basin, Romania). MS  
784 increases here are attributed solely to pedogenesis, via the increase of ultra-fine particles extending into  
785 the SP-SSD threshold interval (20-40 nm). As this threshold decreases with increasing frequency of the  
786 magnetic field, the relative amount of newly formed ultra-fine particles can be determined by the  
787 dependence of MS on the applied frequency (here:  $\chi_{\Delta}$ ; Figure 16 (Liu et al., 2012). Therefore, the  $MS_{fd}$  is  
788 also a valuable and sensitive parameter for incipient soil formation. The interception of the trend line  
789 with the ordinate defines the background susceptibility of raw unweathered loess, which fits well to the  
790 average value determined for Eurasian loess by Forster et al. (1994). In contrast to this generally  
791 accepted explanation for magnetic enhancement in LPS, lowered values of MS in paleosols in high  
792 latitude Alaskan and Siberian loess deposits have been explained by increased wind strength during  
793 glacial periods, which more efficiently transports dense iron oxide particles (wind-vigor model; e.g.  
794 Begét et al., 1990; Evans, 2001). This process, however, is generally inconsequential in controlling  
795 climate-induced variations in MS on the mid latitude Eurasian loess steppes (Buggle et al., 2014).  
796 Likewise, pervasive hydromorphy as the result of water-logged conditions, leading to a reduction of MS  
797 by the dissolution of magnetic particles, is also not a factor in the dry Eurasian steppes, as it might be  
798 elsewhere, especially in the potentially waterlogged Arctic tundra. In summary, loss of magnetic signal in  
799 soils/paleosols, due to waterlogging, is mainly observed in loess from areas affected by periglacial  
800 conditions (Baumgart et al., 2013; Matasova et al., 2001; Taylor et al., 2014).

801 Mineral magnetic patterns in LPS records are fairly concordant throughout Eurasia, at least on  
802 glacial-interglacial time scales. These records show high similarities to oxygen-isotope fluctuations in  
803 deep-sea sediments, and even to the Greenland and Antarctic ice records (Guo et al., 2009; Lambert et  
804 al., 2008; Marković et al., 2015). Such well-expressed linkages are not found to the same extent for loess  
805 or loess-like deposits from other continents, and we therefore focus here on Eurasia. Moreover, on the  
806 CLP, strongly altered and dominantly eolian silt deposits date back to the early Miocene; no equivalent  
807 has yet been found in western Eurasia and on other continents. Nevertheless, the eolian Red-Earth  
808 sequence (also referred to as Red-Clay) in China provides an outstanding paleoclimatic archive for  
809 eastern Eurasia. It has been dated by magnetic polarity and MS stratigraphy, and defines the onset of  
810 desertification in Asia as early as 22 Ma (Guo et al., 2002).

811 The robust correlations between the LPS of Europe and the CLP are of major relevance for  
812 understanding the temporal and spatial variability in paleoclimate within Eurasia (Bronger, 2003;  
813 Marković et al., 2015). Several recent publications have correlated southeastern European LPS with the  
814 CLP, although leaving some inconsistencies (Basarin et al., 2014; Buggle et al., 2009; Marković et al.,  
815 2015; Song et al., 2017). Nonetheless, the studies provide valuable reference records with correlative  
816 age control. In Figure 15 (A) we provide a comparison of established Quaternary paleoclimatic reference  
817 datasets, the LR04 benthic isotope stack (Lisiecki and Raymo, 2005), the Imbrie and Imbrie (1980) ice  
818 model, and a mixture of orbital parameters (Laskar et al., 2004) with the loess MS records from Europe  
819 (Basarin et al., 2014) and China (Hao et al., 2012). In both cases, MS was the primary proxy utilized for  
820 correlation. Over this long glacial-interglacial time scale, where loess units (L) and soil complexes (S)  
821 alternate in the sedimentary profiles, the MS records of LPS from the CLP and southeastern Europe  
822 exhibit similar patterns and amplitudes (Fig. 15). However, prior to ~500 ka the MS record of paleosols in  
823 the CLP shows less amplitude, whereas for European LPS, the amplitude remains similar (e.g., Heslop et  
824 al., 2000; Marković et al., 2015; Necula et al., 2015; Sun et al., 2006). Moreover, it has been suggested  
825 that the Danube Basin in southeastern Europe experienced progressive continentalization throughout  
826 the Middle Pleistocene (Buggle et al., 2013). On the one hand, such sub-continental scale climatic  
827 differentiations additionally complicate the inferred cross-continental correlation among LPS. On the  
828 other hand, if these areas of difference can be better understood, they would allow for deeper insights  
829 into the regionally differentiated past climatic evolution of Eurasia, an issue that has only marginally  
830 been explored to date (Obrecht et al., 2016).

831 MS records resolving millennial scale climatic fluctuations

832           Using Eurasian loess deposits to resolve millennial-scale climate variability is a compelling  
833 research topic, as such deposits had previously been considered too dry to reflect short-term variability  
834 in hydroclimate such as that associated with Greenland stadial-interstadial climate variability.  
835 Nonetheless, Yang and Ding's (2014) data on millennial-scale climatic fluctuations, based on grain-size  
836 records across the CLP, revealed a close match to isotopic records of temperature contained in ice cores  
837 and speleothems and sea surface temperature records. For the western end of the Eurasian loess belt,  
838 Zeeden et al. (in press) and Obreht et al. (2017) recently provided the first multi-site high-resolution MS  
839 and MS<sub>fd</sub> records for the last 50 ka. Figure 15B shows the comparison of Greenland  $\delta^{18}\text{O}$  data (North  
840 Greenland Ice Core Project Members et al., 2004) and the MS<sub>fd</sub> data from SE Romania. This work  
841 highlighted the quality and resolution of paleoenvironmental data which can be extracted from  
842 European loess via mineral magnetic methods. It is evident from these studies that grain size and MS<sub>fd</sub>  
843 can sometimes provide powerful and fine-structured proxy information.

844 Magnetic fabric in loess

845           MS in loess deposits has one additional application. Directional measurements of MS on  
846 oriented samples are used for fabric analyses in LPS. The AMS (anisotropy of magnetic susceptibility)  
847 method is an established structural indicator even in unconsolidated geological materials (Parés, 2015).  
848 Magnetic fabric can be correctly approximated by a second-order symmetric tensor and fabric  
849 magnitude (i.e., degree of anisotropy) and fabric shape (i.e., prolate or oblate). Additionally, the  
850 orientation of principal axes of AMS ellipsoids ( $k_{\max}$ ,  $k_{\text{int}}$ ,  $k_{\min}$ ) can be used for fabric characterization and  
851 quantification (Tarling and Hrouda, 1993).

852           AMS data has its largest applicability in estimating near-surface paleo-wind directions and even  
853 wind intensity (Lagroix and Banerjee, 2004; Zhu et al., 2004; Ge et al., 2014). Additionally, their temporal  
854 evolution can also be reconstructed from loess by such data (Taylor and Lagroix, 2015; Zeeden et al.,  
855 2015). The AMS technique has successfully been applied to western Eurasian (Bradák, et al., 2018;  
856 Nawrocki et al., 2006;) as well as to Chinese and Siberian loess deposits (Liu and Sun, 2012; Matasova et  
857 al., 2001), further illustrating the wide application of loess magnetic properties to paleoenvironmental  
858 research.



859 **Geochemical Approaches to the Study of Loess**

860 E. Arthur Bettis III

861           Geochemistry of loess sediment can be a powerful tool for understanding its origins, transport  
862 pathways and post-depositional alteration. Loess provides a broad, continental-scale sample of the  
863 Earth's upper continental crust (Taylor et al., 1983; Liu et al., 1993; Gallet et al., 1998; McLennan, 2001).  
864 Importantly for loess studies, loess geochemistry varies at subcontinental scales, reflecting variations in  
865 source rock types, alteration along transport pathways, and trends in post-depositional weathering;  
866 these data may provide important insights into paleoclimate, periods of pedogenesis, and other aspects  
867 of Quaternary history. Three primary approaches, sometimes in combination, are used to investigate  
868 loess geochemistry, namely concentrations of: 1) major elements, 2) immobile trace elements (Sc-Th-La-  
869 Zr), and 3) rare earth elements (REE). These data are determined most commonly using X-ray  
870 fluorescence spectrometry (XRF), although inductively coupled plasma-atomic emission spectrometry  
871 has also been used. The use of portable x-ray fluorescence devices, both in the field and benchtop is on  
872 the rise, but more studies of their performance relative to traditional laboratory XRF are needed to  
873 ensure the production of comparable data sets.

874           Major element concentrations in loess reflect the mineral suite present in the sediment.  
875 Bivariate plots of co-occurring elements or elemental oxides' concentrations are often used to display  
876 compositional differences between loess bodies derived from different source rocks or mixtures of  
877 source rocks (Grimley, 2000; Muhs et al., 2003; 2008a; Ujvari et al., 2008). Concentrations of  $\text{Al}_2\text{O}_3$  and  
878  $\text{Fe}_2\text{O}_3$  are often positively correlated because minerals common in loess, such as some smectites and  
879 chlorite, are relatively rich in Al and in Fe. Loess from different regions or source areas are often  
880 distinguishable by plots of such data, because of variations in source rock mineralogy, as illustrated by a  
881 midcontinent United States example (Bettis et al., 2003). In this example, loess from Indiana plots low on  
882 a  $\text{Fe}_2\text{O}_3/\text{Al}_2\text{O}_3$  diagram (Figure 17 a) primarily because of dilution by high amounts of CaO and MgO  
883 (Figure 17b), reflecting significant contributions of calcite and dolomite from carbonate rocks. As  
884 carbonate contributions to the loess decrease from Indiana westward into the Central Plains of  
885 Nebraska, loess data plot higher and farther to the right on the iron/aluminum diagram, and display a  
886 reverse trend on the Mg/Ca diagram.



887           Although loess is dominated by silt-size particles, it does have a range of particle sizes, and these  
888 various size fractions can have potential mineralogical variability that a geochemical study of the “whole  
889 rock” misses. Studies by Eden et al. (1994) and Yang et al. (2006) demonstrated that mineralogy, and  
890 thus geochemistry, varies between different particle-size classes in loess, and that it is therefore  
891 important to understand both the particle-size distribution and the mineralogy of a loess body before  
892 confidently interpreting its geochemistry. Given the likely relationship between loess particle size and  
893 mineralogy, one would expect that geochemical variations within a loess body would also occur along a  
894 transport pathway from a source area. For example, Peoria Loess in western Iowa, USA exhibits  
895 increasing  $\text{Al}_2\text{O}_3$  and  $\text{Fe}_2\text{O}_3$  concentrations with increasing distance from its Missouri River Valley source,  
896 because sand content (a major contributor to  $\text{SiO}_2$  concentrations) decreases as clay contents  
897 (dominantly smectite) increase downwind from this approximately linear source area (Muhs and Bettis,  
898 2000).

899           Paleosols are important components of many loess sequences and they can provide  
900 paleoenvironmental information about periods when loess accumulation was slow or stopped.  
901 Comparing abundances of soluble oxides of major elements (e.g., CaO, MgO,  $\text{Na}_2\text{O}$ ,  $\text{K}_2\text{O}$ ) with  
902 abundances of relatively immobile element oxides (typically  $\text{TiO}_2$  or  $\text{ZrO}_2$ ) is one way to evaluate the  
903 relative degree of weathering in sediment. Muhs et al. (2001) used this approach to demonstrate that  
904 the geochemistry of modern soils formed in loess along the Mississippi River Valley varies systematically  
905 with climate. In a study of the long loess-paleosol record from the Chinese Loess Plateau at Lingtai, Yang  
906 et al. (2006) developed a chemical weathering index,  $(\text{CaO}+\text{MgO}+\text{Na}_2\text{O})/\text{TiO}_2$  to evaluate long-term  
907 trends in loess alteration and found greater mineral weathering during the previous five interglacials  
908 than during the present interglacial. They found evidence for greater weathering of both loess and  
909 intervening paleosols prior to the mid-Pleistocene. They attributed this trend to greater prevalence of  
910 colder and drier conditions that fostered less weathering in the loess source areas since the mid-  
911 Pleistocene.

912           Trace element geochemistry is also an important tool for loess provenance studies (Bugge et al.,  
913 2008; Jahn et al., 2001; Sun, 2002a & b; Muhs et al. 2007; Muhs et al., 2016; Hu and Yang, 2016).  
914 Elements commonly used are those with low mobility in near-surface, low-temperature environments:  
915 Cr, Sc, Ta, Th, Zr, Hf, As, Sb, Y, the rare earth elements (REE) La to Lu, as well as Ti, a minor element. The

916 Sc-Th-La suite of elements is one of the most useful, and these data are usually plotted as a ternary  
917 diagram (Taylor and McLennan, 1985). Muhs et al. (2007, 2008c) used this approach to demonstrate  
918 that silts in loess mantles on the California Channel Islands have trace element concentrations more like  
919 granitic terrain sources of the Mojave Desert (mainland California), than the trace element  
920 concentrations characteristic of the islands' andesite and basalt bedrock. Clays in these soils, on the  
921 other hand, fall between the fields of Mohave dust and those of the local bedrock, suggesting that the  
922 loess clay minerals represent a mixture of clays formed in-situ, as well as clays from distant sources.

923 Rare earth elements (REE) also have low mobility under near-surface conditions, but have an  
924 advantage over other trace elements for loess provenance studies because they occur in both heavy and  
925 light minerals. Thus, they can provide information about both proximal and distal eolian sources. REE  
926 plots typically use abundances normalized to chondritic meteorites. "Flat" REE curves normalized in this  
927 manner, can distinguish little differentiated oceanic crust sources from upper continental crust sources,  
928 which exhibit enrichment of light REE and depletion of heavy REE. The sign and degree of the Eu  
929 "anomaly" provides additional insights into differentiating these sources (Taylor and McLennan, 1985).  
930 Sun (2002a and b) used REE and other geochemical and mineralogical data to isolate potential distal  
931 sources of Chinese Loess Plateau sediments and concluded that likely sources for the Loess Plateau are  
932 silts deflated from alluvial fans flanking the Qilian Mountains in China and the Gobi Altay and Hangayan  
933 Mountains in Mongolia.

934 As these few examples indicate, geochemical approaches can provide insight into a wide range  
935 of loess topics, including source area identification and differentiation, paleoclimatic patterns and  
936 weathering profile evolution. Multi-parameter approaches and the spread of new technologies such as  
937 portable X-ray fluorescence will continue to advance loess geochemical studies that help us better  
938 understand loess systems and sediments.

939

#### 940 **The "Spatial Signatures" Approach to Loess Research**

941

942 Randall J. Schaetzl

943           Loess deposits represent some of the world’s best terrestrial archives of paleoenvironmental  
944 information. The loess itself is a storehouse of information for the period of deposition, and any  
945 intercalated paleosols or weathering profiles can provide data on intervening periods of nondeposition  
946 (or slowed deposition) and soil formation. Knowing this, much has been learned about past terrestrial  
947 environments by studying thick loess deposits, many of which have several intercalated paleosols and  
948 span more than one glacial-interglacial or dry-moist cycle of the Quaternary Period (Heller et al., 1993;  
949 Rousseau and Kukla, 1994; Akram et al., 1998; Buggle et al., 2009; 2011; Marković et al., 2009). Put  
950 another way, thick loess sequences often provide important *temporal* environmental proxy data at a  
951 given location or within a given region (Muhs and Bettis, 2000). In some areas, most of the loess deposit  
952 dates mainly to the last glaciation, or at least to only one instance of recent deposition, e.g., Gild et al.  
953 (2017). Here, this type of “deep” temporal exploration is not possible, or at least less fruitful than in  
954 areas of thick loess that spans more geologic time.

955           All loess, regardless of thickness, can provide investigators with an opportunity to peer into the  
956 spatial variation *across* past landscapes. In other words, thinner loess deposits may not provide insight  
957 into multiple past environments, but by examining the same deposit spatially, information on various  
958 environmental aspects of that landscape while the loess was being deposited can be gained. Although  
959 not commonly performed, similar exploration of spatial trends are possible in thicker loess deposits that  
960 span multiple climate cycles.

961           Indeed, loess is one of the best deposits to examine for spatial patterns and information. Loess  
962 has long been known to become thinner and finer-textured away from the source area (Smith, 1942;  
963 Ruhe, 1954; 1973; Fehrenbacher et al., 1965; Frazee et al., 1970; Kleiss 1973). Mineralogical changes  
964 within the same loess deposit, but across space, are also often predictable and insightful as to  
965 provenance (Muhs and Bettis, 2000; Bettis et al., 2003; Buggle et al., 2008; Chen et al., 2007). Such  
966 information is often developed by studying loess deposits across space, knowing *a priori* the loess  
967 source(s). By knowing which spatial trends in loess deposits are most informative, subsequent work can  
968 then examine the spatial properties of such data, for loess with “less certain” paleoenvironmental  
969 histories. This research has done much to elucidate new loess source areas, refine our understanding of  
970 loess transport systems, and even determine the strength and directional properties of paleowinds  
971 (Stanley and Schaetzl, 2011; Luehmann et al., 2013; 2016; Schaetzl and Attig, 2013; Martignier et al.,

2015; Nyland et al., 2017; Schaetzl et al., 2017; Muhs et al., this issue). In summary, much can be learned about loess deposits by studying their spatial properties.

Historically, researchers have typically examined the spatial properties of loess deposits along transects, (e.g., Frazee et al., 1970; Rutledge et al., 1975; Handy, 1976; Muhs and Bettis, 2000; Martignier et al., 2015; Fig. 18). This early work helped the loess community to understand the distribution of dust from a source, and the processes involved in its generation, transport, and accumulation. Recent work by Schaetzl and colleagues (Scull and Schaetzl, 2011; Stanley and Schaetzl, 2011; Luehmann et al., 2013; 2016; Schaetzl and Attig, 2013) has expanded upon this approach by obtaining loess samples across spatial grids, some of which may include several hundred samples. Typically, these samples are analyzed for grain size and thickness data; future work is likely to include mineralogy and elemental geochemistry data as well. A GPS or a GPS-ready, laptop computer can be used to provide geospatial data for each sample site. Samples are routinely taken with a bucket auger, being careful to obtain some sediment from the entire length of the auger, i.e., the full vertical thickness of the loess deposit must be incorporated into the sample. Lastly, it is suggested that sampling loess within 10-20 cm of any underlying lithologic discontinuity be avoided, as there exists the potential for mixing and contamination (Schaetzl and Luehmann, 2013). Data obtained from the loess, which are presumed to represent loess that was deposited during a discrete time interval, allow the investigator to tease out patterns that can then be used to infer dust source areas or paleowind directions (Schaetzl et al., this issue). Simple characterization techniques such as isoline interpolation or graduate circle symbols are useful for data exploration and interpretation, although more advanced applications such as kriging and inverse distance weighting methods are also commonly applied to such data (Fig. 19).

In summary, much can be gleaned from loess data, when examined spatially. Loess is a highly “spatially organized” deposit, innately lending itself to sampling and analysis across space (landscapes). Although still in its infancy, the spatial signatures, or spatial analysis, approach to loess research discussed here has great potential for future studies of loess depositional and paleoenvironmental systems.

998

**999 Biomarkers and Stable Isotopes in Loess as Paleoenvironmental Indicators**

1000 Michael Zech and Roland Zech

1001           The last few decades have seen considerable advances in biogeochemical analytical techniques,  
1002 e.g., gas chromatography (GC), high performance liquid chromatography (HPLC) and isotope ratio mass  
1003 spectrometry (IRMS). These techniques have enabled investigators to study organic molecules, and their  
1004 stable isotopic composition preserved in various sedimentary archives, as new and valuable proxies for  
1005 paleoenvironmental and climate change. When those organic molecules have more or less specific  
1006 sources, e.g., they are leaf wax or bacterially-derived, they are called biomarkers or molecular fossils  
1007 (Eganhouse 1997, Eglinton and Eglinton 2008). Although biomarker and stable isotope tools have been  
1008 often employed by organic geochemists in the study of marine and lacustrine sediments, applications of  
1009 these methods to loess research have only recently begun (Zech et al. 2011). Concerning the origin of  
1010 bulk organic matter as well as of individual biomarkers in loess, neither a partial contribution by far and  
1011 middle distance aeolian transport nor a partial contribution by postsedimentary illuviation processes nor  
1012 postsedimentary ‘contamination’ by roots/(rhizo-)microbial input can be fully excluded. Hence, such  
1013 processes need to be carefully considered and evaluated as exemplarily highlighted for leaf wax-derived  
1014 *n*-alkanes at the end of the third paragraph.

1015           Amino acids of land snails embedded in loess deposits were among the first loess-associated  
1016 organic molecules investigated (Oches and McCoy 2001). The time-dependent racemization of amino  
1017 acids is used as geochronometer by quantifying the D-enantiomers that have formed from L-  
1018 enantiomers. One of the recent biomarker approaches used in loess research focusses on glycerol dialkyl  
1019 glycerol tetraethers (GDGTs), which are membrane lipids of soil bacteria. These markers can be used to  
1020 reconstruct mean annual temperature and soil pH from loess-paleosol sequences (Jia et al. 2013,  
1021 Schreuder et al. 2016). However, one should keep in mind potential pitfalls of GDGT-based  
1022 reconstructions. For three case studies of well-studied loess-paleosol sequences, Zech R. et al. (2012)  
1023 found major disagreements between GDGT-based temperature reconstructions, as compared to  
1024 expectations based on available stratigraphic, pedological and geochemical data. This finding is in  
1025 agreement with a climate transect study of Dirghangi et al. (2013) reporting that the GDGT-method only  
1026 produces reliable results in humid study areas with mean annual precipitation values > 700-800 mmyr<sup>-1</sup>.

1027           During the last decade, the quantification of the leaf wax-derived long-chain *n*-alkanes *n*C<sub>27</sub>,  
1028 *n*C<sub>29</sub>, *n*C<sub>31</sub> and *n*C<sub>33</sub> from loess sediments has emerged as a potential tool for reconstructing vegetation

1029 changes. Well-preserved *n*-alkanes in the organic matter of loess deposits are mostly interpreted in  
1030 terms of expanding grassland versus forest, respectively (Zhang et al. 2006, Bai et al. 2009, Zech et al.  
1031 2009). It has to be emphasized that such a differentiation based on *n*-alkane patterns does not  
1032 necessarily work on a global scale (Bush and McInerney 2013), and therefore regional calibration studies  
1033 on modern plants may be necessary, as shown by the work of Schäfer et al. (2016b) in Europe. Further  
1034 issues needing consideration are variable *n*-alkane concentrations of different vegetation types,  
1035 potential degradation effects, and the effects of post-sedimentary root or rhizomicrobial sources.  
1036 Gymnosperms yield mostly significantly lower *n*-alkane abundances compared to angiosperms  
1037 (Diefendorf et al. 2011). Although this issue makes the *n*-alkane method insensitive for reconstructing  
1038 conifers (Zech M. et al. 2012), it might be overcome in future studies by investigating additional  
1039 terpenoid and terpenoid-derived biomarkers such as retene and cadalene (Bugge and Zech 2015), as  
1040 well as *n*-alkanoic acid (Schäfer et al. 2016a,b). Concerning degradation effects on *n*-alkane patterns,  
1041 two possible correction procedures were suggested by Bugge et al. (2010) and Zech M. et al. (2009,  
1042 2013a). There is also a discussion as to whether *n*-alkane biomarkers in loess sequences are significantly  
1043 affected by post-depositional root and rhizomicrobial sources, e.g., Wiesenberg and Gocke (2013) vs.  
1044 Zech M. et al. (2013b). This controversy stimulated compound-specific as well as bulk *n*-alkane <sup>14</sup>C dating  
1045 in loess research. Accordingly, comparisons of *n*-alkane <sup>14</sup>C results with independent luminescence  
1046 dating corroborate the stratigraphic integrity of the leaf-wax-derived *n*-alkane biomarkers in loess  
1047 deposits (Häggi et al. 2014, Haas et al. 2017, Zech et al. 2017). Moreover, <sup>14</sup>C dating of bulk leaf waxes,  
1048 which is a relatively straightforward procedure, might become a valuable chronological tool in loess  
1049 research.

1050 By about 1990, the online coupling of elemental analysis with isotope ratio mass spectrometry  
1051 (EA-IRMS) had facilitated the stable carbon ( $\delta^{13}\text{C}$ ) and nitrogen ( $\delta^{15}\text{N}$ ) isotope analysis of soil and  
1052 sediment samples. This is achieved by converting the sample carbon and nitrogen into CO<sub>2</sub> and N<sub>2</sub> in a  
1053 reactor and subsequent transfer of those gases into the IRMS using helium (He) as a carrier gas. Given  
1054 that the  $\delta^{13}\text{C}$  values of plants vary according to photosynthetic pathway, this tool can be applied in loess  
1055 research to reconstruct C3 and C4 vegetation changes (Liu et al. 2005, Hatté et al. 2013, Zech R. et al.  
1056 2013). Potentially challenging issues to be kept in mind are methodological constraints caused by biases  
1057 during acid pre-treatment, when removing carbonates from loess samples (Brodie et al. 2011), as well as  
1058 degradation effects (Zech et al. 2007), sedimentation of reworked and/or transported organic matter,

1059 and illuviation and root contamination. Like the  $\delta^{13}\text{C}$  composition of bulk organic material,  $\delta^{15}\text{N}$  in soils  
1060 and sediments is also affected by degradation (Zech et al. 2011). The few studies that have applied  $\delta^{15}\text{N}$   
1061 to loess deposits therefore have tentatively interpreted the results in terms of a more open versus more  
1062 closed nitrogen (N-)cycle (Schatz et al. 2011, Zech R. et al. 2013, Obrecht et al. 2014).

1063           The large potential for the application of stable hydrogen ( $\delta^2\text{H}$ ) and oxygen ( $\delta^{18}\text{O}$ ) isotopes in  
1064 paleoclimatology is based on the finding that the isotopic composition of precipitation is mainly  
1065 climatically controlled (Dansgaard 1964, Rozanski et al. 1993). Although applications of this method to  
1066 ice cores, speleothems, and lacustrine archives have boosted our understanding of paleoclimate during  
1067 the last decades, applications to loess were hindered because loess and the buried soils within are  
1068 complex from a chemical point of view, comprising a variety of H and O pools. Even worse, some of  
1069 those pools are prone to exchange reactions with percolating water. In a pioneering study, Liu and  
1070 Huang (2005) applied compound-specific  $\delta^2\text{H}$  analyses of leaf wax-derived *n*-alkanes to loess deposits.  
1071 Follow-up studies corroborated that a robust reconstruction of the isotopic composition of  
1072 paleoprecipitation ( $\delta^2\text{H}_{\text{prec}}$ ) is hindered by unknown isotopic enrichment of leaf water due to variable  
1073 evaporative enrichment (Zech R. et al. 2013). Meanwhile, it has become increasingly clear that  $\delta^2\text{H}$  of *n*-  
1074 alkanes in soils and sediments reflect leaf water rather than precipitation (Zech et al. 2015). The same  
1075 holds true for  $\delta^{18}\text{O}$  of plant-derived sugar biomarkers (Tuthorn et al., 2014). This latter new method,  
1076 developed by Zech and Glaser (2009), has been successfully applied to organic-rich permafrost loess-  
1077 paleosol sequences and lake sediments (Zech M. et al. 2013c, 2014), and awaits adaptation to organic-  
1078 poor loess.

1079           The coupling of the  $\delta^2\text{H}_{\text{n-alkane}}$  with the  $\delta^{18}\text{O}_{\text{sugar}}$  biomarker methods has exciting potential for  
1080 paleoclimate research, and particularly, for loess research. First, this coupling has the potential to  
1081 reconstruct  $\delta^2\text{H}/\delta^{18}\text{O}_{\text{prec}}$  much more robustly than a method based on  $\delta^2\text{H}_{\text{n-alkane}}$  or  $\delta^{18}\text{O}_{\text{sugar}}$  alone (Figure  
1082 20). This is realized by tracing back the leaf water evaporation line (EL) until it intersects with the global  
1083 meteoric water line (GMWL). Additionally, the coupling allows for the calculation of paleo relative  
1084 humidity (RH), based on a leaf water enrichment model (Gat and Bowser 1991) and the reconstructed  
1085 so-called deuterium-excess of leaf water. This innovative “paleohygrometer” approach was validated  
1086 recently by Tuthorn et al. (2015) by applying it to modern topsoils along an Argentinean climate



1087 transect, and it was further successfully applied to a Late Quaternary paleosol sequence from Mt.  
1088 Kilimanjaro (Hepp et al. 2017).

1089

1090 **Terrestrial Gastropods in Loess (paleoecology, paleoclimate, geochronology)**

1091 David A. Grimley and Jessica L. Conroy

1092           Gastropod assemblages have been a major component of loess studies for well over a century,  
1093 ever since they were used as key evidence that North American loess deposits have an eolian, rather  
1094 than fluvial, origin (Shimek, 1899). More recently, the presence of land snails has aided in the eolian  
1095 interpretation of Miocene-Pliocene silt deposits in China (Li et al., 2006). Biostratigraphically, mollusks  
1096 have been used to differentiate and characterize loess units (Leonard and Frye, 1960; Rousseau, 2001),  
1097 although only rarely have molluscan species disappeared from Pleistocene geologic record. Rather,  
1098 species have tended to shift geographically in response to climatic and habitat changes, becoming exotic  
1099 rather than extinct (although many are now threatened by human impacts).

1100           Important habitat and ecological inferences are routinely provided by fossil terrestrial gastropod  
1101 assemblages worldwide. For example, their assemblages can reveal whether past landscapes were a  
1102 dense or open woodland, boreal or deciduous forest, steppe-like grassland, or tundra (Miller et al.,  
1103 1994; Marković et al., 2007; Rech et al., 2012). Climatically, many terrestrial gastropods are sensitive to  
1104 temperature and humidity, more so than aquatic gastropod species buffered by lakes or rivers, and can  
1105 thus serve as important proxies for paleoclimate. Land snails are mainly dormant during periods of cold  
1106 temperature, so they are best used as indicators of summer or warm-season climate in mid to high  
1107 latitudes. It was recognized decades ago that many fossil gastropod species in Pleistocene loess (Fig. 21)  
1108 are distinct from local modern faunas and mostly represent cooler glacial or interstadial environments  
1109 (e.g., Baker, 1931). Today, more accurate range maps of terrestrial gastropods (e.g., Nekola and Coles,  
1110 2010, for North America) can provide modern analog distributions and thus better estimates of  
1111 paleoclimate (Moine et al., 2002; Nash et al., 2017). Many examples of climatic (and ecological)  
1112 interpretations from gastropod assemblages in loess-paleosol sequences are reported in Asia (Rousseau  
1113 et al., 2000; Li et al., 2006), Europe (Rousseau, 1991; Marković et al., 2007), and North America



1114 (Rousseau and Kukla, 1994; Rossignol et al., 2004). Such data can fill gaps in the geologic record or can  
1115 complement other terrestrial-aquatic climate records, including pollen, plant macrofossils, insects,  
1116 mammals, and ostracodes (Miller et al., 1994; Karrow et al., 2001).

1117         From a geochronological standpoint, many terrestrial gastropod genera have now been shown  
1118 to be reliable for radiocarbon dating applications, based on dating of modern snails in carbonate-rich  
1119 environments and comparisons with wood and plant macrofossil ages (Pigati et al., 2010, 2013). Various  
1120 tests, including comparisons with independent ages and stratigraphic boundaries in loess (Pigati et al.,  
1121 2013), have confirmed that many small terrestrial genera (when well cleaned of detrital grains and  
1122 secondary carbonate) are statistically accurate or have < 500 years offset from small amounts of old  
1123 carbon; only a few genera should be avoided (Pigati et al., 2010, 2015). For example, *Succinea*, *Catinella*,  
1124 and *Discus*, three genera common to North American loess records (Fig. 21), typically provide accurate  
1125 radiocarbon ages with < 300 years offset (Pigati et al., 2010, 2015). Such success is in large part due to  
1126 the fact that most terrestrial gastropod genera do not readily incorporate old carbon from mineral  
1127 grains into their shells, but rather obtain carbon from plants and the atmosphere.

1128         Beyond the limit of radiocarbon dating (> 50 ka), amino acid racemization studies of gastropod  
1129 shells have been used successfully to provide chronologies for loess units (Clark et al., 1989; Oches and  
1130 McCoy, 2001; Marković et al., 2006; Grimley and Oches, 2015). Early, middle, and late Pleistocene loess  
1131 units, where fossiliferous, can thus be reliably separated, which can be particularly important in regions  
1132 lacking datable volcanic ashes or beds. Although amino acid age estimates have only ~ 20 to 30 %  
1133 precision and include temperature history assumptions, the current use of multiple amino acids (e.g.,  
1134 glutamic acid, aspartic acid) that racemize at different rates is providing more reliable age and  
1135 uncertainty estimates (Kaufman and Manley, 1998; Kosnik et al., 2008). More studies will help to further  
1136 expand molluscan amino chronologies for use in correlating Pleistocene units.

1137         In addition to their utility as chronometers and indicators of past environments, expressed via  
1138 community composition, gastropod shell aragonite holds additional paleoenvironmental information in  
1139 stable isotope ratios of carbon and oxygen (henceforth expressed in standard delta notation,  $\delta^{13}\text{C}$  and  
1140  $\delta^{18}\text{O}$ ). Since the pioneering work of Yapp (1979), gastropod  $\delta^{13}\text{C}$  and  $\delta^{18}\text{O}$  data have been investigated in  
1141 loess deposits across diverse paleoenvironments (e.g., Kehrwald et al., 2010; Yanes et al., 2012;  
1142 Colonese et al., 2013; Yanes, 2015; Banak et al., 2016; Nash et al., 2017). Ideally, shell  $\delta^{13}\text{C}$  values can be

1143 interpreted in the context of changes in gastropod diet between C3 and C4 plants, which may reflect  
1144 changes in local vegetation (Stott, 2002). However, gastropod shell  $\delta^{13}\text{C}$  values are also influenced by  
1145 plant water stress, ingested inorganic carbonate (e.g., limestone), exchange with atmospheric  $\text{CO}_2$ , and  
1146 varying metabolic rates, all of which can complicate interpretations (Zhang et al., 2014; Yanes, 2015).  
1147 Shell  $\delta^{18}\text{O}$  values are controlled by temperature and body water  $\delta^{18}\text{O}$ , which in turn is a function of the  
1148  $\delta^{18}\text{O}$  value of precipitation and atmospheric water vapor, as well as the degree of evaporation, which is  
1149 strongly influenced by relative humidity (Balakrishnan and Yapp, 2004). Despite the seeming complexity  
1150 of shell  $\delta^{18}\text{O}$ , at large spatial scales shell  $\delta^{18}\text{O}$  values largely reflect the  $\delta^{18}\text{O}$  value of warm season  
1151 precipitation (Yanes, 2015). For example, Kehrwald et al. (2010) showed the power of gastropod  $\delta^{18}\text{O}$   
1152 values across large spatial gradients to indicate past atmospheric circulation patterns. Additionally, the  
1153 availability of a straightforward proxy system model for gastropod  $\delta^{18}\text{O}$  (Balakrishnan and Yapp, 2004),  
1154 developed long before the growing popularity and use of such models in other paleoclimate archives  
1155 (Evans et al., 2013), can aid in the interpretation of the climate signal stored in gastropod  $\delta^{18}\text{O}$ . Future  
1156 applications of gastropod stable isotope values for paleoclimate reconstruction will be aided by  
1157 incorporation of this model, as well as comparison with general circulation model simulations of past  
1158 climate (e.g., Eagle et al., 2013; Nash et al., 2017). Finally, studies using clumped stable isotopes (C, O) in  
1159 gastropod shell carbonate as paleothermometers are also ongoing (Eagle et al., 2013) and provide a  
1160 promising avenue of future research.

1161 In sum, terrestrial gastropods are a multi-purpose tool of tremendous value to stratigraphic,  
1162 ecological, chronological, and climatic studies of Pleistocene loess sequences (and even where  
1163 re-sedimented into adjacent lacustrine-wetland records). In the future, high resolution gastropod studies  
1164 and chronologies of glacial and nonglacial loess should help to reveal additional detailed records of  
1165 millennial to centennial variations in sedimentation rates, ecology and climate. Such research may help  
1166 decipher the relationships among finer-scale glacial fluctuations, global and regional climate variability,  
1167 loess sedimentation systems, and incipient paleosol development.

1168

### 1169 **Identifying Abrupt Climate Changes in Loess-Paleosol Sequences**

1170 Denis-Didier Rousseau

1171           Understanding the impacts of atmospheric mineral aerosols (dust) on climate dynamics during  
1172 past glacial periods is a major challenge in modeling the glacial climate (Mahowald et al., 2006). Dust  
1173 content in Greenland ice-cores consistently suggests that atmospheric dynamics were highly variable  
1174 during the last climate cycle (LCC, last 130 kyr), with extremely dusty intervals alternating with non-  
1175 dusty intervals on millennial and shorter timescales. The dust transported to Greenland may have  
1176 originated from Northern Chinese deserts, suggesting that climate variations in these sources reinforced  
1177 or reduced dust emissions. Do other Northern Hemisphere paleodust deposits, exposed to the  
1178 strengthened general atmospheric circulation, also record these abrupt climate changes?

1179           Extensive investigations of European loess along a longitudinal transect at 50°N reveal that the  
1180 millennial-scale climate variations observed in the North-Atlantic marine and Greenland ice-core records  
1181 are well preserved in loess sequences (Rousseau et al., 2007a, 2011, 2017a,b). Among them, the  
1182 Nussloch site, on the right bank of the Rhine valley, yields an important record of the LCC (Antoine et al.,  
1183 2001, 2009b). At this site, the sequence for the interval 45 to 18 ka is exceptionally detailed, and  
1184 supported by an intensive dating effort combining AMS <sup>14</sup>C and luminescence methods (Hatté et al.,  
1185 1999; Lang et al., 2003; Rousseau et al., 2007a; Tissoux et al., 2010; Moine et al., 2017). Alternating  
1186 paleosols and paleodust units (loess) preserved in the LCC record at Nussloch correspond one-to-one  
1187 with Greenland Interstadials (GI - paleosol) and Stadials (GS - paleodust) identified in the Greenland ice-  
1188 cores (Figure 22) (Dansgaard et al., 1993; Johnsen et al., 2001; Moine et al., 2008, 2017; Rousseau et al.,  
1189 2002, 2007a,b, 2017a,b; Antoine et al., 2009b). The morphology of each paleosol observed at Nussloch  
1190 can be related to the duration of the corresponding GIs (Rousseau et al., 2007a, 2017a,b). GI 8, for  
1191 example, the longest interstadial during the 40 ka -15 kyr period, corresponds in the Nussloch  
1192 stratigraphy to a well developed Arctic brown soil, whereas the much shorter GI 3 and 2, among others,  
1193 correspond to tundra gley soils of variable thickness, or to weakly oxidized horizons marked, in part, by  
1194 slightly increased organic contents (Rousseau et al., 2002, 2007a, 2017a,b; Antoine et al., 2009b). Rock  
1195 magnetic investigations (Taylor et al., 2014) of the sediment above the Arctic brown soil at Nussloch  
1196 revealed bands of iron oxide dissolution associated with the formation of tundra gley soils. Iron oxide  
1197 dissolution and the possible iron re-precipitation leading to oxidized horizons represent a diagenetic  
1198 alteration occurring at the base of the active layer, i.e. at the interface with permafrost, during seasonal  
1199 warm and moist intervals. This observation supported the correlation between the paleosols and the GIs

1200 of variable duration, correlations that have been confirmed by recent  $^{14}\text{C}$  dates obtained on earthworm  
1201 calcite granules collected in the paleosols (Moine et al., 2017).

1202           Uncertainties concerning the duration of soil forming intervals pose important chronological  
1203 challenges, especially for interglacial soils in which the upper profile is often eroded. Nevertheless, the  
1204 Arctic brown and tundra gley paleosols do not show evidence of erosion at the outcrops. Furthermore,  
1205 biological remains such as mollusk shells (Moine et al., 2008) and earthworm calcite granules  
1206 (Prud'homme, 2016, 2017), encountered in the upper 10-cm of these paleosols, support the  
1207 interpretation of lack of erosion. This issue is essential to address so that an accurate timescale (Moine  
1208 et al., 2017) can be used for model-data comparisons. Rousseau et al. (2017a) further showed the  
1209 importance of an accurate chronology for correctly estimating the mass accumulation rate (MAR) of the  
1210 sequences for comparison with model estimates, since without a detailed chronology and taking into  
1211 account periods of soil formation, the temporal structure of dust accumulation intervals cannot be  
1212 determined.

1213           The succession of paleosol-loess unit couplets at Nussloch is not unique, but has been observed  
1214 with local and regional variations in sequences ranging from Western Europe eastward to Ukraine  
1215 (Antoine et al., 2009b, 2013; Rousseau et al., 2011, 2017a,b). These paleosol-loess alternations are  
1216 characteristic of the Eurasian loess sequences deposited at about 50°N and higher (North of the Alps  
1217 and the Carpathians); such sequences seem to also exist in Siberia as described by Chlachula et al.  
1218 (2003), Haesaerts et al. (2005) and at lower latitudes in North America (Rousseau et al. 2007) south of  
1219 the last glacial border. Tundra gleys and other indications of permafrost do not occur in southern  
1220 European loess sections but GI – GS forcings may be evident in grain-size or  $\delta^{13}\text{C}$  records in Serbia  
1221 (Antoine et al., 2009a; Hatté et al., 2013; Markovic et al., 2015) and in the Carpathian region (Ujvari et  
1222 al., 2010; Varga, 2011). A pattern similar to the southern European sequences, but without any paleosol  
1223 identified in the LCC, has been identified in grain-size variations in the Chinese loess Plateau  
1224 (Vandenberghe et al., 1997; Vandenberghe, 2003, 2013; Stevens et al., 2006; Sun et al., 2012). In these  
1225 sequences GS corresponds to coarser loess intervals, whereas finer-grained intervals correspond to GI.  
1226 Similar patterns were also observed in cores from the Japan Sea and related to variations in the position  
1227 of the Polar Jetstream as it affected eastward transport of dust particles from east Asian deserts  
1228 (Nagashima et al., 2007, 2011). It is interesting to note that, based on loess data, not only the last glacial

1229 period, but also most of MIS 5 (120-71 ka), experienced several dust episodes at the European scale  
1230 (Rousseau et al., 2013) which are also correlated with abrupt events recorded in the Greenland ice  
1231 cores.

1232           Modeling results point to vegetation changes in response to millennial-scale climate variability  
1233 as a key factor in modulating dust emission (and consequently, also deposition). Model results also point  
1234 to strong seasonality in the annual dust cycle, mainly active in springtime, when the snow cover melts,  
1235 soils begin to thaw, surface winds are still strong (although weaker than in winter), and the surface is  
1236 exposed to wind erosion due to patchy vegetation cover. The colder the climate, the later the emission  
1237 season starts, and the later it ends (about one month delay for a given region between the warmest and  
1238 the coldest simulated climate state, GI vs. Heinrich stadials (Sima et al., 2009, 2013; Rousseau et al.,  
1239 2014)

1240           Understanding how the climate system has operated at both regional and global scales during  
1241 abrupt climatic changes, and at millennial time scales, is a key issue in the last IPCC report (Masson-  
1242 Delmotte et al., 2013). Much emphasis has been given to numerous other classical factors such as  
1243 greenhouse gases and orbital parameters. Paleodust data, however, have been almost neglected  
1244 because of the strong uncertainties associated with the loess paleorecord, uncertainties about its origin  
1245 and transport, and the lack of reliable intercomparisons between models and paleodata. Future  
1246 investigations should attempt to fill this gap.

1247

#### 1248 **“Thin” Loess Deposits**

1249 Randall J. Schaetzl

1250           Most of the world’s best-known loess deposits occur in exposures commonly exceeding meters  
1251 in thickness, thereby providing ready access to the sediment and any intercalated paleosols (Roberts et  
1252 al. 2003; Basarin et al. 2009, Marković et al. 2009, Obrecht et al. 2015). Such deposits are today readily  
1253 recognized as loess, and have proven to be valuable, land-based, paleoenvironmental archives (Lu and  
1254 An 1998, Ding et al. 1993, 1999, Miao et al. 2007, Buggle et al. 2009, Yang and Ding 2014, Marković et al.

1255 2015). Less studied but perhaps more widespread are thinner and/or discontinuous loess deposits. For  
1256 the purposes of this section, I define thin loess deposits as those <2 m in total thickness (Fig. 1A).

1257         Thin loess deposits are part of a continuum from thicker loess deposits to deposits so thin and  
1258 intermixed with the underlying sediment as to be initially unrecognizable (Yaalon and Ganor 1973, Muhs  
1259 2013., Luehmann et al. 2016). Therefore, in the past, many such thin loess deposits went unrecognized  
1260 or misinterpreted. Although much research on thin loess deposits has been focused in the east-central  
1261 USA (Rutledge et al. 1975, Carey et al. 1976, Foss et al. 1978, Schaetzl. and Loope 2008, Stanley and  
1262 Schaetzl 2011, Jacobs et al. 2012, Luehmann et al. 2013, 2016, Schaetzl and Attig 2013), thin loess  
1263 deposits occur worldwide, e.g., Litaor 1987, Hesse and McTainsh (2003), Muhs and Benedict (2006),  
1264 Greene et al. (2009), Lehmkuhl et al. (2014), Gild et al. (2017), Waroszewski et al (2017).

1265         Most commonly, thin loess deposits represent the end member of a loess sheet/deposit that is  
1266 much thicker nearer to its primary source area. The thinning patterns of many loess sheets are well  
1267 known, and can be predicted using statistical models (Fehrenbacher et al. 1965, Frazee et al. 1970, Kleiss  
1268 1973, Ruhe 1973). By recognizing thin loess deposits as the distal “end members” of thicker loess  
1269 deposits, the thinning and fining trends of loess may be more accurately described and analyzed. Some  
1270 thin loess deposits, on the other hand, represent locally sourced sediment that has no association with a  
1271 “thick end member” (Schaetzl 2008, Luehmann et al. 2013). Source regions for such loess deposits may  
1272 have been short-lived, small in areal extent, or simply low overall dust producers.

1273         For many, the identification of thin loess deposits has proven to be problematic. Normally, the  
1274 silty textures and pale colors help to identify loess, where present in thick deposits. But thinner loess is  
1275 often intermixed with the underlying sediment, sometimes making a clear assessment based on texture  
1276 ambiguous (Schaetzl and Weisenborn 2004, Schaetzl 2008, Nyland et al. 2017). Methods used to identify  
1277 loess in thin deposits include (1) changes in texture, often from fine-grained, usually silty, textures in the  
1278 loess to different textures below (These changes are easiest to interpret where the lithologic contact  
1279 and texture changes are sharp, and especially where the underlying sediment contains coarse  
1280 fragments), (2) the presence of quartz or illite (mica) in soils/sediments that have otherwise formed on  
1281 quartz- and mica-free rocks such as basalt, e.g., Rex et al. (1969), (3) different values of quartz oxygen  
1282 isotope ratios or Ti/Zr ratios between the loess and the underlying substrate, as well as (4) distinct and  
1283 regular changes in loess particle size across the landscape (Hesse and McTainsh 2003, Muhs 2013b).

1284 Usually, for 1-3 above, data are plotted as depth functions in order to note changes in one or more of  
1285 these properties with depth (Allan and Hole 1968, Carey et al. 1976).

1286           Although most loess deposits are originally silt-dominated, various post-depositional processes  
1287 have, in some locations, modified their textural character. For this reason, they have often been  
1288 misinterpreted, or simply not recognized as loess, thereby requiring inventive methods for their  
1289 discernment e.g., Scheib et al. (2013). Examples from soils in Michigan, USA illustrate this phenomenon.  
1290 Here, thin loess commonly overlies sandy sediment. Post-depositional pedoturbation (mixing) has  
1291 modified the original loess textures, i.e., sand from below has been mixed into the loess, resulting in  
1292 coarse-loamy textures (Schaetzl and Hook 2008, Schaetzl and Luehmann 2013). Alternatively, sandy  
1293 sediments in the lower part of the loess deposit may have been locally sourced, i.e., deposited via  
1294 saltation; this process may have occurred synchronously with early stages of loess deposition, when  
1295 much of the landscape was not yet loess-covered or fully vegetated. Either scenario can result in loess  
1296 deposits that are sandier than is typical, especially at depth (Schaetzl and Luehmann 2013, Luehmann et  
1297 al. 2016; Fig. 1A), hindering their recognition in the field. Such “compromised” loess often has distinctly  
1298 bimodal particle size curves (Fig. 1B). Ongoing research has shown that, in many areas, soils not known  
1299 for having loess parent materials actually do have silty surface horizons, or if they have coarse-textured  
1300 lower profiles, then the upper profile is loamy. Many of these soils have been impacted by thin loess  
1301 contributions, but until recently, this type of depositional history was not recognized (Munroe et al.  
1302 2015).

1303           Because many thin loess deposits have been texturally altered by post-depositional mixing or by  
1304 additions of other (coarser) eolian sediment during the loess deposition period (Schaetzl and Luehmann  
1305 2013), using texture data from thin loess deposits to examine possible source areas or paleowind-flow  
1306 patterns can be problematic. For this reason, Luehmann et al. (2013) developed a textural “filtering”  
1307 operation that works in most spreadsheet software packages. The filtering method removes the sand  
1308 data from bimodal particle size texture curve and recalculates the remaining particle size data to better  
1309 reflect the character of the original loess (Fig. 1B). The filtering method has been successfully used in  
1310 studies of thin loess in midcontinent USA (Schaetzl and Attig 2013, Luehmann et al. 2016, Nyland et al.  
1311 2017), and awaits further application and refinement elsewhere.



1312 Most thick loess deposits are the focus of scientists who study paleoenvironments, eolian  
1313 systems, or stratigraphy. Alternatively, thin loess deposits commonly fall within the realm of soil  
1314 specialists, many of whom also have an interest in eolian systems. The intellectual draw of thin loess  
1315 deposits to the soil science community is to be expected: soil development is dramatically impacted by  
1316 even small additions of loess (Simonson 1995). Small additions of loess to a preexisting soil often have  
1317 notable impacts on the soil's texture, hydrology, erodibility, and fertility. Soils formed in thin loess  
1318 deposits are impacted not only by the combination of the two sediment types, but also by the  
1319 hydrological impacts of the lithologic contact itself, across which soil permeability values change  
1320 markedly. Loess is commonly finer than the underlying sediment, which causes wetting fronts to "hang"  
1321 at the contact zone for some time, leading potentially to increased duration times for saturated  
1322 conditions, and heightened weathering. This effect can also preferentially cause deposition of illuvial  
1323 substances at the lithologic contact (Schaetzl 1998), and can reduce the rate at which weathering  
1324 byproducts in the overlying loess are removed from the soil. Thus, some soils formed in thin loess  
1325 develop heightened concentrations of soluble substances in the overlying loess (Wilding et al. 1963,  
1326 Indorante 1998). If the loess overlies a paleosol, these impacts may be even more dramatic.

1327 In sum, thin loess deposits, much more widespread and important than previously thought, are  
1328 gaining attention worldwide by pedologists, geologists and eolian scientists. They have great potential to  
1329 inform the scientific community about paleowind patterns, and knowledge of thin loess additions in soils  
1330 can help explain many pedogenic characteristics.

1331

### 1332 **From Coversand to Loess Systems: A Continuous Spectrum**

1333 Jef Vandenberghe

#### 1334 Periglacial aeolian sands

1335 *Sedimentary facies, origin and transport processes*

1336 Aeolian sands formed in periglacial environments with different facies and morphology, from in  
1337 situ to reworked deposits and composing sheet or dune forms. They extend over a vast belt in North

1338 Europe from northern France to northern Russia (Koster, 1988; Kasse, 1997, 2002; Vandenberghe and  
1339 Kasse, 2008) but patchy deposits are also reported in England (Catt, 1977; Bateman, 1998), North  
1340 America (Lea, 1990; Lea and Waythomas, 1990) and SW France (Sitzia et al., 2015; Bertran et al., 2016).  
1341 Their periglacial origin has been evidenced since the pioneering work of Edelman and Crommelin (1939)  
1342 and Van der Hammen et al. (1967). Because of their variegated nature, this paper discusses the different  
1343 kinds of coversand deposits, focusing on their facies, depositional systems, environmental conditions,  
1344 and chronological evolution, and especially their relations with loess deposits. Because of this diversity,  
1345 periglacial aeolian sands have to be categorized. The discussion that follows examines the different  
1346 categories.

1347           Typical '(primary) coversands' (Fig. 24A) are characterized by a specific, very finely horizontal-  
1348 parallel laminated structure. These sands were deposited as a 'cover' bed, preserving the pre-existing  
1349 topography, hence their name. As demonstrated by mineralogical analyses, they have been  
1350 homogenized by saltation over distances on the order of tens of km (Vandenberghe and Krook, 1981,  
1351 1985). As a result, their grain size is surprisingly constant (around 150  $\mu\text{m}$  modal size) over wide  
1352 surfaces, independent of the underlying substrate.

1353           'Reworked (secondary) coversands' (Fig. 24B) originate from primary coversand by post-  
1354 depositional runoff or/and fluvial processes. This reworking has resulted in sedimentary structures  
1355 typical of flowing water (e.g. channel and ripple cross-lamination, thin concave-upward lenses of coarse-  
1356 grained sand), sheetwash (e.g. parallel strata) and even shallow pools of standing water (e.g. clay or silt  
1357 drapes, humic beds) (Ruegg, 1983; Koster, 1988). However, because this transport is limited to relatively  
1358 short distances (tens or hundreds of meters), the deposits have largely maintained the mineralogical  
1359 and granulometric composition of the source coversand. This mixed genesis, also described for present-  
1360 day periglacial environments (Good and Bryant, 1985), is at the origin of their respective designation as  
1361 'fluvio-aeolian' or even 'lacustro-aeolian' sediments (Vandenberghe and Van Huissteden, 1988; Van  
1362 Huissteden et al., 2000), analogous to similar loess deposits (Vandenberghe, 2013, Vandenberghe et al.,  
1363 2017).

1364           'Periglacial dune sands' (Fig. 24C) are characterized by their well-expressed dune morphology,  
1365 some up to a few tens of m in relief. Their sedimentary structure consists of (low- to high-angle) cross-  
1366 bedding, (sub)horizontal lamination and occasionally homogeneous beds. Transport was by saltation or

1367 in low suspension clouds (De Ploey, 1977) over short distances (tens or hundreds of m). In contrast to  
1368 the coversands, these sands have a variable granulometric and mineralogical composition due to their  
1369 local provenance.

1370 *Evolution, age and environmental conditions of European periglacial aeolian sands*

1371 In contrast to loess, periglacial aeolian sands mostly date to the last full glacial period in Europe  
1372 (Weichselian Pleniglacial, ~c. 62-14.7 ka, ~MIS 4-2). Nonetheless, there do exist some rare, Early  
1373 Pleistocene coversand deposits (Kasse, 1993).

1374 During the Weichselian Early and Middle Pleniglacial (~c. 62-30 ka, ~MIS 3-4), reworked aeolian  
1375 sands were dominant (Van Huissteden, 1990). This system is consistent with the generally humid  
1376 conditions during that period, which favored reworking by water on top of a mostly frozen substrate  
1377 (Böse, 1991; Kasse, 1999). The reworking also involved mixing with loess. This system of deposition  
1378 persisted until c. 17 ka, although the silt component gradually decreased over time. Sometimes the  
1379 primary aeolian sands were interbedded with waterlaid sediments during dry climatic phases or/and in  
1380 dry topographic positions (Vandenberghe, 1985; Gozdzik, 1991). Similar processes of dominant  
1381 reworking, occasionally interrupted by pure aeolian activity, before 17 ka have also been documented in  
1382 adjacent loess regions (Mücher and Vreeken, 1981; Huijzer, 1993; Meszner et al., 2014; Lehmkuhl et al.,  
1383 2016).

1384 At the end of the last glacial (after 17 ka), postdating the Last Permafrost Maximum (LPM), the  
1385 "typical" (primary) coversands were deposited across the entire North European coversand belt. (Ruegg,  
1386 1983; Schwan, 1988; Vandenberghe, 1985, 1991; Kasse, 2002; Kasse et al. 2007). This period of pure  
1387 aeolian activity was fostered by increased aridity with reduced vegetation cover, attributed to (apart  
1388 from drier climatic conditions) the disappearance of permafrost that allowed for increased infiltration  
1389 (Kasse, 1997). This important aeolian phase started with widespread deflation, resulting in the  
1390 formation of a characteristic desert pavement ('Beuningen Gravel Bed'; Van der Hammen et al., 1967).  
1391 This prominent (litho-) stratigraphic marker horizon occurs from northern France to northeastern  
1392 Europe (e.g. Zagwijn and Paepe, 1968; Lautridou and Sommé, 1981). It was dated by luminescence  
1393 techniques from the type sections in the eastern Netherlands at 17-15 ka (Bateman and Van Huissteden,

1394 1999; Vandenberghe D. et al 2013), confirmed both in the Netherlands (Kasse et al., 2007) and Belgium  
1395 (Buylaert et al., 2009).

1396 Finally, during the Late Glacial (14.7-11.9 ka) dune formation was most prominent, although  
1397 coversand deposition may have locally continued (Kasse, 1999). Especially during the Older and Younger  
1398 Dryas, dunes expanded considerably in north-central Europe (e.g. Nowaczyck, 1986; Bohncke et al.  
1399 1995; Zeeberg, 1998), and during the very dry end of the Younger Dryas (10.5-10.1 ka) in North Europe  
1400 (e.g. Vandenberghe, 1983; Bohncke et al., 1993). Dunes formed especially along valley margins where  
1401 sand supplied from (braided) floodplains was captured by the vegetation on the adjacent higher dry  
1402 areas (Vandenberghe, 1983, 1991). In poorly vegetated areas, dune formation continued into the early  
1403 Holocene (Kozarski, 1990; Schwan, 1991; Manikowska, 1994).

#### 1404 The transitional zone between loess and coversand

1405 Macroscopically there is often a sharp spatial boundary between areas of Late Pleniglacial  
1406 coversands and loess areas. However, loess adjacent to the coversand belt shows distinct transitional  
1407 properties, e.g., in average grain-size distribution. One example occurs in central Flanders (called the  
1408 'sandloess belt' by Paepe and Sommé, 1970), at the northern fringe of the Central Loess Plateau (e.g.  
1409 Liu, 1985; Nugteren and Vandenberghe, 2004) and in SW France (Bertran et al., 2011). Texturally, the  
1410 transitional sandloess here is distinctly bimodal, with a fine coversand grain size (c. 150 µm) and a  
1411 typical silt-loess mode (c. 40 µm). This double composition reflects transport both by saltation and in  
1412 suspension. Possible source regions of both coversand and loess (possibly the vast Nordic proglacial  
1413 areas, floodplains or large river deltas) and wind directions (varying from N to SW) are still under  
1414 discussion (e.g. Lautridou et al., 1984; Schwan, 1988; Renssen et al., 2007; Schatz et al., 2015). The  
1415 spatial distribution of the sandloess facies illustrates the downwind transition from coversand to  
1416 sandloess to loess, roughly NNW-SSE both in W Europe (Renssen et al., 2007) and in northern China  
1417 (Nugteren and Vandenberghe, 2004). Further, it appears that in the southern Netherlands and Flanders  
1418 this sandloess occurred more to the north (in proximal position) before the Beuningen desert pavement  
1419 formed than after, i.e., the coversand belt advanced distally after that episode (Vandenberghe and  
1420 Krook, 1985).

#### 1421 The periglacial loess depositional system

1422            Generally, three modes of primary loess deposition, each with specific grain-size distributions,  
1423 may be distinguished (Bagnold, 1941; Pye, 1995; Vandenberghe, 2013). Fine sandy deposits are  
1424 principally transported by saltation (type 1a in Vandenberghe, 2013), while two finer-grained  
1425 populations are transported in suspension (types 1b-c).

1426            Loess type 1b (mainly medium-to-coarse silt (25 to 65  $\mu\text{m}$ )) is transported in short-term, near-  
1427 surface to low-suspension clouds (Tsoar and Pye, 1987) probably during cyclonal dust storm outbreaks,  
1428 and especially under cold conditions (Prins et al., 2007). Grain sizes of 35-40  $\mu\text{m}$  are common worldwide  
1429 in primary loess (e.g. Bokhorst et al., 2011, Novothny et al., 2011; Vandenberghe et al., 2014 in central  
1430 and east Europe; Prins et al., 2007, Vriend et al., 2011, Ijmker et al., 2012; Dietze et al., 2013;  
1431 Nottebaum et al., 2015 in China, and Muhs and Bettis, 2003 in N. America). However, this grain size may  
1432 vary slightly according to differing wind energy, and thus transport capacity, which can be influenced by  
1433 the local topography and surface conditions, including vegetation cover (Schaetzl and Attig, 2013  
1434 Vandenberghe, 2013). The sandloess type from the transitional zone (see above) may be considered as a  
1435 mixture of loess types 1a and 1b.

1436            Loess type 1c is a fine (clayey) silt with modal diameters between 4 and 22  $\mu\text{m}$ . It has been  
1437 interpreted as background dust transported in high-suspension clouds over long distances (Zhang et al.,  
1438 1999; Prins et al., 2007; Vriend et al., 2011) and incorporated in the high-level westerlies (Pye and Zhou,  
1439 1989; Pye, 1995; Sun et al., 2002), cf. the ‘small dust’ (Stuut et al., 2009) and the very fine dust  
1440 transported from Central Asia. This dust type is deposited mostly in combination with the coarser-  
1441 grained silt fraction 1b. It is deposited continuously over time but it is best expressed in relatively warm  
1442 conditions when cyclonic dust storms are relatively weak (Vandenberghe et al., 2006; Prins et al., 2007;  
1443 Vriend et al., 2011).

1444

#### 1445 **Loess and Past Cultures**

1446 Piotr Owczarek and Ian Smalley

1447            Changes to farming and stock keeping, along with other measures of development of past  
1448 cultures, were crucial to the growth and rapid expansion of human groups (Dani and Masson, 1992;

1449 Simmons, 2011). The agrarian Neolithic societies in Europe and the rich ancient proto-urban and urban  
1450 civilization in Asia developed under favourable environmental conditions created by access to water and  
1451 fertile loess soils. The appearance of early man in China and the development of the Chinese culture  
1452 have long been associated with loess (Andersson, 1934; Watson, 1966; Clark and Pigott, 1965). The  
1453 traditional view, as expressed by these scholars, indicates that the distribution of loess corresponds  
1454 approximately to the areas assigned to the Neolithic tradition of the north, in particular the painted  
1455 pottery of the Yang-shao people. Ho (1976) demarcated loess regions as the ‘Cradle of the East’ and has  
1456 clearly demonstrated the links between loess and the Chinese Neolithic. This loess-based Chinese  
1457 society is the only one of the great ancient civilizations to have survived to the present day. Roxby  
1458 (1938) was perhaps the first to link the societal development specifically to loess, and his ideas were  
1459 developed by Smalley (1968). Smalley postulated unreasonable amounts of glaciation as a precursor to  
1460 loess deposit formation but recent studies have shown that loess material originated in High Asia and its  
1461 deposition was much influenced by the Yellow River (Stevens et al., 2013b). The formation mechanisms  
1462 for the Chinese loess and the links to early societies now seem to be firmly established.

1463           Central Asia, regarded by many authors as one of the classic loess provinces (Dodonov, 2007),  
1464 includes different loess deposits extending from the marginal zones of Taklamakan desert, valleys and  
1465 piedmont of the Pamir-Alay and Tian Shan mountains to the southeastern coast of the Caspian Sea  
1466 (Dodonov, 1991; Dodonov and Zhou, 2008) (Fig. 25). These areas played a key role in the development  
1467 of the first agricultural civilizations in this part of Asia. The earliest known remains of production-based  
1468 economy in Central Asia date to the sixth millennium BC (Sarianidi 1992). Early agricultural sites here are  
1469 known from the area between the Pamir forelands, the upper Amu Darya (Oxus) River and southern  
1470 margin of the Karakum desert. These settlements developed on loess patches, as did the First Persian  
1471 Empire (Achaemenid Empire), and in the next millennia Parthia, Khwarezm, Sogdiana and Bactria (Dani  
1472 and Masson, 1992). In the past, more humid climatic conditions occurred in these modern semi-desert  
1473 or desert landscapes (Yang et al. 2009; Chen et al. 2010). The rise and fall of societies inhabiting central  
1474 Asia coincided with these climatic fluctuations (Yin et al., 2016).

1475           The first Neolithic cultures also appeared in areas of loess in Europe. Clark (1952) produced an  
1476 interesting map suggesting the relationship of the settlement of Central Europe by Neolithic Danubian  
1477 peasants to locations of loess deposits. He placed Neolithic sites on a base map of the Grahmann loess

1478 map (1932) of Europe and showed impressive correlations. Neolithic and earlier Bronze Age settlement  
1479 systems on the central European uplands and Carpathian forelands also correspond strongly with areas  
1480 of loess (Kruk et al., 1996; Kruk and Milisauskas, 1999). The spread of the Neolithic to Central Europe,  
1481 between the 6<sup>th</sup> and 4<sup>th</sup> millennium BC (Gronenborn, 2010), took place along fertile loess uplands  
1482 occurring on the northern Sudetes and Carpathians forelands.

1483           Loess deposits are interconnected along the course of the Silk Route (Fig. 25), whose peak of  
1484 influence occurred during the Tang Dynasty, in the second part of the first millennium AD (Liu, 2010).  
1485 From Chang'an (Xi'an) in the Chinese Empire, through the rich ancient kingdoms of Loulan, Khotan,  
1486 Sogdiana and Khwarezm to the coast of the Caspian Sea, the route clearly coincided with loess areas,  
1487 where many agricultural settlements occurred. The development of a network of towns and settlements  
1488 along the Silk Road during this period was possible thanks to fertile loess soils and abundant water  
1489 (oases, rivers) (Dani and Masson, 1992; Abazow, 2008; Owczarek et al., 2017). Climate change during  
1490 the last two millennia, along with human impacts such as deforestation and intensive agriculture,  
1491 influenced the rise and fall, and in some cases even the emergence of new settlements in this area,  
1492 especially in the western piedmont of Pamir and Tian Shan mountains in the Sogdiana (Marshak, 2003).  
1493 An example of the close relationship between favorable environmental conditions and climate change  
1494 may be the ancient cities of the Niya, Loulan and Panjikent. Niya and Loulan, centers of the rich Khotan  
1495 and Loulan kingdoms, were located on the southern and eastern edge of Taklamakan desert (Yong and  
1496 Sun, 1994). Both of the cities were developed on the basis of irrigation of loess soils on the terraces of  
1497 the Niya and Tarim Rivers. Increases in precipitation at ca. 2.1 – 1.9 ka, noted in the Tarim Basin  
1498 (Wünnemann et al., 2006; Chen et al., 2010), led to the rapid political and economic development of this  
1499 area. These rich cities lost their importance after the 2<sup>nd</sup> century AD, due to long-term drought and  
1500 shifting and drying of river channels and lakes, and were completely abandoned by the early 5<sup>th</sup> century  
1501 (Yong and Sun, 1994). As these kingdoms located on the edge of Taklamakan desert in the Tarim Basin  
1502 declined, the Sogdiana in the western central Asia grew. The Sogdian settlement network, like those of  
1503 Samarqand and Bukhara, developed on loess patches in the piedmont of Pamir-Alay along the Zarafshan  
1504 River. One of the towns erected along the Silk Road in the 5<sup>th</sup> century was Panjikent, which by the end of  
1505 the 7<sup>th</sup> century was the most important urban settlement in this part of Central Asia (Grenet and de la  
1506 Vaissière, E., 2002; Marshak, 2003). The city was founded on the upper, loess-mantled terrace of the  
1507 Zarafshan River (Owczarek et al., 2017). The ancient town was abandoned in the 9<sup>th</sup> and 10<sup>th</sup> centuries.



1508 The fall of Panjikent was associated with a political crisis connected to Arab conquest in 722 AD (Grenet  
1509 and de la Vaissière, E., 2002), during a shift to a drier climate in the 8<sup>th</sup>-9<sup>th</sup> centuries, and an  
1510 accompanying decline in natural and agricultural resources due to human impacts and erosion of its  
1511 loess soils (Owczarek et al., 2017).

1512 The cultural and economic development of human societies is strongly affected by  
1513 environmental resources. Areas with fertile soil and access to water, characteristics common to most  
1514 areas of loess, have been shown throughout history to be predisposed for a “Neolithic revolution”,  
1515 which became a later impulse for the development of modern societies.

1516

## 1517 **Loess Geochronology**

1518 Helen M. Roberts

1519 Loess deposits often provide impressive paleoclimatic and paleoenvironmental records.  
1520 Accurate geochronological data play a critical role in understanding these important terrestrial archives.  
1521 A number of approaches have been used to establish the timing of events preserved within the loess  
1522 record, including relative dating techniques and methods to establish age-equivalence, as well as  
1523 radiometric dating techniques to establish numerical ages. The purpose of this section is to consider  
1524 these different geochronologic approaches and their contribution to the study of loess, and comment on  
1525 the likely future research directions for loess geochronology.

1526 The striking visible changes between alternating intercalated loess and paleosol units that can  
1527 be seen in many loess exposures attests directly to the rhythm of changing climatic conditions through  
1528 time. This stratigraphy offers a simple relative chronology back through time, across glacial-interglacial  
1529 cycles, solely based on appearance. If assumptions are made about continuous accumulation rates and  
1530 preservation of the loess deposits over time, then simple top-down layer-counting of the loess-paleosol  
1531 units can be used to establish the likely ages of the individual units, which in turn allows correlation to  
1532 other loess sequences on the basis of likely age-equivalence, and correlation to other dust-bearing  
1533 deposits such as terrestrial lake deposits, marine sediments, and ice cores. Correlations of all kinds are  
1534 dramatically strengthened where isochronous stratigraphic markers preserved in the deposits, e.g., a

1535 geochemically-distinct tephra, can be identified and used to establish age-equivalence; this is especially  
1536 key for loess deposits. Where the age of these distinctive markers is already known from records  
1537 elsewhere, this is particularly valuable, e.g., the widespread Campanian Ignimbrite/Y5 tephra, dated to ~  
1538 40 ka, is a key chronostratigraphic marker across the Mediterranean and southeastern Europe (Veres et  
1539 al., 2013).

1540           Records of paleomagnetic reversals and geomagnetic excursions due to changes in the Earth's  
1541 geomagnetic field have also played an important role in linking long terrestrial loess sequences to each  
1542 other, and enabling correlation to other long records such as the marine record of Lisiecki and Raymo  
1543 (2005). However, the delay between the deposition of sediment and the immobilization of the magnetic  
1544 signal results in the apparent downward displacement of the paleomagnetic signature preserved in  
1545 different records (Zhou and Shackleton, 1999; Sun et al., 2013; Zhao et al., 2014). This 'lock-in effect'  
1546 requires careful consideration or potentially much higher-resolution sampling (Maher, 2016), if high-  
1547 precision magnetostratigraphy is to be used to link sites with greater temporal precision and accuracy.

1548           Beyond this broad framework of tie-points offered through stratigraphy, opportunistic tephra  
1549 correlation, and magnetostratigraphy, further detail and opportunities for correlation between these  
1550 indirectly-dated records can be provided by fluctuations in records of magnetic susceptibility, grain-size,  
1551 dust-flux, and the degree of amino-acid racemization in land snails, which are used to establish age-  
1552 equivalence on the basis of the pattern of their signatures within loess and paleosol units. Magnetic  
1553 susceptibility and grain size fluctuations in particular have been widely used for correlation between  
1554 loess records on the basis of "wobble-matching" (e.g., Yang and Ding, 2014, Markovic, this issue); they  
1555 are often interpreted as climate-related signatures, inasmuch as climate cycles largely drive silt-  
1556 generation and loess depositional systems. In some cases, a chronology is established by linking these  
1557 records to other non-loess records for which more detailed chronologic information may have already  
1558 been established, such as records from lacustrine, marine and ice cores, and speleothems (e.g.,  
1559 Bloemendal et al., 1995; Vandenberghe et al., 1997; Porter and An, 1995; Yang and Ding, 2014); in other  
1560 cases, these records are directly tuned to orbital cycles (Sun et al, 2006; Ding et al., 2002).

1561           Where only a broad chronostratigraphic framework or methods to establish age-equivalence are  
1562 used, or where proxy records of climate are tuned to orbital frequencies, it is necessary to assume that  
1563 (1) loess accumulation rates were essentially continuous over time, with no major hiatuses or erosional

1564 events, and (2) the rates were constant between chronologic tie-points. However, these assumptions  
1565 are being increasingly recognized as an oversimplification of the nature of many loess records, as large  
1566 (i.e., order of magnitude) fluctuations in accumulation rates have been reported within (Roberts et al.,  
1567 2003; Muhs et al., 2013; Stevens et al., 2016b), as well as between, loess units (Sun and An, 2005).  
1568 Additionally, significant hiatuses have been identified (Lu et al., 2006; Terhorst et al., 2011). Additionally,  
1569 indirect dating methods and/or tuning of proxy records to a climate driver, such as orbital cycles, has  
1570 other potential problems: (1) it involves assumptions about the nature and timing of the records or  
1571 proxies being investigated, (2) it brings the potential for circular reasoning, and (3) it precludes the  
1572 opportunity to investigate leads and lags between proxy records of climate change. In contrast,  
1573 independent numerical dating using radiometric techniques allows loess-paleosol sequences to be  
1574 linked unambiguously to each other, and to other records with accurate, independent numerical  
1575 chronologies. This approach allows proxy records and their correlations to be explored within and  
1576 between sites, rather than being assumed to have the same meaning, timing, and significance at each  
1577 site. For example, a comparison of several Chinese loess sections with independent radiometric age  
1578 control (Dong et al., 2015) revealed the time-transgressive nature across the sites of rapid changes in  
1579 the magnetic susceptibility signal inferred to represent the Pleistocene/Holocene transition. The sites  
1580 spanned a climatic gradient across the Loess Plateau, and the age for the inferred Pleistocene/Holocene  
1581 transition was asynchronous across the sites, varying by ~3-4 ka along the northwest (drier, less-  
1582 weathered) to southeast (wetter, more-weathered) transect. Furthermore, none of these  
1583 independently-derived numerical ages were synchronous with the age of the marine isotope stage 2/1  
1584 boundary that would otherwise have been assumed for the Pleistocene/Holocene transition at each site,  
1585 had there been no independent radiometric chronology to support the magnetic susceptibility data  
1586 (Dong et al., 2015). This example emphasizes the importance of independent numerical dating, where  
1587 possible.

1588           The key radiometric dating techniques that have helped establish numerical chronologies for  
1589 loess-paleosol sequences are (1) radiocarbon dating and (2) luminescence dating. Since the earliest  
1590 application to loess-paleosol sequences, radiocarbon dating has benefitted from advances in methods of  
1591 analysis, improvements in instrumentation, and extensions and refinements to the radiocarbon  
1592 calibration curve (e.g. Hajdas, 2008). The radiocarbon method relies upon finding suitable, sufficient, in  
1593 situ organic material for dating, and has therefore been particularly applied to paleosols and snail shells

1594 in loess deposits (Wang et al., 2014; Pigati et al., 2013), although other organic materials such as  
1595 calcareous earthworm granules have also been used (Moine et al., 2017). One key issue regarding the  
1596 use of radiocarbon techniques for dating loess deposits is the relatively low maximum age that can be  
1597 achieved, compared to the temporally extensive nature of many loess records. Luminescence dating  
1598 techniques extend beyond the upper age limit of radiocarbon dating, and have played an increasingly  
1599 significant role in deciphering the chronology of loess-paleosol sequences, as both the accuracy and  
1600 precision of techniques have improved over time.

1601 Luminescence dating exploits the steady build-up of a time-dependent signal acquired during  
1602 burial of mineral grains of quartz and feldspar. The event being dated is the last exposure to sunlight  
1603 during transport, prior to deposition and burial. Luminescence techniques are therefore highly  
1604 appropriate for application to loess sequences, as the fine-grained nature of this eolian sediment implies  
1605 long-transport distances, and hence ample time for bleaching of any pre-existing luminescence signal  
1606 prior to deposition; additionally, the method dates the deposition event directly. The method does not  
1607 typically suffer from lack of suitable materials for dating, being applied to mineral grains of quartz and  
1608 feldspar which are abundant in loess and available throughout the sedimentary sequence. One  
1609 important parameter that does need to be considered though is water content over the depositional  
1610 period, as water in the pore spaces between grains absorbs radiation that would otherwise reach the  
1611 sediment grains. Careful assessment must be made as the final luminescence age calculated can change  
1612 by a little over 1% per 1% change in water content. A combination of local knowledge of water history at  
1613 the site, and measurements of the lower and upper limits of water content are therefore used to define  
1614 a suitable average value for the water content over the depositional history of the sediments (see also  
1615 Nelson and Rittenour, 2015).

1616 Today, a family of luminescence techniques exists, and the range of signals available for dating  
1617 continues to expand. The optically stimulated luminescence (OSL) signal from quartz grains, measured  
1618 using a single-aliquot regenerative dose protocol, remains the luminescence signal of choice for dating  
1619 where conditions are appropriate (see review by Roberts, 2008). Unfortunately, the annual dose rate in  
1620 loess is relatively high, and hence the maximum age limit for quartz OSL is typically significantly less than  
1621 100 ka (Chapot et al., 2012). In contrast, infrared stimulated luminescence (IRSL) signals from feldspar  
1622 have a greater saturation dose and hence a greater potential upper age limit. In the past, however, the

1623 widespread use of feldspars for dating was impeded by the phenomenon of anomalous fading, leading  
1624 to age underestimations. A resurgence of interest in the use of feldspars for dating has recently  
1625 occurred, driven by the discovery of more stable ‘post-IR IRSL’ signals with minimal rates of anomalous  
1626 fading (see reviews by Buylaert et al., 2012; Li and Li, 2012). Feldspars offer a higher upper age limit of  
1627 several hundreds of thousand years in loess. Ongoing and future luminescence work relevant to loess  
1628 studies will likely focus on the development of techniques to reliably extend the upper limit of dating  
1629 even further. Examples include the infrared photon-luminescence (IRPL) signal from feldspars, which  
1630 appears not to suffer from anomalous fading (Prasad et al., 2017), the use of the thermally-transferred  
1631 OSL (TT-OSL) signal from quartz (Wang et al., 2006), and the violet stimulated luminescence (VSL) signal,  
1632 which has been used by Ankjærgaard et al. (2016) to significantly extend the age range from quartz by  
1633 an order of magnitude to ~ 600 ka in loess.

1634           Aided by the expansion of the range of radiometric techniques available, and an increasingly  
1635 large number of ages generated, future work within the area of loess geochronology will likely focus on  
1636 investigating the validity of previous assumptions regarding the steady accumulation rates and quasi-  
1637 continuous nature of loess accumulation. Future research can address questions relating to the degree  
1638 of continuity of thick loess records, and explore the existence and durations of major hiatuses in the  
1639 loess sedimentary record. The increased use of independent radiometric dating will also permit further  
1640 investigation of the degree of (a)synchrony of the proxy records preserved across networks of loess-  
1641 paleosol sequences, and cross-correlations to other long sedimentary records such as marine and ice-  
1642 core records. This work will, however, necessitate an increasingly dense sampling strategy for  
1643 radiometric dating, in order to capture the detail required to address these questions. An increased  
1644 density of independent numerical age determinations will also enable the application of Bayesian  
1645 statistics to such datasets, giving rise to age-depth models which will further increase the accuracy and  
1646 precision of loess-paleosol chronologies.

1647

#### 1648 **Zircon U-Pb and Single Grain Provenance Techniques in Loess Research**

1649 Thomas Stevens

1650 Knowledge of loess sources provides information on past dust sources and production, allows  
1651 proper interpretation of climate proxies, and can yield insights into landscape evolution (Smalley et al.,  
1652 2009; Nie et al., 2015). However, substantial debates still exist over the dust sources of many of the  
1653 world's loess deposits (Aleinikoff et al., 2008; Crouvi et al., 2008; Újvári et al., 2012; Stevens et al.,  
1654 2013a). Due to the dominance of silt-size particles and the well-known distance-sorting properties of  
1655 eolian systems, bulk sediment techniques have traditionally been used to address these debates (Chen  
1656 et al., 2007; Buggle et al., 2008). Although they provide valuable information on the fine silt/clay sources  
1657 and overall compositional characteristics of loess, bulk sediment analyses average out provenance  
1658 signatures, which may mask specific provenance data if the loess was derived from multiple sources  
1659 (Stevens et al., 2010).

1660 In order to circumvent such problems there has been a surge in use of single-grain techniques to  
1661 identify loess sources (Aleinikoff et al., 1999; Aleinikoff et al., 2008; Stevens et al., 2010; Újvári et al.,  
1662 2012). To date, most such studies have focused on U-Pb ages of multiple individual zircon grains ( $\text{ZrSiO}_4$ ).  
1663 Zircons are heavy minerals ( $4.65 \text{ g cm}^{-3}$ ) that are resistant to weathering and act as geochemically closed  
1664 systems through most surface and crustal processes. They crystallize at high temperatures from silica  
1665 rich melts and at high grades of metamorphism, with Pb and U retained up to c. 900 °C. They are nearly  
1666 ubiquitous in upper crustal rocks and as an accessory mineral in detrital sediments (Hawkesworth and  
1667 Kemp, 2006). Zircons reject radiogenic Pb during their formation, which means that the ages of  
1668 individual grains, isolated from bulk samples via density and magnetic separation, can be constrained  
1669 using U-Pb isotopic analysis, often measured using Laser Ablation Inductively Coupled Mass  
1670 Spectrometry (LA-ICP-MS) or Secondary Ion Mass Spectrometry (SIMS) (Fedo et al., 2003). Zircon U-Pb  
1671 ages can be highly diagnostic of sediment source, due to the variety of distinct formation ages of their  
1672 protosource terranes, and the often characteristic zircon U-Pb age distributions in different detrital  
1673 sediments and rocks. As such, the technique is one of the most widely used provenance methods (Fedo  
1674 et al., 2003) and zircon U-Pb age data are abundant for many loess potential source areas.

1675 Provenance assignment is undertaken via comparisons of zircon U-Pb age assemblages in target  
1676 loess sediments to zircon U-Pb data in potential source areas. This comparison is usually based on some  
1677 graphical form of probability density estimation, for example a probability density function (PDF) or  
1678 kernel density estimator (KDE) diagram (Fig. 26), but also potentially via mixture modelling or other

1679 statistical approaches. The identification of discrete peaks of specific zircon U-Pb ages or age ranges in a  
1680 sample facilitates the identification or exclusion of possible sources based on the presence of zircons of  
1681 these ages in potential source rock samples. A specific example from China is shown in Figure 26, and  
1682 described below. Since preparation and analysis of samples is relatively time consuming, sampling is  
1683 often undertaken at rather coarse intervals (m to 10's of m scale) within a loess section. To ensure  
1684 sufficient yield of zircons, it is advisable to take  $\approx 1$  kg of loess material per sample at the cleaned  
1685 section. After extraction, grains are usually imaged (often using cathodoluminescence) to check for  
1686 damage, zonation, etc., and to set up targets for analyses. Analyses numbers vary greatly between  
1687 studies (discussed below) but at a minimum it is generally accepted that >110 zircon ages are needed to  
1688 utilize age peak presence as a provenance indicator (Vermeesch, 2004), whereas to analyze the absence  
1689 of ages or the relative heights of peaks generally requires substantially more data (Pullen et al., 2014).

1690           Significant zircon U-Pb data sets exist from both North American (Aleinikoff et al., 1999;  
1691 Aleinikoff et al., 2008) and European (Újvári et al., 2012) loess, although the majority of data are from  
1692 Chinese Loess Plateau deposits (Stevens et al., 2010; 2013a; Pullen et al., 2011; Xiao et al., 2012; Che  
1693 and Li, 2013; Licht et al., 2016; Fenn et al., in press). Debate about the origin/provenance of Chinese  
1694 loess has been rather polarized, with multiple potential source areas, some being thousands of  
1695 kilometres apart. Chinese Loess Plateau zircon U-Pb age distributions exhibit a distinctive 'double peak'  
1696 of ages of around 260-290 Ma and 440-460 Ma; these ages comprise 80-90% of the zircon grains (Fig.  
1697 26). Small numbers of grains have ages of 700-1100 Ma and 1700-2000 Ma. The protosources of these  
1698 zircon grains must be crystalline/high grade metamorphic rocks formed at those times, with prime  
1699 candidates being Northern Tibetan Plateau and Gobi Altay mountain terranes (Stevens et al., 2010).  
1700 These age peaks can be compared to data obtained from potential source sediments, as they may be  
1701 indicative of the most recent sediment transport step. Nie et al. (2015) proposed that the Yellow River  
1702 system was the source for Chinese Loess Plateau deposits, as it transported eroded NE Tibetan Plateau  
1703 sediment (Fig. 26) that is readily available for deflation and eolian transport to the Chinese Loess  
1704 Plateau. This major revision of prevailing ideas implies that the summer monsoon controls incision of  
1705 the Tibetan plateau and may be responsible for the accelerated rates of loess deposition on the Plateau,  
1706 post 3.6 Ma. A number of further U-Pb studies have tested these conclusions (Bird et al., 2015; Licht et  
1707 al., 2016; Zhang et al., 2016; Fenn et al., in press). Licht et al. (2016) argued that although many  
1708 potential Chinese loess source areas yield similar zircon age peaks, deriving large datasets ( $n=400-1000$



1709 grains per sample) permits differences in peak proportions to be used to differentiate these source  
1710 areas. As such, they grouped age data together into loess, paleosol and potential source area groups,  
1711 and applied mixture-modelling techniques; their work supports the idea that the Yellow River system is  
1712 indeed the dominant sediment source to the Loess Plateau (Fig. 26). Licht et al. (2016) further argued  
1713 that sediments from the north Tibetan Plateau Qaidam Basin also contributed an equal proportion of  
1714 sediment to both loess and paleosol units (Fig. 26). As different dust storm tracks likely existed between  
1715 glacial and interglacial phases, this similar source assemblage implies that pre-deposited glacial loess  
1716 material was eroded during interglacials and contributed to accretion of soil units, in a process of  
1717 internal reworking or ‘eolian cannibalism’ (Licht et al., 2016).

1718           A key challenge is to extend these comprehensive analyses to Pliocene red clay deposits that  
1719 underlie the loess. Although some red clay zircon U-Pb studies have been published (Nie et al., 2014,  
1720 Shang et al., 2016; Gong et al., 2017) the necessary preparation and analysis of smaller zircon grains in  
1721 the red clays make this work difficult. A further challenge is that the large sample numbers in recent  
1722 studies require improved analysis and visualization of the resultant datasets. One method to address  
1723 this is multi-dimensional scaling (MDS) (Vermeesch, 2013). MDS constructs a 2D map of individual points  
1724 that represents samples with multiple analyses numbers; distances on the map indicate the degree of  
1725 similarity among points (c.f. Stevens et al., 2013b). Such dimensional reduction techniques are likely to  
1726 become more important with the increasing importance of ‘big data’ (an internet-era term used by  
1727 Vermeesch and Garzanti (2015) to describe the large and complex multi-sample, multi-method datasets  
1728 now being generated in many provenance studies). Big datasets also open up the potential for  
1729 quantification of source contributions from zircon U-Pb data; this is a major topic of interest, with a  
1730 number of recent approaches proposed (Stevens et al., 2010; Licht et al., 2016; Zhang et al., 2016).  
1731 However, a note of caution has also recently been sounded by Fenn et al. (in press), who demonstrated  
1732 that grouping of sample data together can result in spurious trends. Clearly, high analysis numbers and  
1733 statistical representativity are important, although the number of analyses required depends on the  
1734 complexity of source assemblages and the specific property of U-Pb age distributions being examined  
1735 (Vermeesch, 2004; Pullen et al., 2014). Nonetheless, the goal should be larger numbers of analyses from  
1736 individual samples, with caution exercised in grouping sample datasets (Fenn et al., in press).

1737 Zircon U-Pb data are not without limitations, e.g., (1) the effect of sedimentary recycling  
1738 through multiple phases is hard to diagnose, (2) zircon sources may not always be representative of  
1739 those of the main sediment body, (3) as zircon is a heavy mineral, zircon U-Pb ages will likely reflect  
1740 more proximal sources, and (4) zircon fertility in source rocks exerts a key control over detrital zircon  
1741 assemblages (Sláma and Košla, 2012). As such, a major goal of future research should be to introduce  
1742 other single-grain analyses that complement zircon U-Pb age analyses. Some initial attempts at this have  
1743 been made in Chinese loess, combining zircon U-Pb dating with zircon fission-track and heavy mineral  
1744 analysis (Stevens et al., 2013b; Nie et al., 2014; Nie et al., 2015) and with garnet chemistry (Fenn et al.,  
1745 in press). In central-eastern European loess deposits, attempts have been made to combine zircon U-Pb  
1746 dating with both geochemistry of rutile (Újvári et al., 2013) and zircon Hf isotopes (Újvári and Klötzli,  
1747 2015), as well as bulk geochemical indicators (Újvári et al., 2012). Zircon U-Pb analyses have also been  
1748 combined with Pb isotope analysis of isolated aliquots of K-feldspars in loess in the United States  
1749 (Aleinikoff et al., 1999; 2008). Garnet type and rutile trace element composition in particular have great  
1750 potential to complement zircon U-Pb dating, especially where source terranes show overlapping zircon  
1751 U-Pb ages but are comprised of rocks of varying metamorphic grade and formation temperatures (Újvári  
1752 et al., 2013; Fenn et al., in press).

1753 In sum, single-grain provenance analysis is a rapidly emerging tool in loess research. Although in  
1754 many loess regions major breakthroughs in constraining loess-dust sources can be made through the  
1755 straightforward application of detrital zircon U-Pb dating, multi-technique single-grain approaches  
1756 promise even more accurate and precise dust sourcing for loess deposits globally.

1757

1758

1759 FIGURES

1760 Figure 1. Participants taking turns examining thin loess in a soil pit at one of the several field trip  
1761 stops at the 2016 LoessFest in western Wisconsin, USA. Photo by R. Schaetzl.

- 1762 Figure 2. Map of loess deposits (yellow) on the Chinese Loess Plateau. Arrows indicate the direction of  
1763 the East Asian winter and summer monsoonal winds. Inset shows the location of the Chinese Loess  
1764 Plateau in Euroasia. After Yang et al. (2015).
- 1765 Figure 3. Photograph of the eolian deposits at Luochuan (Fig. 1), in the central Chinese Loess Plateau,  
1766 with loess (L)–soil (S) couplets for the L<sub>1</sub>–L<sub>6</sub> portion indicated. For details on stratigraphic nomenclature  
1767 of Chinese loess, see Rutter et al. (1991) and Ding et al. (1993). Photo by Shiling Yang.
- 1768 Figure 4. Loess distribution along the core Central Asian piedmonts in the rain shadow of the Asian high  
1769 mountains, showing geographic associations of loess deposits to glaciated regions, major rivers and  
1770 deserts, as well as key regions and localities. After Dodonov (1991).
- 1771 Figure 5. Loess distribution map (Haase et al., 2007) including LGM maximum extent (Ehlers et al., 2004,  
1772 2011), dry continental shelf (Willmes, 2015), LGM permafrost distribution (Vandenberghe et al., 2014)  
1773 and northern LGM timberline (Grichuk, 1992).
- 1774 Figure 6. A Middle Pleistocene loess-paleosol sequence from Mircea Voda (Dobrogea, Romania). The  
1775 approximately 25m high sequence represents the dry steppe loess facies of the Lower Danube Basin.  
1776 Note the characteristic uppermost double paleosol (S<sub>2</sub>) that corresponds to MIS 7, while the lowermost  
1777 strongly developed paleosol (S<sub>6</sub>) represents MIS 17 (Bugge et al., 2009). Photo by Ulrich Hambach.
- 1778 Figure 7. Principal stratigraphic subdivisions and important paleosols within the lithologic/loess record  
1779 for the last 130 ka, for five main sites throughout Europe. Vertical scales on the diagrams are not  
1780 uniform. In order to better match the graphics to the legend, each soil has been numbered and the  
1781 numbers placed next to the stratigraphic profiles. After Markovic et al. (2008).
- 1782 Figure 8. A. The general loess stratigraphy found in eastern Nebraska, U.S.A., as represented by core 3-  
1783 B-99 (41°29'N, 96°13'W) (Mason et al., 2007). Peoria Loess, Gilman Canyon Formation, and Loveland  
1784 Loess are correlated with specific parts of marine isotope record based on numerical dating. Ages  
1785 assigned to Loveland Loess are based on luminescence dating at the paratype locality in western Iowa  
1786 (Forman and Pierson, 2002); ages assigned to Kennard Formation are based on its stratigraphic position  
1787 between Loveland Loess and Lava Creek B tephra, supported by burial dating of Balco et al. (2005). B.  
1788 Loess stratigraphy in the Elba Cut section of central Nebraska (41°18'N, 98°31'W), interpreted by J.

1789 Mason by comparison with eastern Nebraska sections (Mason et al., 2007). Note person at base of  
1790 section for scale. The tephra present in this section (to left of area shown here) is the Lava Creek B (E.A.  
1791 Bettis III, personal communication).

1792 Figure 9. Map of Alaska showing the distribution of Quaternary loess deposits and the distribution of  
1793 modern glaciers. Lettered dots refer to localities discussed in the text. After Muhs et al., (2003).

1794 Figure 10. DEM image of southern South America with general location of the Pampean plain, Chaco,  
1795 Puna and other areas discussed in the text. Localities referred to in the text are keyed to the legend in  
1796 the lower right of the figure.

1797 Figure 11. A. Spatial distribution of loess in Africa and Arabia, active sand seas and Arenosols (sandy  
1798 soils) (FAO/IIASA/ISRIC/ISSCAS/JRC, 2009). Near surface dominant wind directions for January and June  
1799 are based on Breed et al. (1979). Silt (content in %, 24 $\mu$ m mode) in oceanic sediments off the West  
1800 Africa coast deposited during the last glacial maximum (Sarnthein et al., 1981). See text for further  
1801 details on the Negev loess, Israel. After Crouvi et al. (2010). B. Map of Israel and its surroundings,  
1802 showing the distribution of sand dunes (white polygons with black dots) and loessial (dark grey) and  
1803 sandy (light grey) soils in the Negev and Sinai deserts (the soils were mapped only in Israel). Mean  
1804 annual rainfall (mm) in Israel for the period 1961–1990 is shown by dashed isohyets. Black arrows are  
1805 the inferred westerly winds prevalent during sand incursion. Insert shows the location of Israel in the  
1806 eastern Mediterranean region and the mean annual rainfall isohyets (mm). After Crouvi et al. (2008).

1807 Figure 12. The Mircea Voda loess section in Dobrogea, Romania is a good example of alternations of  
1808 loess layers (from L1 to L5) and pedological horizons, or paleosols (from S0 to S5). These data are  
1809 additionally illustrated by variations in magnetic susceptibility ranging from low values in loess units to  
1810 high values in paleosols (Bugge et al., 2009; Timar-Gabor et al., 2011).

1811 Figure 13. Direct comparisons between the A: marine LR04 stack (Lisiecki and Raymo, 2005) and B:  
1812 Serbian loess (Marković et al., 2015) and C: Chinese loess (Sun et al., 2006) magnetic susceptibility  
1813 records plotted on time-scale.

1814 Figure 14. Comparisons between classic Pleistocene stratigraphic subdivisions (Gibbard and Cohen,  
1815 2008), Marine Isotope Stages (e.g., Lisiecki and Raymo, 2005), and L&S nomenclature initially presented  
1816 by Kukla and An (1989).

1817 Figure 15. Comparisons of established Quaternary reference datasets. A: A comparison of the LR04  
1818 benthic isotope stack (Lisiecki and Raymo, 2005), the Imbrie and Imbrie (1980) ice model (parameterized  
1819 as by LR04), and a mixture of orbital parameters eccentricity (E), tilt/obliquity (T) and precession (P;  
1820 Laskar et al., 2004), along with loess MS data from Europe (Basarin et al., 2014) and the Chinese Loess  
1821 Plateau (Hao et al., 2012). In both cases, loess MS (and other information) was used for correlative time  
1822 scale construction. Marine Isotope Stages (MIS) and loess (L) and paleosol (S) units are indicated, using a  
1823  $\delta^{18}\text{O}$  cutoff of 4.3. B: A comparison of Greenland  $\delta^{18}\text{O}$  data (North Greenland Ice Core Project Members  
1824 et al., 2004) with two datasets of the  $\text{MS}_{\text{fd}}$  from Uurluia (Obrecht et al., 2017) and Rasova (Zeeden et al., in  
1825 press). Note that the Campanian Ignimbrite volcanic tephra causes additional signal at ca. 40 ka.

1826 Figure 16. A scatter-plot of the  $\chi_{\text{lf}}$  (ordinate) vs.  $\chi_{\Delta}$  (abscissa) and the trend of the “true loess line” as  
1827 suggested by Zeeden et al. (2016) and based on Forster et al. (1994). The grey data points show the  
1828 magnetic enhancement trend for the Semail LPS (recent to  $\approx 400$  ka; SE Pannonian Basin, Romania;  
1829 modified after Zeeden et al., 2016) as a function of increasing pedogenesis for dry steppe loess. The  
1830 interception of the “true loess line” with the ordinate defines the background susceptibility of raw,  
1831 unweathered loess, which fits well to the average value determined for Eurasian loess by Forster et al.  
1832 (1994).

1833 Figure 17. Contents of various major elements in last glacial loess of Midcontinent USA. Fe and Al  
1834 contents generally increase east to west from Indiana to Nebraska, as calcite and dolomite (reflected by  
1835 CaO and MgO percentages, respectively) generally decrease. These changes reflect decreasing  
1836 contributions of carbonate rock sources to the loess from east to west. After Pye and Johnson (1988),  
1837 Muhs and Bettis (2000), and Muhs et al. (2001).

1838 Figure 18. Examples of loess data derived from two-dimensional transects away from a known loess  
1839 source. Both rivers are in the central US. The use of scatterplots and regression equations in the analysis  
1840 of such data is commonplace.

1841 Figure 19. Examples of spatial display/analytical approaches that have been applied to loess data in the  
1842 USA. A: Graduated circle map of a loess textural attribute across the loess-covered plains of central  
1843 Wisconsin. Loess is mapped here on areas shown as light brown; the dark brown area is the Late  
1844 Wisconsin (MIS 2) end moraine. Major rivers, which flow north-to-south in this area, are also shown. The  
1845 size of the circles, in this case, is proportional to content of the 35-75  $\mu\text{m}$  fraction in the loess (coarse silt  
1846 and the finest of the very fine sand). Loess samples were obtained in areas that are not currently  
1847 mapped as having loess, but the loess here contains little of this size fraction. Areas with larger amounts  
1848 of the mapped size fraction are downwind (to the SE) of topographic obstructions to loess transport: (1)  
1849 bedrock uplands, (2) the end moraine, and (3) major river valleys. B: Kriged, interpolated isoline map of  
1850 the contents of fine and medium silt (6-35  $\mu\text{m}$ ) in the thin loess of Michigan's western Upper Peninsula  
1851 and northeastern Wisconsin. Potential loess source areas are shown in yellow (outwash plains) and  
1852 brown (end moraines). Isolines are only shown in areas where mapped thicknesses of loess occur. After  
1853 Schaetzl and Attig (2013). C: Kriged, interpolated isoline map of the contents of silt and very fine sand  
1854 (6-125  $\mu\text{m}$ ) across the thin loess of Michigan's western Upper Peninsula. This map also shows sample  
1855 site locations (some are covered by the isolines). The loess here varies considerably across the  
1856 landscape. Luehmann et al. (2013) identified four "core" areas of loess in this region. The figure also  
1857 provides compiled data, as histograms, for other kinds of loess data within the heart of each loess  
1858 "core"; average loess thickness, mean weighted particle size ( $\mu\text{m}$ ), total silt (6-50 $\mu\text{m}$ ), medium silt  
1859 through very fine sand (25-125 $\mu\text{m}$ ), and total very fine and fine sand (50-250  $\mu\text{m}$ ). D: Interpolated,  
1860 kriged map of sorting coefficients (Trask 1932) for a thin (< 1 m) loess deposit in southwestern Michigan.  
1861 Across this study area, loess deposits are discontinuous, and therefore, in this display method,  
1862 interpolated data are shown only in areas where soils are mapped that presumably formed in loess. That  
1863 is, the figure is also a loess distribution map. The presumed loess source for this area is the glacial  
1864 meltwater valley, outlined in white. After Luehmann et al. (2016).

1865 Figure 20: Conceptual diagram of the proposed "paleohygrometer" based on a coupled  $^2\text{H}$ - $^{18}\text{O}$   
1866 biomarker approach (modified after Zech M. et al. 2013c and Tuthorn et al. 2015). Apart from enabling  
1867 the reconstruction of relative atmospheric humidity (RH) by using  $\delta^2\text{H}_{\text{n-alkane}}$  and  $\delta^{18}\text{O}_{\text{sugar}}$  and resultant  
1868 deuterium-(d-) excess of leaf water, the approach additionally allows for the reconstruction of  
1869  $\delta^2\text{H}/\delta^{18}\text{O}_{\text{prec}}$  much more robustly than one based on  $\delta^2\text{H}_{\text{n-alkane}}$  or  $\delta^{18}\text{O}_{\text{sugar}}$  alone.

1870 Figure 21. Examples of six species of fossil terrestrial gastropods of the more than 25 genera and 50  
1871 species found in last glacial loess (Peoria Silt) of the central USA. Photos include (A) *Succinea* sp. from  
1872 Scott County, Illinois (Leonard and Frye, 1960; ABL#7), (B) *Discus whitneyi* from Rocks Section, Union  
1873 County, Kentucky, (C) *Vertigo modesta* from Demazenod Section, St. Clair County, Illinois, (D) *Columella*  
1874 *alticola* from Rocks Section, Union County, Kentucky, (E) *Anguispira alternata* from Burdick Branch  
1875 Section, Madison County, Illinois (Leonard and Frye, 1960; ABL#2), and (F) *Carychium exile* from New  
1876 Cottonwood School Section, Cass County, Illinois (Nash et al., 2017). The yellow scale bar is 1 mm in all  
1877 images. Shells of the genera *Succinea* (A) and *Discus* (B) are among the best for radiocarbon dating. The  
1878 shells pictured in (C) and (D), where found, are representative of much cooler boreal environments to  
1879 perhaps borderline tundra conditions (Nekola and Coles, 2010). Species (E) and (F) have relatively broad  
1880 distributions today in forested landscapes of the eastern USA and southern Canada.

1881 Figure 22. Stratigraphic correlations between Nussloch paleosols and NGRIP interstadials (GIs) (modified  
1882 from Rousseau et al., 2017a,b). Map of Northern Hemisphere during the LGM (Patton et al., 2016)  
1883 showing the location of the main ice sheets, the reconstructed jet stream tracks (Kutzbach, 1987), and  
1884 the reference sequence of Nussloch.  $\delta^{18}\text{O}$  (‰, in blue) and the dust concentration (part/ $\mu\text{L}$ , in brown)  
1885 records in the NGRIP ice core over the interval between 60 ka and 15 ka. Nussloch stratigraphic column  
1886 modified from Antoine et al. (2016).

1887 Figure 23. Textural data for two different thin loess deposits in Michigan, USA. A: A profile image, with  
1888 corresponding texture data, for a soil formed in  $\approx 96$  cm of loess over glacial outwash. Texture curves  
1889 indicate the varying amounts of mixing of the two sediments, both above and below the lithologic  
1890 contact. Tape increments in cm. After Luehmann et al. (2016). B: Example of texture data for a thin loess  
1891 deposit in northern Michigan. Note the distinct bimodality in the raw data, but not in the filtered data.  
1892 After Luehmann et al. (2013).

1893 Figure 24. A: Characteristic horizontal parallel laminated coversand in the type region of Lutterzand  
1894 (eastern Netherlands); vertical extent of image is 100 cm. B: Fluvio-eolian sands consisting of alternating  
1895 beds of medium-coarse sands, fine sands and silty fine sands interrupted by phases of non-deposition  
1896 during which frost cracks could form, e.g., indicated by arrows (eastern Netherlands). Length of trowel is  
1897 15 cm. C: Typical cross-laminated and high-angle bedded sand in a dune of Younger Dryas age  
1898 (Bosscherheide, Netherlands); activation surfaces are indicated by arrows. Length of spade is 50 cm.



1899 Figure 25. Map of loess and loess-like deposits in Asia, with the locations of the most important towns  
1900 and Silk Road branches on the background of the main kingdoms and empires of the 2<sup>nd</sup> – 3<sup>rd</sup> centuries  
1901 AD. After Dodonov (2007) Dodonov and Zhou (2008) and Owczarek et al. (2017).

1902 Figure 26. Kernel Density Estimator (KDE) diagrams (Vermeesch, 2012) of compiled zircon U-Pb age data  
1903 from studies of the Chinese Loess Plateau. Compiled from Fenn et al. (in press; see paper for sources).  
1904 ‘Chinese Loess Plateau’ includes all data from the plateau combined, whereas ‘loess’ and ‘paleosol’ are  
1905 combined data for Chinese Loess Plateau loess and soil units respectively. Yellow River (U) refers to the  
1906 upper river reaches (Nie et al., 105); Mu Us (E) and (W) refer to data from eastern and western parts of  
1907 the desert respectively (Stevens et al., 2013).

1908

1909

1910

1911 **References**

- 1912 Abazow, R, 2008. Palgrave Concise Historical Atlas of Central Asia. Palgrave Macmillan US.
- 1913 Akram, H., Yoshida, M., Ahmad, M.N., 1998. Rock magnetic properties of the late Pleistocene loess-  
1914 paleosol deposits in Haro River area, Attock Basin, Pakistan: Is magnetic susceptibility a proxy measure  
1915 of paleoclimate? *Earth Planets Space* 50, 129-139.
- 1916 Aleinikoff, J.N., Muhs, D.R., Saner, R.R., Fanning, C.M., 1999. Late Quaternary loess in northeastern  
1917 Colorado: Part II - Pb isotopic evidence for the variability of loess sources. *Geological Society of America*  
1918 *Bulletin* 111, 1876-1883.
- 1919 Aleinikoff, J.N., Muhs, D.R., Bettis, E.A., III, Johnson, W.C., Fanning, C.M., Benton, R., 2008. Isotopic  
1920 evidence for the diversity of late Quaternary loess in Nebraska: Glaciogenic and nonglaciogenic sources.  
1921 *Geological Society of America Bulletin* 120, 1362-1377.
- 1922 Allan, R.J., Hole, F.D., 1968. Clay accumulation in some Hapludalfs as related to calcareous till and  
1923 incorporated loess on drumlins in Wisconsin. *Soil Science Society of America Proceedings* 32, 403-408.
- 1924 Amit, R., Enzel, Y., Crouvi, O., 2016. Distance-impacted grain size of loess and dust result in the  
1925 formation of diverse soil types around the Mediterranean. *Geological Society of America, Abstracts with*  
1926 *Programs*. Vol. 48, No. 7 doi: 10.1130/abs/2016AM-282202
- 1927 Andersson, J.G., 1934. *Children of the Yellow Earth*. Kegan Paul, Trench, Tubner, London.
- 1928 Ankjærgaard, C., Guralnik, B., Buylaert, J.-P., Reimann, T., Yi, S.W., Wallinga, J., 2016. Violet stimulated  
1929 luminescence dating of quartz from Luochuan (Chinese Loess Plateau): Agreement with independent  
1930 chronology up to ~600 ka. *Quaternary Geochronology* 34, 33-46.
- 1931 An, Z., Kukla, G.J., Porter, S.C., Xiao, J., 1991a. Magnetic susceptibility evidence of monsoon variation on  
1932 the Loess Plateau of central China during the last 130,000 years. *Quaternary Research* 36, 29–36.
- 1933 An, Z.S., Kukla, G., Porter, S.C., Xiao, J.L., 1991b. Late Quaternary dust flow on the Chinese Loess Plateau.  
1934 *Catena* 18, 125–132.

- 1935 Antoine, P., Rousseau, D.D., Lautridou, J.P., Hatté, C., 1999. Last interglacial-glacial climatic cycle in  
1936 loess-paleosol successions of north-western France. *Boreas* 28, 551-563.
- 1937 Antoine, P., Catt, J., Lautridou, J.-P., Sommé, J., 2003. The loess and coversands of northern France and  
1938 southern England. *Journal of Quaternary Sciences* 18, 309–318.
- 1939 Antoine, P., Rousseau, D.-D., Moine, O., Kunesch, S., Hatté, C., Lang, A., Tissoux, H., Zöller, L., 2009.  
1940 Rapid and cyclic aeolian deposition during the Last Glacial in European loess: a high-resolution record  
1941 from Nussloch, Germany. *Quaternary Science Reviews* 28, 2955–2973.
- 1942 Antoine, P., Rousseau, D.-D., Degeai, J.-P., Moine, O., Lagroix, F., Kreutzer, S., Fuchs, M., Hatté, C.,  
1943 Gauthier, C., Svoboda, J., Lisá, L., 2013. High-resolution record of the environmental response to climatic  
1944 variations during the Last Interglacial–Glacial cycle in Central Europe: the loess-palaeosol sequence of  
1945 Dolní Věstonice (Czech Republic). *Quaternary Science Reviews* 67, 17–38.
- 1946 Assallay, A.M., Rogers, C.D.F., Smalley, I.J., Jefferson, I.F., 1998. Silt: 2-62 micron, 9-4 phi. *Earth-Science*  
1947 *Reviews* 45, 61-88.
- 1948 Aubekerov, B.J., 1993. Stratigraphy and Paleogeography of the Plain Zones of Kazakhstan during the Late  
1949 Pleistocene and Holocene, Development of Landscape and Climate of Northern Asia, Late Pleistocene  
1950 and Holocene. Nauka, Moscow, pp. 101-110.
- 1951 Auclair, M., Lamothe, M., Lagroix, F., Banerjee, S.K., 2007. Luminescence investigation of loess and  
1952 tephra from Halfway House section, Central Alaska. *Quaternary Geochronology* 2, 34-38.
- 1953 Avni, Y., 2005. Gully incision as a key factor in desertification in an arid environment, the Negev  
1954 highlands, Israel. *Catena* 63, 185-220.
- 1955 Avni, Y., Porat, N., Plakht, J., Avni, G., 2006. Geomorphic changes leading to natural desertification  
1956 versus anthropogenic land conservation in an arid environment, the Negev Highlands, Israel.  
1957 *Geomorphology* 82, 177-200.
- 1958 Bagnold, R., 1941. The physics of blown sand and desert dunes. Chapman & Hall, London, 265pp.

- 1959 Bai, Y., Fang, X., Nie, J., Wang, Y., Wu, F., 2009. A preliminary reconstruction of the paleoecological and  
1960 paleoclimatic history of the Chinese Loess Plateau from the application of biomarkers. *Palaeogeography,*  
1961 *Palaeoclimatology, Palaeoecology* 271, 161-169.
- 1962 Baker, F.C., 1931. Pulmonate mollusca peculiar to the Pleistocene Period, particularly the loess deposits.  
1963 *Journal of Paleontology* 5, 270-292
- 1964 Balakrishnan, M., Yapp, C.J., 2004. Flux balance models for the oxygen and carbon isotope compositions  
1965 of land snail shells. *Geochimica Cosmochimica Acta* 68, 2007-2024.
- 1966 Balco, G., Stone, J.O.H., Mason, J.A., 2005. Numerical ages for Plio-Pleistocene glacial sediment  
1967 sequences by Al-26/Be-10 dating of quartz in buried paleosols. *Earth and Planetary Science Letters* 232,  
1968 179-191.
- 1969 Banak, A., Mandic, O., Sprovieri, M., Lirer, F., Pavelić, D., 2016. Stable isotope data from loess  
1970 malacofauna: Evidence for climate changes in the Pannonian Basin during the Late Pleistocene.  
1971 *Quaternary International* 415, 15-24.
- 1972 Basarin, B., Vandenberghe, D.A.G., Marković, S.B., Catto, N., Hambach, U., Vasiliniuc, S., Derese, C.,  
1973 Rončević, S., Vasiljević, D.A., Rajić, L., 2009. The Belotinac section (Southern Serbia) at the southern limit  
1974 of the European loess belt: Initial results. *Quaternary International* 240, 128-138.
- 1975 Basarin, B., Buggle, B., Hambach, U., Marković, S.B., Dhand, K.O., Kovačević, A., Stevens, T., Guo, Z.,  
1976 Lukić, T., 2014. Time-scale and astronomical forcing of Serbian loess-palaeosol sequences. *Global and*  
1977 *Planetary Change* 122, 89–106.
- 1978 Bateman, M.D., 1998. The origin and age of coversand in north Lincolnshire, UK Permafrost and  
1979 *Periglacial Processes* 9, 313-325.
- 1980 Bateman, M.D., Van Huissteden, J., 1999. The timing of last-glacial periglacial and aeolian events,  
1981 Twente, eastern Netherlands. *Journal of Quaternary Science* 14, 277-283.

- 1982 Baumgart, P., Hambach, U., Meszner, S., Faust, D., 2013. An environmental magnetic fingerprint of  
1983 periglacial loess: Records of Late Pleistocene loess–palaeosol sequences from Eastern Germany.  
1984 *Quaternary international*, 296, 82-93
- 1985 Begét, J., 1990. Middle Wisconsinan climate fluctuations recorded in central Alaskan loess. *Géographie*  
1986 *Physique et Quaternaire* 44, 3-13.
- 1987 Begét, J.E., 1996. Tephrochronology and paleoclimatology of the last interglacial-glacial cycle recorded in  
1988 Alaskan loess deposits. *Quaternary International* 34-36, 121-126.
- 1989 Begét, J.E., Hawkins, D.B., 1989. Influence of orbital parameters on Pleistocene loess deposition in  
1990 central Alaska. *Nature* 337, 151-153.
- 1991 Begét, J.E., Stone, D.B., Hawkins, D.B., 1990. Paleoclimatic forcing of magnetic susceptibility variations in  
1992 Alaskan loess during the Quaternary. *Geology* 18, 40-43.
- 1993 Begét, J., Edwards, M., Hopkins, D., Keskinen, M., Kukla, G., 1991. Old Crow tephra found at the  
1994 Palisades of the Yukon, Alaska. *Quaternary Research* 35, 291-297.
- 1995 Ben Israel, M., Enzel, Y., Amit, R., Erel, Y., 2015. Provenance of the various grain-size fractions in the  
1996 Negev loess and potential changes in major dust sources to the Eastern Mediterranean. *Quaternary*  
1997 *Research* 83, 105-115.
- 1998 Berger, G.W., 2003. Luminescence chronology of late Pleistocene loess-paleosol and tephra sequences  
1999 near Fairbanks, Alaska. *Quaternary Research* 60, 70-83.
- 2000 Bertran, P., Bateman, M.D., Hernandez, M., Mercier, N., Millet, D., Sitzia, L., Tastet, J.-P., 2011. Inland  
2001 aeolian deposits of south-west France: facies, stratigraphy and chronology. *Journal of Quaternary*  
2002 *Science* 26, 374-388.
- 2003 Bertran, P., Liard, M., Sitzia, L., Tissoux, H., 2016. A map of Pleistocene aeolian deposits in Western  
2004 Europe, with special emphasis on France. *Journal of Quaternary Sciences* 31, 844-856.

- 2005 Bettis, E.A., III, Muhs, D.R., Roberts, H.M., Wintle, A.G., 2003. Last Glacial loess in the conterminous USA.  
2006 *Quaternary Science Reviews* 22, 1907-1946.
- 2007 Bird, A., Stevens, T., Rittner, M., Vermeesch, P., Carter, A., Andò, S., Garzanti, E., Lu, H., Nie, J., Zeng, L.,  
2008 Zhang, H., Xu, Z., 2015. Quaternary dust source variation across the Chinese Loess Plateau.  
2009 *Palaeogeography, Palaeoclimatology, Palaeoecology* 435, 254-264.
- 2010 Björck, S., Walker, M.J.C., Cwynar, L.C., Johnsen, J., Knudsen, K.L., Lowe, J.J., Wohlfarth, B., 1998. An  
2011 event stratigraphy for the Last Termination in the North Atlantic region based on the Greenland ice-core  
2012 record: a proposal by the INTIMATE group. *Journal of Quaternary Science* 13/4, 283-292.
- 2013 Bloemendal, J., Liu, X.M., and Rolph, T.C., 1995. Correlation of the magnetic-susceptibility stratigraphy of  
2014 Chinese loess and the marine oxygen-isotope record – chronological and paleoclimatic implications.  
2015 *Earth and Planetary Science Letters* 131, 371-380.
- 2016 Bohncke, S., Vandenberghe, J., Huijzer, A.S., 1993. Periglacial environments during the Weichselian Late  
2017 Glacial in the Maas valley, The Netherlands. *Geologie en Mijnbouw* 72, 193-210.
- 2018 Bohncke, S., Kasse, C., Vandenberghe, J., 1995. Climate induced environmental changes during the  
2019 Vistulian Lateglacial at Zabinko, Poland. *Quaestiones Geographicae, Spec. Issue 4 'Late-Quaternary relief  
2020 evolution and environment changes'*, 43-64.
- 2021 Boixadera, J., Poch, R.M., Lowick, S.E., Balasch, J.C., 2015. Loess and soils in the eastern Ebro Basin,  
2022 *Quaternary International* 376, 114-133.
- 2023 Bokhorst, M., Vandenberghe, J., Sümegei, P., Lanczont, M., Gerasimenko, N.P., Matviishina, Z.N.,  
2024 Markovic, S.B., Frechen, M., 2011. Atmospheric circulation patterns in Central and Eastern Europe during  
2025 the Weichselian Pleniglacial inferred from loess grain-size records. *Quaternary International* 234, 62-74.
- 2026 Böse, M., 1991. A palaeoclimatic interpretation of frost-wedge casts and aeolian sand deposits in the  
2027 lowlands between Rhine and Vistula in the Upper Pleniglacial and Late Glacial. *Zeitschrift für  
2028 Geomorphologie* 90, 15-28.

- 2029 Bradák, B., Újvári, G., Seto, Y., Hyodo, M., Végh, T., 2018. A conceptual magnetic fabric development  
2030 model for the Paks loess in Hungary. *Aeolian Research*, 30, 20-31.
- 2031 Breed, C.S., Fryberger, S.G., Andrews, S., McCauley, C., Lennartz, F., Gebel, D., Horstman, K., 1979.  
2032 Regional studies of sand seas, using Landsat (ERTS) imagery, In: McKee, E.D. (Ed.), *A study of global sand*  
2033 *seas*. United States Geological Survey, pp. 305-397.
- 2034 Brodie, C., Leng, M., Casford, J., Kendrick, C., Lloyd, J., Yongqiang, Z., Bird, M., 2011. Evidence for bias in  
2035 C and N concentrations and  $\delta^{13}\text{C}$  composition of terrestrial and aquatic organic materials due to pre-  
2036 analysis acid preparation methods. *Chemical Geology* 282, 67-83.
- 2037 Bronger, A., 1976. Zur quartären Klima- und Landschaftsentwicklung des Karpatenbeckens auf (paläo)  
2038 pedologischer und bodengeographischer Grundlage. In: *Kieler geographische Schriften* 45. Selbstverlag  
2039 des Geographischen Instituts der Universität Kiel, Kiel.
- 2040 Bronger, A., 2003. Correlation of loess-paleosol sequences in East and Central Asia with SE Central  
2041 Europe - Towards a continental Quaternary pedostratigraphy and paleoclimatic history. *Quaternary*  
2042 *International* 106/107, 11-31.
- 2043 Bronger, A., Heinkele, T., 1989. Micromorphology and genesis of paleosols in the Luochuan loess  
2044 section, China: Pedostratigraphical and environmental implications. *Geoderma* 45, 123-143.
- 2045 Bronger, A., Winter, R., Sedov, S., 1998. Weathering and clay mineral formation in two Holocene soils  
2046 and in buried paleosols in Tadjikistan towards a Quaternary paleoclimatic record in Central Asia. *Catena*  
2047 34, 19-34.
- 2048 Buggle, B., Zech, M., 2015. New frontiers in the molecular based reconstruction of Quaternary  
2049 paleovegetation from loess and paleosols. *Quaternary International* 372, 180-187.
- 2050 Buggle, B., Glaser, B., Zöller, L., Hambach, U., Marković, S., Glaser, I., Gerasimenko, N., 2008.  
2051 Geochemical characterization and origin of Southeastern and Eastern European loesses (Serbia,  
2052 Romania, Ukraine). *Quaternary Science Reviews* 27, 1058-1075.



- 2053 Buggle, B., Hambach, U., Glaser, B., Gerasimenko, N., Marković, S.B., Glaser, I., Zöller, L., 2009.  
2054 Stratigraphy and spatial and temporal paleoclimatic trends in East European loess paleosol sequences.  
2055 *Quaternary International* 196, 86-106.
- 2056 Buggle, B., Wiesenberg, G., Glaser, B., 2010. Is there a possibility to correct fossil n-alkane data for  
2057 postsedimentary alteration effects? *Applied Geochemistry* 25, 947-957.
- 2058 Buggle, B., Glaser, B., Hambach, U., Gerasimenko, N., Marković, S., 2011. An evaluation of geochemical  
2059 weathering indices in loess-paleosol studies. *Quaternary International* 240, 12-21.
- 2060 Buggle, B., Hambach, U., Kehl, M., Marković, S.B., Zöller, L., Glaser, B., 2013. The progressive evolution  
2061 of a continental climate in SE-Central European lowlands during the Middle Pleistocene recorded in  
2062 loess paleosol sequences. *Geology* 41, 771–774.
- 2063 Buggle, B., Hambach, U., Müller, K., Zöller, L., Marković, S.B., Glaser, B., 2014. Iron mineralogical proxies  
2064 and Quaternary climate change in SE-European loess–paleosol sequences. *Catena* 117, 4–22.
- 2065 Bush, R., McInerney, F., 2013. Leaf wax n-alkane distributions in and across modern plants: Implications  
2066 for paleoecology and chemotaxonomy. *Geochimica et Cosmochimica Acta* 117, 161-179.
- 2067 Buylaert, J.-P., Ghysels, G., Murray, A.S., Thomsen, K.J., Vandenberghe, D., De Corte, F., Heyse, I., Van  
2068 den haute, P., 2009. Optical dating of relict sand wedges and composite-wedge pseudomorphs in  
2069 Flanders, Belgium. *Boreas* 38, 160–175.
- 2070 Buylaert, J.-P., Jain, M., Murray, A. S., Thomsen, K. J., Thiel, C., Sohbaty, R., 2012. A robust feldspar  
2071 luminescence dating method for Middle and Late Pleistocene sediments. *Boreas* 41, 435–451.
- 2072 Campbell, G.E., Walker, R.T., Abdrakhmatov, K., Jackson, J., Elliott, J.R., Mackenzie, D., Middleton, T.,  
2073 Schwenninger, J.L., 2015. Great earthquakes in low strain rate continental interiors: An example from SE  
2074 Kazakhstan. *Journal of Geophysical Research: Solid Earth* 120, 5507-5534.
- 2075 Carey, J.B., Cunningham, R.L., Williams, E.G., 1976. Loess identification in soils of southeastern  
2076 Pennsylvania. *Soil Science Society of America Journal* 40, 745-750.

- 2077 Catt, J.A., 1977. Loess and coversands. In: Shotton, F.W. (Ed.) *British Quaternary Studies: recent*  
2078 *advances*, Oxford University Press, 221-229.
- 2079 Chapot, M.S., Roberts, H.M., Duller, G.A.T., Lai, Z.P., 2012. A comparison of natural and laboratory-  
2080 generated dose response curves for quartz optically stimulated luminescence signals from Chinese  
2081 Loess. *Radiation Measurements* 47, 1045-1052.
- 2082 Che, X., Li, G., 2013. Binary sources of loess on the Chinese Loess Plateau revealed by U-Pb ages of  
2083 zircon. *Quaternary Research* 80, 545–551.
- 2084 Chen, J., An, Z.S., Head, J., 1999. Variation of Rb/Sr ratios in the loess-paleosol sequences of central  
2085 China during the last 130000 years and their implications for monsoon paleoclimatology. *Quaternary*  
2086 *Research* 51, 215–219.
- 2087 Chen, J., Li, G.J., Yang, J.D., Rao, W.B., Lu, H.Y., Balsam, W., Sun, Y.B., Ji, J.F., 2007. Nd and Sr isotopic  
2088 characteristics of Chinese deserts: Implications for the provenances of Asian dust. *Geochimica et*  
2089 *Cosmochimica Acta* 71, 3904-3914.
- 2090 Chen, F.H., Chen, J.H., Holmes, J., Boomer, I., Austin, P., Gates, J.B., Wang, N.L., Brooks, S.J., Zhang, J.W.,  
2091 2010. Moisture changes over the last millennium in arid central Asia: a review, synthesis and comparison  
2092 with monsoon region, *Quaternary Science Reviews* 29 (7–8), 1055-1068.
- 2093 Chlachula, J., Evans, M.E., Rutter, N.W., 1998. A magnetic investigation of a Late Quaternary  
2094 loess/palaeosol record in Siberia. *Geophysical Journal International* 132, 128-132.
- 2095 Clark, G., Pigott, S., 1965. *Prehistoric Societies*. Hutchinson, London.
- 2096 Clark, J.G.D., 1952. *Prehistoric Europe: the Economic Basis*. Methuen, London.
- 2097 Clark, P.U., Pollard, D., 1998. Origin of the middle Pleistocene transition by ice sheet erosion of regolith.  
2098 *Paleoceanography* 13, 1-9.
- 2099 Clark, P.U., Nelson, A.R., McCoy, W.D., Miller, B.B., Barnes, D.K., 1989. Quaternary aminostratigraphy of  
2100 Mississippi valley loess. *Geological Society of America Bulletin* 101, 918–926.

- 2101 Colonese, A.C., Zanchetta, G., Fallick, A.E., Manganelli, G., Saña, M., Alcade, G., Nebot, J., 2013.  
2102 Holocene snail shell isotopic record of millennial-scale hydrological conditions in western  
2103 Mediterranean: Data from Bauma del Serrat del Pont (NE Iberian Peninsula). *Quaternary International*  
2104 303, 43-53.
- 2105 Coude-Gaussen, G., 1987. The perisaharan loess: Sedimentological characterization and paleoclimatical  
2106 significance. *GeoJournal* 15, 177-183.
- 2107 Cremaschi, M., Zerboni, A., Nicosia, C., Negrino, F., Rodnight, H., Spötl, C., 2015. Age, soil-forming  
2108 processes, and archaeology of the loess deposits at the Apennine margin of the Po plain (northern Italy):  
2109 New insights from the Ghiardo area. *Quaternary International* 376, 173-188.
- 2110 Crouvi, O., 2009. Sources and formation of loess in the Negev desert during the late Quaternary, with  
2111 implications for other worldwide deserts, Institute of Earth Sciences. The Hebrew University of  
2112 Jerusalem, Jerusalem, p. 141.
- 2113 Crouvi, O., Amit, R., Enzel, Y., Porat, N., Sandler, A., 2008. Sand dunes as a major proximal dust source  
2114 for late Pleistocene loess in the Negev desert, Israel. *Quaternary Research* 70, 275-282.
- 2115 Crouvi, O., Amit, R., Enzel, Y., Gillespie, A.R., 2010. The role of active sand seas in the formation of desert  
2116 loess. *Quaternary Science Reviews* 29, 2087-2098.
- 2117 Crouvi, O., Barzilai, O., Goldsmith, Y., Amit, R., Porat, N., Enzel, Y., 2015. Middle to Late Pleistocene  
2118 drastic change in eolian silt grains additions into Mediterranean soils at the Levant's desert fringe, Israel  
2119 Geological Society Annual Meeting, Kinar, Israel.
- 2120 Crouvi, O., Amit, R., Ben Israel, M., Enzel, Y., 2017a. Loess in the Negev Desert: Sources, Loessial Soils,  
2121 Palaeosols, and Palaeoclimatic Implications, in: Enzel, Y., Bar-Yosef, O. (Eds.), *Quaternary Environments,*  
2122 *Climate Change and Humans in the Levant*. Cambridge University Press, Cambridge.
- 2123 Crouvi, O., Dayan, U., Amit, R., Enzel, Y., 2017b. An Israeli haboob: Sea breeze activating local  
2124 anthropogenic dust sources in the Negev loess. *Aeolian Research* 24, 39-52.

- 2125 Danin, A., Ganor, E., 1991. Trapping of airborne dust by mosses in the Negev Desert, Israel. *Earth Surface*  
2126 *Processes and Landforms* 16, 153-162.
- 2127 Dani, A.H., Masson, V.M. (Eds.) 1992. History of civilizations of Central Asia I: The dawn of civilization:  
2128 earliest times to 700 BC. UNESCO Publishing, Paris.
- 2129 Dansgaard, P., 1964. Stable isotopes in precipitation. *Tellus*, 16, 436-468.
- 2130 De Ploey, J., 1977. Some experimental data on slopewash and wind action with reference to Quaternary  
2131 morphogenesis in Belgium. *Earth Surface Processes* 2, 101-115.
- 2132 Dettman, D.L., Kohn, M.J., Quade, J., Ryerson, F.J., Ojha, T.P., Hamidullah, S., 2001. Seasonal stable  
2133 isotope evidence for a strong Asian monsoon throughout the past 10.7 m.y. *Geology* 29, 31-34.
- 2134 Diefendorf, A., Freeman, K., Wing, S., Graham, H., 2011. Production of n-alkyl lipids in living plants and  
2135 implications for the geologic past. *Geochimica et Cosmochimica Acta* 75, 7472-7485.
- 2136 Dietze, E., Wünnemann, B., Hartmann, K., Diekmann, B., Jin, H., Stauch, G., Yang, S., Lehmkuhl, F., 2013.  
2137 Early to mid-Holocene lake high-stand sediments at Lake Gonggi Cona, Northeastern Tibetan Plateau,  
2138 China. *Quaternary Research* 79, 325-336.
- 2139 Ding, Z., Rutter, N., Liu, T.S., 1993. Pedostratigraphy of Chinese loess deposits and climatic cycles in the  
2140 last 2.5 Myr. *Catena* 20, 73-91.
- 2141 Ding, Z.L., Yu, Z.W., Rutter, N.W., Liu, T.S., 1994. Towards an orbital time scale for Chinese loess  
2142 deposits. *Quaternary Science Reviews* 13, 39–70.
- 2143 Ding, Z., Sun, J., Rutter, N.W., Rokosh, D., Liu, T., 1999. Changes in sand content of loess deposits along a  
2144 north-south transect of the Chinese Loess Plateau and the implications for desert variations. *Quaternary*  
2145 *Research* 52, 56-62.
- 2146 Ding, Z.L., Derbyshire, E., Yang, S.L., Yu, Z.W., Xiong, S.F., Liu, T.S., 2002a. Stacked 2.6-Ma grain size  
2147 record from the Chinese loess based on five sections and correlation with the deep-sea  $\delta^{18}\text{O}$  record.  
2148 *Paleoceanography* 17, 1033.

- 2149 Ding, Z.L., Ranov, V., Yang, S.L., Finaev, A., Han, J.M., Wang, G.A., 2002b. The loess record in southern  
2150 Tajikistan and correlation with Chinese loess. *Earth and Planetary Science Letters* 200, 387-400.
- 2151 Ding, Z.L., Derbyshire, E., Yang, S.L., Sun, J.M., Liu, T.S., 2005. Stepwise expansion of desert environment  
2152 across northern China in the past 3.5 Ma and implications for monsoon evolution. *Earth and Planetary  
2153 Science Letters* 237, 45–55.
- 2154 Dirghangi, S., Pagani, M., Hren, M., Tipple, B., 2013. Distribution of glycerol dialkyl glycerol tetraethers in  
2155 soils from two environmental transects in the USA. *Organic Geochemistry* 59, 49-60.
- 2156 Dodonov, A.E., 1991. Loess of Central Asia. *GeoJournal* 24, 185-194.
- 2157 Dodonov, A.E., 2002. Quaternary of Middle Asia: Stratigraphy, Correlation, Paleogeography. *Geos,  
2158 Moscow* (in Russian).
- 2159 Dodonov, A.E., 2007. Loess records - Central Asia. In: Elias, S. (Ed.), *The Encyclopedia of Quaternary  
2160 Sciences*. Elsevier, Amsterdam, pp. 1418–1429.
- 2161 Dodonov, A.E., Baiguzina, L.L., 1995. Loess stratigraphy of Central Asia: Palaeoclimatic and  
2162 palaeoenvironmental aspects. *Quaternary Science Reviews* 14, 707-720.
- 2163 Dodonov, A.E., Zhou L., 2008. Loess deposition in Asia: its initiation and development before and during  
2164 the Quaternary. *Episodes* 31 (2), 222–225.
- 2165 Dodonov, A.E., Sadchikova, T.A., Sedov, S.N., Simakova, A.N., Zhou, L.P., 2006. Multidisciplinary  
2166 approach for paleoenvironmental reconstruction in loess-paleosol studies of the Darai Kalon section,  
2167 Southern Tajikistan. *Quaternary International* 152-153, 48-58.
- 2168 Dong, Y., Wu, N., Li, F., Huang, L., and Wen, W., 2015. Time-transgressive nature of the magnetic  
2169 susceptibility record across the Chinese loess plateau at the Pleistocene/Holocene transition. *PLoS ONE*  
2170 10, e0133541.

- 2171 Eagle, R.A., Risi, C., Mitchell, J.L., Eiler, J.M., Seibt, U., Neelin, J.D., Li, G., Tripathi, A.K., 2013. High regional  
2172 climate sensitivity over continental China constrained by glacial-recent changes in temperature and the  
2173 hydrological cycle. *Proceedings of the National Academy of Sciences* 110, 8813-8818.
- 2174 Edelman, C.H., Crommelin, R.D., 1939. Ueber die periglaziale Natur des Jungpleistozäns in den  
2175 Niederlanden. *Abhandlungen Natur Verzeichnis Bremen* 31/2, 307-318.
- 2176 Eden D.N., Qizhong, W., Hunt, J.L., Whitton, J.S., 1994. Mineralogical and geochemical trends along the  
2177 Loess Plateau, North China. *Catena* 21, 73-90.
- 2178 Ehlers, J., Eissmann L., Lippstreu L., Stephan H.-J., Wansa S., 2004. Pleistocene glaciation of North  
2179 Germany, In: Ehlers J. and Gibbard P.L. (Eds.), *Quaternary Glaciation – Extent and Chronology, Part I:  
2180 Europe (Developments in Quaternary Sciences, 2)*. Elsevier, Amsterdam, pp. 135-146.
- 2181 Ehlers, J., Grube, A., Stephan, H.J., Wansa, S., 2011. Pleistocene glaciation of North Germany – New  
2182 results, In: Ehlers J., Gibbard P.L. and Hughes P.D. (Eds.), *Quaternary Glaciation – Extent and Chronology.  
2183 A Closer Look (Developments in Quaternary Sciences, 15)*. Elsevier, Amsterdam, pp. 149-162.
- 2184 Eganhouse, R.P. (Ed.), 1997. *Molecular Markers in Environmental Geochemistry*. ACS Symposium Series  
2185 671, Washington, DC.
- 2186 Eglinton, T., Eglinton, G., 2008. Molecular proxies for paleoclimatology. *Earth and Planetary Science  
2187 Letters* 275, 1-16.
- 2188 Espizúa L.E., 2004. Pleistocene glaciations in the Mendoza Andes, Argentina. In: Ehlers, J., Gibbard, J.P.  
2189 (Eds), *Quaternary Glaciations -Extent and Chronology, Part III: South America, Asia, Africa, Australasia,  
2190 Antarctica*. Elsevier, Cambridge, pp 69–73.
- 2191 Evans, M.E., 2001. Magnetoclimatology of aeolian sediments. *Geophysical Journal International* 144,  
2192 495–497.
- 2193 Evans, M.E., Heller, F., 2003. *Environmental Magnetism – Principles and Applications of  
2194 Enviromagnetics*. Academic Press, Amsterdam.

- 2195 Evans, M.N., Tolwinski-Ward, S.E., Thompson, D.M., Anchukaitis, K.J., 2013. Applications of proxy system  
2196 modeling in high resolution paleoclimatology. *Quaternary Science Reviews* 76, 16-28.
- 2197 FAO/IIASA/ISRIC/ISSCAS/JRC, 2009. Harmonized World Soil Database (version 1.1). FAO, Rome, Italy and  
2198 IIASA, Laxenburg, Austria.
- 2199 Fedo, C.M., Sircombe, K.N., Rainbird, R.H., 2003. Detrital zircon analysis of the sedimentary record.  
2200 *Reviews in Mineralogy and Geochemistry* 53, 277-303.
- 2201 Fehrenbacher, J.B., White, J.L., Ulrich, H.P., Odell, R.T., 1965. Loess distribution in southeastern Illinois  
2202 and southwestern Indiana. *Soil Science Society of America Proceedings* 29, 566-572.
- 2203 Feng, Z.D., Ran, M., Yang, Q.L., Zhai, X.W., Wang, W., Zhang, X.S., Huang, C.Q., 2011. Stratigraphies and  
2204 chronologies of late Quaternary loess-paleosol sequences in the core area of the central Asian arid zone.  
2205 *Quaternary International* 240, 156-166.
- 2206 Fenn, K., Stevens, T., Bird, A., Limonta, M., Rittner, M., Vermeesch, P., Andò, S., Garzanti, E., Lu, H.,  
2207 Zhang, H., Lin, Z., in press. Insights into the provenance of the Chinese Loess Plateau from joint zircon U-  
2208 Pb and garnet geochemical analysis of last glacial loess. *Quaternary Research*.
- 2209 Fink, J., 1956. Zur Korrelation der Terrassen und Lössen in Österreich. *Eiszeitalter und Gegenwart* 7, 49-  
2210 77.
- 2211 Fink, J., 1962. Studien zur absoluten und relativen Chronologie der fossilen Böden in Österreich, II  
2212 Wetzleinsdorf und Stillfried. *Archaeol. Austriaca* 31, 1- 18.
- 2213 Fink, J., Haase, G., Ruske, R., 1977. Bemerkungen zur Lößkarte von Europe 1:2,5 Mio. *Petermanns*  
2214 *Geographische Mitteilungen* 2 (77), 81–94.
- 2215 Fink, J., Kukla, G., 1977. Pleistocene climates in Central Europe: at least 17 interglacials after the Olduvai  
2216 event. *Quaternary Research* 7, 363–371.
- 2217 Fisher, R.V., 1961. Proposed classification of volcanoclastic sediments and rocks. *Geological Society of*  
2218 *America Bulletin* 72, 1409-1414.



- 2219 Fitzsimmons, K.E., Sprafke, T., Zielhofer, C., Günter, C., Deom, J.-M., Sala, R., Iovita, R., in press. Loess  
2220 accumulation in the Tian Shan piedmont: Implications for palaeoenvironmental change in arid Central  
2221 Asia. *Quaternary International*.
- 2222 Fitzsimmons, K., Marković, S.B., Hambach, U., 2012. Pleistocene environmental dynamics recorded in  
2223 the loess of the middle and lower Danube basin. *Quaternary Science Reviews* 41, 104–118.
- 2224 Follmer, L.R., 1996. Loess studies in central United States: Evolution of concepts. *Engineering Geology*  
2225 45, 287-304.
- 2226 Forman, S.L., Pierson, J., 2002. Late Pleistocene luminescence chronology of loess deposition in the  
2227 Missouri and Mississippi river valleys, United States. *Palaeogeography Palaeoclimatology Palaeoecology*  
2228 186, 25-46.
- 2229 Forman, S.L., Bettis, E.A., III, Kemmis, T.J., Miller, B.B., 1992. Chronological evidence for multiple periods  
2230 of loess deposition during the Late Pleistocene in the Missouri and Mississippi River Valleys, U.S.:  
2231 Implications for the activity of the Laurentide Ice Sheet. *Palaeogeography Palaeoclimatology*  
2232 *Palaeoecology* 93, 71-83.
- 2233 Forster, T., Evans, M.E., Heller, F., 1994. The frequency dependence of low field susceptibility in loess  
2234 sediments. *Geophysical Journal International*. 118, 636–642.
- 2235 Foss, J.E., Fanning, D.S., Miller, F.P., Wagner, D.P., 1978. Loess deposits of the eastern shore of  
2236 Maryland. *Soil Science Society of America Journal* 42, 329-334.
- 2237 Frazee, C.J., Fehrenbacher, J.B., Krumbein, W.C., 1970. Loess distribution from a source. *Soil Science*  
2238 *Society of America Proceedings* 34, 296-301.
- 2239 Gallet, S., Jahn, B.M., Torii, M., 1996. Geochemical characterization of the Luochuan loess-paleosol  
2240 sequence China, and paleoclimatic implications. *Chemical Geology* 133, 67–88.

- 2241 Gallet, S., Jahn, B., Van Vliet-Lannoë, B., Dia, A., Rossello, E.A., 1998. Loess geochemistry and its  
2242 implications for particle origin and composition of the upper continental crust. *Earth and Planetary  
2243 Science Letters* 156, 157-172.
- 2244 Gao, X. B., Hao, Q. Z., Wang, L., Oldfield, F., Bloemendal, J., Deng, C. L., Song, Y., Ge, J. Y., Wu, H. B., Xu,  
2245 B., Li, F. J., Han, L., Fu, Yu, Guo, Z.T., 2018. The different climatic response of pedogenic hematite and  
2246 ferrimagnetic minerals: Evidence from particle-sized modern soils over the Chinese Loess Plateau.  
2247 *Quaternary Science Reviews*, 179, 69-86
- 2248 Gat, J.R., Bowser, C., 1991. The heavy isotope enrichment of water in coupled evaporative systems. In:  
2249 Taylor, H.P., O'Neil, J.R., Kaplan, I.R. (Eds.), *Stable Isotope Geochemistry: A Tribute to Samuel Epstein*.  
2250 The Geochemical Society, Lancaster, pp. 159–168.
- 2251 Ge, J. Y., Guo, Z. T., Zhao, D. A., Zhang, Y., Wang, T., Yi, L., Deng, C. L., 2014. Spatial variations in  
2252 paleowind direction during the last glacial period in North China reconstructed from variations in the  
2253 anisotropy of magnetic susceptibility of loess deposits. *Tectonophysics*, 629, 353-361.
- 2254 Gerasimenko, N. P., 2006. Upper Pleistocene loess-palaeosol and vegetational successions in the Middle  
2255 Dnieper Area, Ukraine. *Quaternary International* 149, 5566.
- 2256 Gibbard, P.L., Cohen, K.M., 2008. Global chronostratigraphical correlation table for the last 2.7 million  
2257 years. *Episodes* 31, 243-247.
- 2258 Gild, C., Geitner, C., Sanders, D., 2017. Discovery of a landscape-wide drape of late-glacial aeolian silt in  
2259 the western Northern Calcareous Alps (Austria): First results and implications. *Geomorphology* 301, 39-  
2260 52.
- 2261 González Bonorino, F., 1966. Soil clay mineralogy of the Pampas plain, Argentina. *Journal of Sedimentary  
2262 Petrology* 36, 1026-1035.
- 2263 Good, T.R., Bryant, I.D., 1985. Fluvio-aeolian sedimentation - an example from Banks island, N.W.T.  
2264 Canada. *Geografiska Annaler* 67A, 33-46.

- 2265 Gong, H., Xie, W., Zhang, R., Zhang, Y., 2017. U-Pb ages of detrital zircon and provenances of Red Clay in  
2266 the Chinese Loess Plateau. *Journal of Asian Earth Sciences* 138, 495-501.
- 2267 Gozdzik, J., 1991. Sedimentological record of aeolian processes from the Upper Plenivistulian and the  
2268 turn of Pleni-and Late Vistulian in Central Poland. *Zeitschrift für Geomorphologie, Suppl. Bd. 90*, 51-60.
- 2269 Grahmann, R., 1932. Der Löss in Europa. *Mitteilungen der Gesellschaft für Erkunde Leipzig* 51, 5-24.
- 2270 Greene, R.S.B., Cattle, S.R., McPherson, A.A., 2009. Role of eolian dust deposits in landscape  
2271 development and soil degradation in southeastern Australia. *Australian Journal of Earth Sciences* 56,  
2272 S55–S65.
- 2273 Grenet, F., de la Vaissière, E., 2002. The Last Days of Panjikent. *Silk Road Art and Archaeology* 8, 155–96.
- 2274 Grichuk, V. P., 1992. Main types of vegetation (ecosystems) for the maximum cooling of the last  
2275 glaciation. In: Frenzel, B., Pecsli, B. Velichko, A.A. (Eds.), *Atlas of Palaeoclimates and Palaeoenvironments*  
2276 *of the Northern Hemisphere*. INQUA/Hungarian Academy of Sciences, Budapest, pp. 123-124.
- 2277 Grimley, D.A., 1996. Stratigraphy, Magnetic Susceptibility, and Mineralogy of Loess-Paleosol sequences  
2278 in Southwestern Illinois and Eastern Missouri. Ph.D. thesis, University of Illinois, Urbana.
- 2279 Grimley, D.A., 2000. Glacial and nonglacial sediment contributions to Wisconsin Episode loess in the  
2280 central United States. *Geological Society of America Bulletin* 112, 1475-1495.
- 2281 Grimley, D.A., Oches, E.A., 2015. Amino acid geochronology of gastropod-bearing Pleistocene units in  
2282 Illinois, central USA. *Quaternary Geochronology* 25, 10-25.
- 2283 Gronenborn, D. 2010. Climate, crises, and the neolithisation of central Europe between IRD-events 6 and  
2284 4. In: Gronenborn, D., Petrasch, J. (Eds.) *The Spread of the Neolithic to central Europe*. International  
2285 Symposium, Mainz 24 June–26 June 2005, Mainz: Verlag des Römisch-Germanischen Zentralmuseums,  
2286 pp. 61–81.

- 2287 Grützner, C., Carson, E., Walker, R.T., Rhodes, E.J., Mukambayev, A., Mackenzie, D., Elliott, J.R.,  
2288 Campbell, G., Abdrakhmatov, K., 2017. Assessing the activity of faults in continental interiors:  
2289 Palaeoseismic insights from SE Kazakhstan. *Earth and Planetary Science Letters* 459, 93-104.
- 2290 Gullentops, F., 1954. Contributions à la chronologie du pleistocène et des formes du relief en Belgique.  
2291 *Mémoires Institut Géologique de Louvain* 18, 125-252.
- 2292 Guo, Z. T., Ruddiman, W. F., Hao, Q. Z., Wu, H. B., Qiao, Y. S., Zhu, R. X., Peng, S. Z., Wei, J. J., Yuan, B. Y.,  
2293 Liu, T. S., 2002. Onset of Asian desertification by 22 Myr ago inferred from loess deposits in China.  
2294 *Nature*, 416(6877), 159-163.
- 2295 Guo, Z. T., Berger, A., Yin, Q. Z., Qin, L., 2009. Strong asymmetry of hemispheric climates during MIS-13  
2296 inferred from correlating China loess and Antarctica ice records. *Climate of the Past*, 5(1), 21-31.
- 2297 Haase, D., Fink, J., Haase, G., Ruske, R., Pécsi, M., Richter, H., Altermann, M., Jäger, K.D., 2007. Loess in  
2298 Europe—its spatial distribution based on a European Loess Map, scale 1:2,500,000. *Quaternary Science*  
2299 *Reviews*, 26, 1301-1312.
- 2300 Haas, M., Bliedtner, M., Borodynkin, I., Salazar, G., Szidat, S., Eglinton, T., Zech, R., 2017. Radiocarbon  
2301 Dating of Leaf Waxes in the Loess-Paleosol Sequence Kurtak, Central Siberia. *Radiocarbon* 59(1), 165-  
2302 176.
- 2303 Haesaerts, P., Borziak, I., Chirica, V., Damblon, F., Koulakovska, L., van der Plicht, J., 2003. The east  
2304 Carpathian loess record: a reference for the middle and late pleniglacial stratigraphy in central Europe.  
2305 *Quaternaire* 14, 163-188.
- 2306 Haesaerts, P., Damblon, F., Gerasimenko, N., Spagna, P., Pirson, S., 2016. The Late Pleistocene loess-  
2307 palaeosol sequence of Middle Belgium. *Quaternary International* 411, 25-43.
- 2308 Hajdas, I., 2008. Radiocarbon dating and its application in Quaternary studies. *E&G Quaternary Science*  
2309 *Journal* 57, 2-24.

- 2310 Hambach, U., 2010. Palaeoclimatic and Stratigraphic Implications of High Resolution Magnetic  
2311 Susceptibility Logging of Würmian Loess at the Upper Palaeolithic Krems-Wachtberg Site, in: Friesinger,  
2312 H. (Ed.), *New Aspects of the Central and Eastern European Upper Palaeolithic – methods, chronology,*  
2313 *technology and subsistence*, Mitteilungen der Prähistorischen Kommission. Verlag der Österreichischen  
2314 Akademie der Wissenschaften, Wien, pp. 295–304.
- 2315 Hamilton, T.D., Craig, J.L., Sellmann, P.V., 1988. The Fox permafrost tunnel: A late Quaternary geologic  
2316 record in central Alaska: *Geological Society of America Bulletin* 100, 948-969.
- 2317 Handy, R., 1976. Loess distribution by variable winds. *Geological Society of America Bulletin* 87, 915-927.
- 2318 Hao, Q., Guo Z., 2004. Magnetostratigraphy of a late Miocene-Pliocene loess-soil sequence in the  
2319 western Loess Plateau in China. *Geophysical Research Letters*, 31: L092099.
- 2320 Hao, Q.Z., Wang, L., Oldfield, F., Peng, S.Z., Qin, L., Song, Y., Xu, B., Qiao, Y., Bloemendal, J., Guo, Z.T.,  
2321 2012. Delayed build-up of Arctic ice sheets during 400,000-year minima in insolation variability. *Nature*  
2322 490, 393–396.
- 2323 Hatté, C., Fontugne, M., Rousseau, D.D., Antoine, P., Zöller, L., Tisnérat-Laborde, N., Bentaleb, I., 1998.  
2324  $\delta^{13}\text{C}$  variations of loess organic matter as a record of the vegetation response to climatic changes  
2325 during the Weichselian. *Geology* 26, 583-586.
- 2326 Hatté, C., Gauthier, C., Rousseau, D.D., Antoine, P., Fuchs, M., Lacroix, F., Markovic, S.B., Moine, O.,  
2327 Sima, A., 2013. Excursions to C4 vegetation recorded in the upper Pleistocene loess of Surduk (Northern  
2328 Serbia): An organic isotope geochemistry study. *Climate of the Past* 9, 1001-1014.
- 2329 Häggi, C., Zech, R., McIntyre, C., Zech, M., Eglinton, T., 2014. On the stratigraphic integrity of leaf-wax  
2330 biomarkers in loess paleosol. *Biogeosciences* 11, 2455-2463.
- 2331 Hawkesworth, C.J., Kemp, A.I.S., 2006. Using hafnium and oxygen isotopes in zircons to unravel the  
2332 record of crustal evolution. *Chemical Geology* 226, 144-162.
- 2333 Heller F, Evans, M.A. 1995. Loess Magnetism. *Reviews of Geophysics* 33, 211-240.

- 2334 Heller, F., Liu, T., 1982. Magnetostratigraphical dating of loess deposits in China. *Nature* 300, 431–433.
- 2335 Heller F, Liu T., 1984. Magnetism of Chinese loess deposits. *Journal of the Royal Astronomical Society* 77,  
2336 125–141.
- 2337 Heller, F., Liu, X., Liu, T., Xu, T., 1991. Magnetic susceptibility of loess in China. *Earth and Planetary*  
2338 *Science Letters* 103, 301–310.
- 2339 Heller, F., Shen, C.D., Beer, J., Liu, X.M., Liu, T.S., Bronger, A., Suter, M., Bonani, G., 1993. Quantitative  
2340 estimates of pedogenic ferromagnetic mineral formation in Chinese loess and paleoclimatic  
2341 implications. *Earth and Planetary Science Letters* 114, 385-390.
- 2342 Hepp, J., Zech, R., Rozanski, K., Tuthorn, M., Glaser, B., Greule, M., Keppler, F., Huang, Y., Zech, W., Zech,  
2343 M., 2017. Late Quaternary relative humidity changes from Mt. Kilimanjaro, based on a coupled  $^2\text{H}$ - $^{18}\text{O}$   
2344 biomarker paleohygrometer approach. *Quaternary International* 438, Part B, 116-130.
- 2345 Heslop, D., Langereis, C.G., Dekkers, M.J., 2000. A new astronomical timescale for the loess deposits of  
2346 Northern China. *Earth and Planetary Science Letters* 184, 125–139.
- 2347 Hesse, P.P., McTainsh, G.H., 2003. Australian dust deposits: modern processes and the Quaternary  
2348 record. *Quaternary Science Reviews* 22, 2007–2035.
- 2349 Ho, P., 1976. *The Cradle of the East: An enquiry into the indigenous origins of techniques and ideas of*  
2350 *Neolithic and Early Historic China 5000-1000 BC*. Chinese University of Hong Kong Press, Hong Kong.
- 2351 Höfle, C., Ping, C.-L., 1996. Properties and soil development of late- Pleistocene paleosols from Seward  
2352 Peninsula, northwest Alaska. *Geoderma* 71, 219–243.
- 2353 Höfle, C., Edwards, M.E., Hopkins, D.M., and Mann, D.H., 2000. The full-glacial environment of the  
2354 northern Seward Peninsula, Alaska, reconstructed from the 21,500-year-old Kitluk paleosol. *Quaternary*  
2355 *Research* 53, 143-153.
- 2356 Hopkins, D.M., 1963. *Geology of the Imuruk Lake area, Seward Peninsula, Alaska*. U.S. Geological Survey  
2357 *Bulletin* 1141-C.

- 2358 Hu, J., Yang, X., 2016. Geochemical and geomorphological evidence for the provenance of the eolian  
2359 deposits in the Badain Jaran Desert, northwestern China. *Quaternary Science Reviews* 131, 179-192.
- 2360 Huijzer, A.S., 1993. Cryogenic microfabrics and macrostructures: interrelations, processes and  
2361 paleoclimatic significance. PhD Thesis, Vrije Universiteit, Amsterdam, 245 pp.
- 2362 Hunt, R.M., 1990. Taphonomy and sedimentology of Arikaree (lower Miocene) fluvial, eolian, and  
2363 lacustrine paleoenvironments, Nebraska and Wyoming: a paleobiota entombed in fine-grained  
2364 volcanoclastic rocks, In: Lockley, M.G., Rice, A. (Eds.), *Volcanism and fossil biotas*. Geological Society of  
2365 America, Special Paper 244, Boulder, Colorado, pp. 69-112.
- 2366 Ijmker, J., Stauch, G., Dietze, E., Hartmann, K., Diekmann, B., Lockot, G., Opitz, S., Wünnemann, B.,  
2367 Lehmkuhl, F., 2012. Characterisation of transport process and sedimentary deposits by statistical end-  
2368 member mixing analysis of terrestrial sediments in the Donggi Cona lake catchment, NE Tibet Plateau.  
2369 *Sedimentary Geology* 281, 166-179.
- 2370 Imbrie, J., Imbrie, J.Z., 1980. Modeling the Climatic Response to Orbital Variations. *Science* 207, 943–  
2371 953.
- 2372 Indorante, S.J., 1998. Introspection of natric soil genesis on the loess-covered till plain in south central  
2373 Illinois. *Quaternary International* 51, 41-42.
- 2374 Iriondo M., 1990. Map of the South American plains – Its present state. *Quaternary of South America*  
2375 *and Antarctic Peninsula*. Vol. 6. pp. 297–308.
- 2376 Iriondo, M.H., Kröhling, D.M., 2007. Non-classical types of loess. *Sedimentary Geology* 202, 352-368.
- 2377 Jacobs, P.M., Knox, J.C., 1994. Provenance and petrology of a long-term Pleistocene depositional  
2378 sequence in Wisconsin's Driftless Area. *Catena* 22, 49-68.
- 2379 Jacobs, P.M., Mason, J.A., Hanson, P.R., 2012. Loess mantle spatial variability and soil horizonation,  
2380 southern Wisconsin, USA. *Quaternary International* 265, 42-53.



- 2381 Janh, B., Gallet, S., Han, J., 2001. Geochemistry of the Xining, Xifeng and Jixian sections, Loess Plateau of  
2382 China: eolian dust provenance and paleosol evolution during the last 140 ka. *Chemical Geology* 178, 71-  
2383 94.
- 2384 Jensen, B.J.L., Reyes, A.V. Froese, D.G., Stone, D.B., 2013. The Palisades is a key reference site for the  
2385 middle Pleistocene of eastern Beringia: new evidence from paleomagnetism and regional  
2386 tephrostratigraphy. *Quaternary Science Reviews* 63, 91-108.
- 2387 Jensen, B.J.L., Evans, M.E., Froese, D.G., Kravchinsky, V.A., 2016. 150,000 years of loess accumulation in  
2388 central Alaska. *Quaternary Science Reviews* 135, 1-23.
- 2389 Jia, G., Rao, Z., Zhang, J., Li, Z., Chen, F., 2013. Tetraether biomarker records from a loess-paleosol  
2390 sequence in the western Chinese Loess Plateau. *Frontiers in Microbiology* 4,  
2391 doi:10.3389/fmicb.2013.00199.
- 2392 Jiang, W., Cheng, Y., Yang, X., Yang, S., 2013. Chinese Loess Plateau vegetation since the Last Glacial  
2393 Maximum and its implications for vegetation restoration. *Journal of Applied Ecology* 50, 440–448.
- 2394 Jiang, W., Yang, X., Cheng, Y., 2014. Spatial patterns of vegetation and climate on the Chinese Loess  
2395 Plateau since the Last Glacial Maximum. *Quaternary International* 334-335, 52–60.
- 2396 Jipa, D. C., 2014. The conceptual sedimentary model of the Lower Danube loess basin: Sedimentogenetic  
2397 implications. *Quaternary International* 351, 14-24.
- 2398 Johnson, W.C., Willey, K.L., 2000. Isotopic and rock magnetic expression of environmental change at the  
2399 Pleistocene-Holocene transition in the central Great Plains. *Quaternary International* 67, 89-106.
- 2400 Johnson, W.C., Willey, K.L., Mason, J.A., May, D.W., 2007. Stratigraphy and environmental  
2401 reconstruction at the middle Wisconsinan Gilman Canyon Formation type locality, Buzzard's Roost,  
2402 southwestern Nebraska, USA. *Quaternary Research* 67, 474-486.
- 2403 Kasse, C., 1993. Periglacial environments and climate development during the Early Pleistocene Tiglian  
2404 stage (Beerse Glacial) in northern Belgium. *Geologie en Mijnbouw* 72, 107-123.

- 2405 Kasse, C., 1997. Cold-Climatic aeolian sand-sheet formation in North-Western Europe (c. 14-12.4 ka): a  
2406 response to permafrost degradation and increased aridity. *Permafrost and Periglacial Processes* 8, 295-  
2407 311.
- 2408 Kasse, C., 1999. Late Pleniglacial and Late Glacial aeolian phases in The Netherlands. In: Schirmer (ed.)  
2409 "Dunes and fossil soils". *GeoArchaeoRhein* 3, 61-82.
- 2410 Kasse, C., 2002. Sandy aeolian deposits and environments and their relation to climate during the Last  
2411 Glacial Maximum and Lateglacial in northwest and central Europe. *Progress in Physical Geography* 26,  
2412 507–532.
- 2413 Kasse, C., Vandenberghe, D., De Corte, F., Van den Haute, P., 2007. Late Weichselian fluvio-aeolian sands  
2414 and coversands of the type locality Grubbenvorst (southern Netherlands): sedimentary environments,  
2415 climate record and age. *Journal of Quaternary Science* 22, 695–708.
- 2416 Karrow, P.F., McAndrews, J.H., Miller, B.B., Morgan, A.V., Seymour, K.L., White, O.L., 2001. Illinoian to  
2417 Late Wisconsinan stratigraphy at Woodbridge, Ontario. *Canadian Journal of Earth Science* 38: 921–942.
- 2418 Kaufman, D.S., Manley, W.F., 1998. A new procedure for determining D/L amino acid ratios in fossils  
2419 using reverse phase liquid chromatography. *Quaternary Science Reviews* 17, 987-1000.
- 2420 Kaufman, D.S., Manley, W.F., Ager, T.A., Axford, Y., Balascio, N.L., Begét, J.E., Brigham-Grette, J., Briner,  
2421 J.P., Bundtzen, T.K., Carraara, P., Hamilton, T.D., Lubinski, D.J., Reger, R.D., Schmoll, H.R., Thorson, R.M.,  
2422 Waythomas, C.F., Weber, F.R., Werner, A., Wilson, F.H., 2004. Pleistocene maximum and late  
2423 Wisconsinan glacier extents across Alaska, U.S.A. In: Ehlers, J., Gibbard, P.L., eds., *Quaternary*  
2424 *Glaciations-Extent and Chronology, Part II*. Amsterdam, Elsevier, *Developments in Quaternary Science* 2,  
2425 pp. 9-27.
- 2426 Kehl, M., Sahvati, R., Ahmadi, H., Frechen, M., Skowronek, A., 2005. Loess paleosol-sequences along a  
2427 climatic gradient in Northern Iran. *Eiszeitalter und Gegenwart* 55, 149-173.

- 2428 Kehrwald, N.M., McCoy, W.D., Thibeault, J., Burns, S.J., Oches, E.A., 2010. Paleoclimatic implications of  
2429 the spatial patterns of modern and LGM European land-snail shell d18O. *Quaternary Research* 74, 166-  
2430 176.
- 2431 Kleiss, H.J., 1973. Loess distribution along the Illinois soil-development sequence. *Soil Science* 115, 194-  
2432 198.
- 2433 Koloszar, L., 2010. The thickest and the most complete loess sequence in the Carpathian basin: the  
2434 borehole Udvari-2A. *Open Geosciences* 2, 165-174.
- 2435 Koppes, M., Gillespie, A.R., Burke, R.M., Thompson, S.C., Stone, J., 2008. Late Quaternary glaciation in  
2436 the Kyrgyz Tien Shan. *Quaternary Science Reviews* 27, 846-866.
- 2437 Koster, E., 1988. Ancient and modern cold-climate aeolian sand deposition. *Journal of Quaternary*  
2438 *Science* 3, 69-83.
- 2439 Kozarski, S., 1990. Pleni-and Late Vistulian aeolian phenomena in Poland : new occurrences,  
2440 palaeoenvironmental and stratigraphic interpretations. *Acta Geographica Debrecina* 1987-1988, 26-27,  
2441 31-45.
- 2442 Kruk, J., Milisauskas, S., 1999. The Rise and Fall of Neolithic Societies [In Polish]. Polish Academy of  
2443 Sciences, Cracow.
- 2444 Kruk, J., Alexadrowicz, S., Milisauskas, S., Śnieszko, Z., 1996. Environmental Changes and Settlement on  
2445 the Loess Uplands [In Polish]. Polish Academy of Sciences, Cracow.
- 2446 Kukla, G.J., 1975. Loess stratigraphy of Central Europe, In: After the Australopithecines, Butzer, K.W.,  
2447 Isaac, L.I. (Eds). Mouton Publishers, The Hague, pp. 99-187.
- 2448 Kukla, G., 1977. Pleistocene land-sea correlations. 1. Europe. *Earth-Science Reviews* 13, 307-374.
- 2449 Kukla, G., 1987. Loess stratigraphy in central China. *Quaternary Science Reviews* 6, 191-219.

- 2450 Kukla, G., An, Z., 1989. Loess stratigraphy in Central China. *Palaeogeography, Palaeoclimatology,*  
2451 *Palaeoecology* 72, 203-225.
- 2452 Kukla, G., Heller, F., Liu, X., Xu, T., Liu, T., An, Z., 1988. Pleistocene climates in China dated by magnetic  
2453 susceptibility. *Geology*, 16(9), 811-814.
- 2454 LaGarry, H.E., 1998. Lithostratigraphic revision and redescription of the Brule Formation (White River  
2455 Group) of northwestern Nebraska,, In: Terry, D.O., Jr, LaGarry, H.E., Hunt, R.M., Jr (Eds.), *Depositional*  
2456 *Environments, Lithostratigraphy, and Biostratigraphy of the White River and Arikaree Groups (Late*  
2457 *Eocene-Early Miocene, North America)*. Geological Society of America Special Paper 325, Boulder,  
2458 Colorado, pp. 63-91.
- 2459 Lagroix, F., Banerjee, S. K., 2004. The regional and temporal significance of primary aeolian magnetic  
2460 fabrics preserved in Alaskan loess. *Earth and Planetary Science Letters*, 225(3), 379-395.
- 2461 Lambert, F., Delmonte, B., Petit, J. R., Bigler, M., Kaufmann, P. R., Hutterli, M. A., Stocker, T. F., Ruth, U.,  
2462 Steffensen, J. P., Maggi, V., 2008. Dust-climate couplings over the past 800000 years from the EPICA  
2463 Dome C ice core. *Nature*, 452, 616–619.
- 2464 Laskar, J., Robutel, P., Joutel, F., Gastineau, M., Correia, A.C.M., Levrard, B., 2004. A long-term numerical  
2465 solution for the insolation quantities of the Earth. *Astronomy Astrophysics* 428, 261–285.
- 2466 Lautridou, J.-P., 1981. Lithostratigraphie et chronostratigraphie des loess de Haute Normandie. In: Pécsi,  
2467 M. (Ed.), *Studies on Loess. Acta Geol. Acad. Sciences Hungaricae* 1979, 22, 1-4, 125-132.
- 2468 Lautridou, J.-P., Sommé, J., 1981. L'extension des niveaux repères périglaciaires et grandes fentes de gel  
2469 de la stratigraphie du Pleistocène Récent de la France du Nord-Ouest. *Biuletyn Peryglacjalny* 28, 179-  
2470 185.
- 2471 Lautridou J.P., Sommé J., Jamagne M., 1984. Sedimentological, mineralogical and geochemical  
2472 characteristics of the loess of North-Western France. In: Pécsi, M. (ed.) *Lithology and Stratigraphy of*  
2473 *Loess and Paleosols*. Geographical Research Institute of the Hungarian Academy of Science, Budapest,  
2474 121-132.

- 2475 Lea, P.D., 1990. Pleistocene periglacial eolian deposits in southwestern Alaska: sedimentary facies and  
2476 depositional processes. *Journal of Sedimentary Petrology* 60, 582-591.
- 2477 Lea, P.D., Waythomas, C.F., 1990. Late-Pleistocene eolian sand sheets in Alaska. *Quaternary Research*  
2478 34, 269-281.
- 2479 Leigh, D.S., 1994. Roxana Silt of the Upper Mississippi Valley: Lithology, source, and paleoenvironment.  
2480 *Geological Society of America Bulletin* 106, 430-442.
- 2481 Leigh, D.S., Knox, J.C., 1994. Loess of the Upper Mississippi Valley Driftless Area. *Quaternary Research*  
2482 42, 30-40.
- 2483 Lehmkuhl, F., Haselein, F., 2000. Quaternary paleoenvironmental change on the Tibetan Plateau and  
2484 adjacent areas (Western China and Western Mongolia). *Quaternary International* 65, 121-145.
- 2485 Lehmkuhl, F., Hilgers, A., Fries, S., Hülle, D., Schlütz, F., Shumilovskikh, L., Felauer, T., Protze, J., 2011.  
2486 Holocene geomorphological processes and soil development as indicator for environmental change  
2487 around Karakorum, Upper Orkhon Valley (Central Mongolia). *Catena* 87, 31-44.
- 2488 Lehmkuhl, F., Schulte, P., Zhao, H., Hülle, D., Protze, J., Stauch, G., 2014. Timing and spatial distribution  
2489 of loess and loess-like sediments in the mountain areas of the northeastern Tibetan Plateau. *Catena* 117,  
2490 23-33.
- 2491 Lehmkuhl, F., Zens, J., Krauß, L., Schulte, P., Kels, H., 2016. Loess-paleosol sequences at the northern  
2492 European loess-belt in Germany: distribution, geomorphology and stratigraphy. *Quaternary Science*  
2493 *Reviews* 153: 11-30.
- 2494 Leonard, A.B., Frye, J.C., 1960. Wisconsinan molluscan faunas of the Illinois Valley region. *Illinois*  
2495 *Geological Survey Circular* 304, 32 p.
- 2496 Li, B., Li, S.-H., 2012. Luminescence dating of Chinese loess beyond 130 ka using the non-fading signal  
2497 from K-feldspar. *Quaternary Geochronology* 10, 24–31.

- 2498 Li, F., Wu, N., Pei, Y., Hao, Q., Rousseau, D-D. 2006. Wind-blown origin of Dongwan late Miocene–  
2499 Pliocene dust sequence documented by land snail record in western Chinese Loess Plateau. *Geology* 34,  
2500 405-408.
- 2501 Li, Y., Yang, S., Wang, X., Hu, J., Cui, L., Huang, X., Jiang, W., 2016a. Leaf wax n-alkane distributions in  
2502 Chinese loess since the Last Glacial Maximum and implications for paleoclimate. *Quaternary*  
2503 *International* 399, 190–197.
- 2504 Li, Y., Song, Y., Chen, X., Li, J., Mamadjanov, Y., Aminov, J., 2016b. Geochemical composition of Tajikistan  
2505 loess and its provenance implications. *Palaeogeography, Palaeoclimatology, Palaeoecology* 446, 186-  
2506 194.
- 2507 Liang, Y., Yang, T. B., Velichko, A. A., Zeng, B., Shi, P. H., Wang, L. D., Chen, Y., 2016. Paleoclimatic record  
2508 from Chumbur-Kosa section in Sea of Azov region since Marine Isotope Stage 11. *Journal of Mountain*  
2509 *Science* 13, 985-999.
- 2510 Licht, A., Pullen, A., Kapp, P., Abell, J., Gieser, N., 2016. Eolian cannibalism: reworked loess and fluvial  
2511 sediment as the main sources of the Chinese Loess Plateau. *Geological Society of America Bulletin* 128,  
2512 944-956.
- 2513 Lisiecki, L. E., M. E. Raymo., 2005. A Pliocene-Pleistocene stack of 57 globally distributed benthic  $\delta^{18}\text{O}$   
2514 records, *Paleoceanography*, 20, PA1003.
- 2515 Litaor, M.I., 1987. The influence of eolian dust on the genesis of alpine soils in the Front Range,  
2516 Colorado. *Soil Science Society of America Journal* 51, 142-147.
- 2517 Liu, C.-Q., Masuda, A., Okada, A., Yabuki, S., Zhang, J., Fan, Z.-L., 1993. A geochemical study of loess and  
2518 desert sand in northern China: implications for continental crust weathering and composition. *Chemical*  
2519 *Geology* 106, 359-374.
- 2520 Liu, J., Murray, A.S., Buylaert, J.-P., Jain, M., Chen, J., Lu, Y., 2016. Stability of fine-grained TT-OSL and  
2521 post-IR IRSL signals from a c. 1 Ma sequence of aeolian and lacustrine deposits from the Nihewan Basin  
2522 (northern China). *Boreas* 45, 703-714.

- 2523 Liu, Q. S., A. P. Roberts, J. C. Larrasoana, S. K. Banerjee, Y. Guyodo, L. Tauxe, F. Oldfield, 2012.  
2524 Environmental magnetism: Principles and applications. *Reviews of Geophysics* 50, RG4002.
- 2525 Liu, T.S., 1966. *Composition and Texture of Loess*. Science Press, Beijing.
- 2526 Liu, T. S, 1985. *Loess and Environment*. China Ocean Press, Beijing 1-106.
- 2527 Liu, T., Ding, Z., 1998. Chinese loess and the paleomonsoon. *Annual Review of Earth and Planetary*  
2528 *Sciences* 26, 111–145.
- 2529 Liu, W., Huang, Y., 2005. Compound specific D/H ratios and molecular distributions of higher plant leaf  
2530 waxes as novel paleoenvironmental indicators in the Chinese Loess Plateau. *Organic Geochemistry*, 36,  
2531 851-860.
- 2532 Liu, W., Sun, J. 2012. High-resolution anisotropy of magnetic susceptibility record in the central Chinese  
2533 Loess Plateau and its paleoenvironment implications. *Science China Earth Science* 55(3), 488–494.
- 2534 Liu, W., Huang, Y., An, Z., Clemens, S.C., Li, L., Prell, W.L., Ning, Y., 2005. Summer monsoon intensity  
2535 controls C<sub>4</sub>/C<sub>3</sub> plant abundance during the last 35 ka in the Chinese Loess Plateau: Carbon isotope  
2536 evidence from bulk organic matter and individual leaf waxes. *Palaeogeography, Palaeoclimatology,*  
2537 *Palaeoecology* 220, 243-254.
- 2538 Liu, W., Yang, H., Sun, Y., Wang, X., 2011.  $\delta^{13}\text{C}$  Values of loess total carbonate: A sensitive proxy for Asian  
2539 summer monsoon in arid northwestern margin of the Chinese loess plateau. *Chemical Geology* 284,  
2540 317–322.
- 2541 Liu, X, 2010. *The Silk Road in World History*. Oxford University Press.
- 2542 Lorenzo, F., Mehl A., Zárate M., 2017. Dinámica fluvial y sedimentología del humedal Bañados del Atuel,  
2543 provincia de La Pampa, Argentina ACTAS XX Congreso Geológico Argentino, San Miguel de Tucumán, 91-  
2544 93.
- 2545 Lu, H., An, Z., 1998. Paleoclimatic significance of grain size of loess-palaeosol deposit in Chinese Loess  
2546 Plateau. *Science in China* 41D, 626-631.



- 2547 Lu, H., Stevens, T., Yi, S., and Sun, X., 2006. An erosional hiatus in Chinese loess sequences revealed by  
2548 closely spaced optical dating. *Chinese Science Bulletin* 51, 2253-2259.
- 2549 Lu, H.Y., Wu, N.Q., Liu, K.B., Jiang, H., Liu, T.S., 2007. Phytoliths as quantitative indicators for the  
2550 reconstruction of past environmental conditions in China II: palaeoenvironmental reconstruction in the  
2551 Loess Plateau. *Quaternary Science Reviews* 26, 759–772.
- 2552 Luehmann, M.D., Schaetzl, R.J., Miller, B.A., Bigsby, M., 2013. Thin, pedoturbated and locally sourced  
2553 loess in the western Upper Peninsula of Michigan. *Aeolian Research* 8, 85-100.
- 2554 Luehmann, M.D., Peter, B., Connallon, C.B., Schaetzl, R.J., Smidt, S.J., Liu, W., Kincare, K., Walkowiak,  
2555 T.A., Thorlund, E., Holler, M.S., 2016. Loamy, two-storied soils on the outwash plains of southwestern  
2556 Lower Michigan: Pedoturbation of loess with the underlying sand. *Annals of the Association of American*  
2557 *Geographers* 106, 551-571.
- 2558 Maat, P.B., Johnson, W.C., 1996. Thermoluminescence and new C-14 age estimates for late Quaternary  
2559 loesses in southwestern Nebraska. *Geomorphology* 17, 115-128.
- 2560 Machalet, B., Oches, E.A., Frechen, M., Zöller, L., Hambach, U., Mavlyanova, N.G., Markovic, S.B.,  
2561 Endlicher, W., 2008. Aeolian dust dynamics in Central Asia during the Pleistocene: driven by the long-  
2562 term migration, seasonality and permanency of the Asiatic polar front. *Geophysics, Geochemistry and*  
2563 *Geosystems* 9, Q08Q09.
- 2564 Maher, B. A., 2011. The magnetic properties of Quaternary aeolian dusts and sediments, and their  
2565 palaeoclimatic significance. *Aeolian Research*, 3(2), 87-144.
- 2566 Maher, B. A., 2016. Palaeoclimatic records of the loess/palaeosol sequences of the Chinese Loess  
2567 Plateau. *Quaternary Science Reviews*, 154, 23-84.
- 2568 Maher, B.A., Thompson, R., 1992. Paleoclimatic significance of the mineral magnetic record of the  
2569 Chinese loess and paleosols. *Quaternary Research* 37, 155–170.

- 2570 Mancini, M. V., Paez M. M., Prieto, A. R., Stutz S., Tonello M., Vilanova I., 2005. Mid-Holocene climatic  
2571 variability reconstruction from pollen records (32°-52°S, Argentina). *Quaternary International* 132, 47-  
2572 59.
- 2573 Manikowska, B., 1994. Etat des études des processus éoliens dans la région de Lodz (Pologne centrale).  
2574 *Biuletyn Peryglacjalny* 33, 107-131.
- 2575 Markewich, H.W., Wysocki, D.A., Pavich, M.J., Rutledge, E.M., Millard, H.T., Rich, F.J., Maat, P.B., Rubin,  
2576 M., McGeehin, J.P., 1998. Paleopedology plus TL, Be-10, and C-14 dating as tools in stratigraphic and  
2577 paleoclimatic investigations, Mississippi River Valley, USA. *Quaternary International* 51-2, 143-167.
- 2578 Marković, S.B., Oches, E.A., Sümegi, P., Jovanovic, M., Gaudenyi, T., 2006. An introduction to the Middle  
2579 and Upper Pleistocene loess-paleosol sequence at Ruma brickyard, Vojvodina, Serbia. *Quaternary*  
2580 *International* 149, 80-86.
- 2581 Marković, S.B., Oches, E.A., McCoy, W.D., Gaudenyi, T., Frechen, M. 2007. Malacological and  
2582 sedimentological evidence for “warm” climate from the Irig loess sequence (Vojvodina, Serbia).  
2583 *Geophysics, Geochemistry and Geosystems* 8, p. Q09008.
- 2584 Marković, S.B. Bokhorst, M, Vandenberghe, J., Oches, E.A., Zöller, L., McCoy, W.D., Gaudenyi, T.,  
2585 Jovanović, M., Hambach, U., Machalet, B., 2008. Late Pleistocene loess-paleosol sequences in the  
2586 Vojvodina region, North Serbia. *Journal of Quaternary Science* 23, 73-84.
- 2587 Marković, S.B., Hambach, U., Catto, N., Jovanović, M., Buggle, B., Machalet, B., Zöller, L., Glaser, B.,  
2588 Frechen, M., 2009. Middle and Late Pleistocene loess sequences at Batajnica, Vojvodina, Serbia.  
2589 *Quaternary International* 198, 255-266.
- 2590 Marković, S. B., Hambach, U., Stevens, T., Kukla, G.J., Heller, F., William D. McCoy, W.D., Oches, E.A.,  
2591 Buggle, B., Zöller, L., 2011. The last million years recorded at the Stari Slankamen loess-palaeosol  
2592 sequence: revised chronostratigraphy and long-term environmental trends. *Quaternary Science Reviews*  
2593 30, 1142-1154.

- 2594 Marković, S.B., Stevens, T., Kukla, G.J., Hambach, U., Fitzsimmons, K.E., Gibbard, P., Buggle, B., Zech, M.,  
2595 Guo, Z., Hao, Q., Wu, H., O'Hara Dhand, K., Smalley, I.J., Újvári, G., Sümegei, P., Timar-Gabor, A., Veres, D.,  
2596 Sirocko, F., Vasiljević, D.A., Jary, Z., Svensson, A., Jović, V., Lehmkuhl, F., Kovács, J., Svirčev, Z., 2015.  
2597 Danube loess stratigraphy - Towards a pan-European loess stratigraphic model. *Earth-Science Reviews*  
2598 148, 228–258.
- 2599 Marković, S.B., Fitzsimmons, K.E., Sprafke, T., Gavrilovic, D., Smalley, I.J., Jovic, V., Svirčev, Z., Gavrilov,  
2600 M.B., Bešlin, M., 2016. The history of Danube loess research. *Quaternary International* 399, 86-99.
- 2601 Martignier, L., Nussbaumer, M., Adatte, T., Gobat, J.-M., Verrecchia, E.P., 2015. Assessment of a locally-  
2602 sourced loess system in Europe: The Swiss Jura Mountains. *Aeolian Research* 18, 11-21.
- 2603 Marshak, B.I., 2003. The Archaeology of Sogdiana. *The Silk Road* 1 (2), 2 -8 .
- 2604 Mason, J.A., Jacobs, P.M., Hanson, P.R., Miao, X.D., Goble, R.J., 2003. Sources and paleoclimatic  
2605 significance of Holocene Bignell Loess, Central Great Plains, USA. *Quaternary Research* 60, 330-339.
- 2606 Mason, J.A., Joeckel, R.M., Bettis, E.A., III, 2007. Middle to Late Pleistocene loess record in eastern  
2607 Nebraska, USA, and implications for the unique nature of Oxygen Isotope Stage 2. *Quaternary Science*  
2608 *Reviews* 26, 773-792.
- 2609 Mason, J.A., Miao, X.D., Hanson, P.R., Johnson, W.C., Jacobs, P.M., Goble, R.J., 2008. Loess record of the  
2610 Pleistocene-Holocene transition on the northern and central Great Plains, USA. *Quaternary Science*  
2611 *Reviews* 27, 1772-1783.
- 2612 Matasova, G., Petrovský, E., Jordanova, N., Zykina, V., Kapika, A., 2001. Magnetic study of Late  
2613 Pleistocene loess/palaeosol sections from Siberia: palaeoenvironmental implications. *Geophysical*  
2614 *Journal International* 147, 367-380.
- 2615 Matthews, N.E., Vasquez, J.A., Calvert, A.T., 2015. Age of the Lava Creek supereruption and magma  
2616 chamber assembly at Yellowstone based on <sup>40</sup>Ar/<sup>39</sup>Ar and U-Pb dating of sanidine and zircon crystals.  
2617 *Geochemistry Geophysics Geosystems* 16, 2508-2528.

- 2618 McDowell, P.F., Edwards, M.E., 2001. Evidence of Quaternary climatic variations in a sequence of loess  
2619 and related deposits at Birch Creek, Alaska: implications for the Stage 5 climatic chronology. *Quaternary*  
2620 *Science Reviews* 20, 63-76.
- 2621 McLennan, S.M., 2001. Relationships between the trace element composition of sedimentary rocks and  
2622 upper continental crust. *Geochemistry, Geophysics, Geosystems* 2, 2000GC000109.
- 2623 McTainsh, G., 1987. Desert loess in Northern Nigeria. *Zeitschrift für Geomorphologie*. N. F. 31, 145-165.
- 2624 Meszner, S., Kreutzer, S., Fuchs, M., Faust, D., 2014. Identifying depositional and pedogenetic controls of  
2625 Late Pleistocene loess-palaeosol sequences (Saxony, Germany) by combined grain size and microscopic  
2626 analyses. *Zeitschrift für Geomorphologie* 58, Suppl. 3, 63-90.
- 2627 Miao, X.D., Mason, J.A., Johnson, W.C., Wang, H., 2007. High-resolution proxy record of Holocene  
2628 climate from a loess section in Southwestern Nebraska, USA. *Palaeogeography Palaeoclimatology*  
2629 *Palaeoecology* 245, 368-381.
- 2630 Miller, B.B., Graham, R.W., Morgan, A.V., Norton, G.M., McCoy, W.D., Palmer, D.F., Smith, A.J., Pilny, J.J.,  
2631 1994. A biota associated with Matuyama-age sediments in west-central Illinois. *Quaternary Research* 41,  
2632 350–365.
- 2633 Moine, O., 2014. Weichselian Upper Pleniglacial environmental variability in north-western Europe  
2634 reconstructed from terrestrial mollusc faunas and its relationship with the presence/absence of human  
2635 settlements. *Quaternary International* 337, 90–113.
- 2636 Moine, O., Rousseau, D.-D., Jolly, D., Vianey-Liaud, M., 2002. Paleoclimatic reconstruction using mutual  
2637 climatic range on terrestrial mollusks. *Quaternary Research* 57, 162-172.
- 2638 Moine, O., Antoine, P., Hatté, C., Landais, A., Mathieu, J.C., Prud'homme, C., and Rousseau, D., 2017.  
2639 The impact of Last Glacial climate variability in west-European loess revealed by radiocarbon dating of  
2640 fossil earthworm granules. *PNAS* 114, 6209–6214.

- 2641 Mùcher, H., Vreeken, W., 1981. (Re)deposition of loess in southern Limburg. The Netherlands. II.  
2642 Micromorphology of the lower silt loam complex and comparison with deposits produced under  
2643 laboratory conditions. *Earth Surface Processes and Landforms*, 6, 355-363.
- 2644 Muhs, D.R., 2013a. Loess and its Geomorphic, Stratigraphic, and Paleoclimatic Significance in the  
2645 Quaternary, in: *Treatise on Geomorphology*. Academic Press, San Diego, pp. 149–183.
- 2646 Muhs, D.R., 2013b. The geologic records of dust in the Quaternary. *Aeolian Research* 9, 3-48.
- 2647 Muhs, D.R., Benedict, J.B. 2006. Eolian additions to late Quaternary alpine soils, Indian Peaks Wilderness  
2648 Area, Colorado Front Range. *Arctic, Antarctic and Alpine Research* 38, 120-130.
- 2649 Muhs, D.R., Bettis, E.A. III., 2000. Geochemical variations in Peoria Loess of western Iowa indicate  
2650 paleowinds of midcontinental North America during last glaciation. *Quaternary Research* 53, 49-61.
- 2651 Muhs, D.R., Bettis, E.A. III, 2003. Quaternary Loess-Paleosol Sequences as Examples of Climate-driven  
2652 Sedimentary Extremes. *Geological Society of America Special Paper* 370, 53-74.
- 2653 Muhs, D.R., Budahn, J.R., 2006. Geochemical evidence for the origin of late Quaternary loess in central  
2654 Alaska. *Canadian Journal of Earth Sciences* 43, 323-337.
- 2655 Muhs, D.R., Bettis, E.A. III, Been, J., McGeehin, J., 2001. Impact of climate and parent material on  
2656 chemical weathering in loess-derived soils of the Mississippi River Valley. *Soil Science Society of America*  
2657 *Journal* 65, 1761-1777.
- 2658 Muhs, D.R., Ager, T.A., Been, J., Bradbury, J.P., Dean, W.E., 2003a. A late Quaternary record of eolian silt  
2659 deposition in a maar lake, St. Michael Island, western Alaska. *Quaternary Research* 60, 110-122.
- 2660 Muhs, D.R., Ager, T.A., Bettis, E.A., III, McGeehin, J., Been, J.M., Begét, J.E., Pavich, M.J., Stafford, T.W.,  
2661 Jr., Stevens, D.S.P., 2003b. Stratigraphy and paleoclimatic significance of late Quaternary loess-paleosol  
2662 sequences of the last interglacial-glacial cycle in central Alaska. *Quaternary Science Reviews*, 22, 1947-  
2663 1986.

- 2664 Muhs, D.R., McGeehin, J.P., Beann, J., Fisher, E., 2004. Holocene loess deposition and soil formation as  
2665 competing processes, Matanuska Valley, southern Alaska. *Quaternary Research* 61, 265-276.
- 2666 Muhs, D.R., Budahn, J., Reheis, M., Beann, J., Skipp, G., Fisher, E., 2007. Airborne dust transport to the  
2667 eastern Pacific Ocean off southern California: Evidence from San Clemente Island. *Journal of Geophysical*  
2668 *Research*, 112, D13203, doi:10.1029/2006JD007577.
- 2669 Muhs, D.R., Bettis, E.A., III, Aleinikoff, J.N., McGeehin, J.P., Beann, J., Skipp, G., Marshall, B.D., Roberts,  
2670 H.M., Johnson, W.C., Benton, R., 2008a. Origin and paleoclimatic significance of late Quaternary loess in  
2671 Nebraska: Evidence from stratigraphy, chronology, sedimentology, and geochemistry. *Geological Society*  
2672 *of America Bulletin* 120, 1378-1407.
- 2673 Muhs, D.R., Ager, T.A., Skipp, G., Beann, J., Budahn, J.R., McGeehin, J.P., 2008b. Paleoclimatic  
2674 significance of chemical weathering in loess-derived paleosols of subarctic central Alaska. *Arctic,*  
2675 *Antarctic, and Alpine Research* 40, 396-411.
- 2676 Muhs, D.R., Budahn, J., Johnson, D.L., Rehis, M., Beann, J., Skipp, G., Fisher, E., Jones, J.A., 2008c.  
2677 Geochemical evidence for airborne dust additions to soils in Channel Islands National Park, California.  
2678 *Geological Society of America Bulletin* 120, 106-126.
- 2679 Muhs, D.R., Bettis, E.A., III, Roberts, H.M., Harlan, S.S., Paces, J.B., Reynolds, R.L., 2013a. Chronology and  
2680 provenance of last-glacial (Peoria) loess in western Iowa and paleoclimatic implications. *Quaternary*  
2681 *Science Reviews* 80, 468-481.
- 2682 Muhs, D.R., Budahn, J.R., McGeehin, J.P., Bettis, E.A. III, Skipp, G., Paces, J.B., Wheeler, E.A., 2013b.  
2683 Loess origin, transport, and deposition over the past 10,000 years, Wrangell-St. Elias National Park,  
2684 Alaska: *Aeolian Research* 11, 85-99.
- 2685 Muhs, D.R., Roskin, J., Tsoar, H., Skipp, G., Budahn, J.R., Sneh, A., Porat, N., Stanley, J.-D., Katra, I.,  
2686 Blumberg, D.G., 2013c. Origin of the Sinai–Negev erg, Egypt and Israel: mineralogical and geochemical  
2687 evidence for the importance of the Nile and sea level history. *Quaternary Science Reviews* 69, 28-48.

- 2688 Muhs, D.R., Budahn, J.R., Skipp, G.L., McGeehin, J.P., 2016. Geochemical evidence for seasonal controls  
2689 on the transportation of Holocene loess, Matanuska Valley, southern Alaska, USA. *Aeolian Research* 21,  
2690 61-73.
- 2691 Muhs, D.R., Pigati, J.S., Budahn, J.R., Skipp, G.L., Bettis, E.A. III, Jensen, B., 2018. Origin of last-glacial  
2692 loess in the western Yukon-Tanana Upland, central Alaska, U.S.A. *Quaternary Research: this issue*.
- 2693 Munroe, J.S., Attwood, E.C., O’Keefe, S.S., Quackenbush, P.J.M., 2015. Eolian deposition in the alpine  
2694 zone of the Uinta Mountains, Utah, USA. *Catena* 124, 119-129.
- 2695 Nash, T.A., Conroy, J.L., Grimley, D.A., Guenther, W.R., Curry, B.B., 2017. Episodic deposition of Illinois  
2696 Valley Peoria Silt in association with Lake Michigan Lobe fluctuations during the last glacial maximum.  
2697 *Quaternary Research*, 1-17.
- 2698 Nawrocki, J., Polechonska, O., Boguckij, A., Lanczont, M., 2006. Palaeowind directions recorded in the  
2699 youngest loess in Poland and western Ukraine as derived from anisotropy of magnetic susceptibility  
2700 measurements. *Boreas* 35, 266-271.
- 2701 Necula, C., Dimofte, D., Panaiotu, C., 2015. Rock magnetism of a loess-palaeosol sequence from the  
2702 western Black Sea shore (Romania). *Geophysical Journal International* 202, 1733–1748.
- 2703 Nekola, J.C., Coles, B.F., 2010. Pupillid land snails of eastern North America. *American Malacological*  
2704 *Bulletin* 28, 29-57.
- 2705 Nelson, M.S., Rittenour, T.M., 2015. Using grain-size characteristics to model soil water content:  
2706 Application to dose-rate calculation for luminescence dating. *Radiation Measurements* 81, 142-149.
- 2707 Nie, J., Stevens T., Rittner, M., Stockli, D., Garzanti, E., Limonta, M., Bird, A., Andò, S., Vermeesch, P.,  
2708 Saylor, J., Lu, H., Breecker, D., Hu, X., Liu, S., Resentini, A., Vezzoli, G., Peng, W., Carter, A., Ji, S., Pan, B.,  
2709 2015. Loess Plateau storage of Northeastern Tibetan Plateau-derived Yellow River sediment. *Nature*  
2710 *Communications* 6, 1-10.

- 2711 North Greenland Ice Core Project Members, Andersen, K.K., Azuma, N., Barnola, J.-M., Bigler, M.,  
2712 Biscaye, P., Caillon, N., Chappellaz, J., Clausen, H.B., Dahl-Jensen, D., Fischer, H., others, 2004. High-  
2713 resolution record of Northern Hemisphere climate extending into the last interglacial period. *Nature*  
2714 431, 147–151.
- 2715 Nottebaum, V., Stauch, G., Hartmann, K., Zhang, J., Lehmkuhl, F., 2015. Unmixed loess grain size  
2716 populations along the northern Qilian Shan (China): relationships between geomorphologic,  
2717 sedimentologic and climatic controls. *Quaternary International* 372, 151-166.
- 2718 Novotny, A., Frechen, M., Horvath, E., Wacha, L., Rolf, C., 2011. Investigating the penultimate and last  
2719 glacial cycles of the Süttö loess section (Hungary) using luminescence dating, high-resolution grain size,  
2720 and magnetic susceptibility data. *Quaternary International* 234, 75-85.
- 2721 Nowaczyk, B., 1986. The age of dunes, their textural and structural properties against atmospheric  
2722 circulation pattern of Poland during the Late Vistulian and Holocene. A. Mickiewicz University Press,  
2723 *Seria Geografia* 28. 245 pp.
- 2724 Nugteren, G., Vandenberghe, J., 2004. Spatial climatic variability on the Central Loess Plateau (China) as  
2725 recorded by grain size for the last 250 kyr. *Global and Planetary Change* 41, 185-206.
- 2726 Nyland, K.E., Schaetzl, R.J., Ignatov, A., Miller, B.A., 2017. A new depositional model for sand-rich loess  
2727 on the Buckley Flats outwash plain, northwestern Lower Michigan. *Aeolian Research*: in press.
- 2728 Obreht, I., Buggle, B., Catto, N., Marković, S.B., Bösel, S., Vandenberghe, D.A.G., Hambach, U., Svirčev, Z.,  
2729 Lehmkuhl, F., Basarin, B., Gavrilov, M.B., Jović, G., 2014. The Late Pleistocene Belotinac section  
2730 (southern Serbia) at the southern limit of the European loess belt: environmental and climate  
2731 reconstruction using grain size and stable C and N isotopes. *Quaternary International* 334–335, 10–19.
- 2732 Obreht, I., Zeeden, C., Schulte, P., Hambach, U., Eckmeier, E., Timar-Gabor, A., Lehmkuhl, F., 2015.  
2733 Aeolian dynamics at the Orlovat loess–paleosol sequence, northern Serbia, based on detailed textural  
2734 and geochemical evidence. *Aeolian Research* 18, 69-81.



- 2735 Obreht, I., Zeeden, C., Hambach, U., Veres, D., Marković, S.B., Böskén, J., Svirčev, Z., Bačević, N., Gavrilov,  
2736 M.B., Lehmkuhl, F., 2016. Tracing the influence of Mediterranean climate on Southeastern Europe  
2737 during the past 350,000 years. *Scientific Reports* 6, 36334.
- 2738 Obreht, I., Hambach, U., Veres, D., Zeeden, C., Böskén, J., Stevens, T., Marković, S.B., Klasen, N., Brill, D.,  
2739 Burow, C., Lehmkuhl, F., 2017. Shift of large-scale atmospheric systems over Europe during late MIS 3  
2740 and implications for Modern Human dispersal. *Scientific Reports* 7, s41598-017-06285-x-017.
- 2741 Oches, E.A., McCoy, W.D., 2001. Historical developments and recent advances in amino acid  
2742 geochronology applied to loess research: examples from North America, Europe, and China. *Earth-*  
2743 *Science Reviews* 54(1–3), 173–192
- 2744 Oches, E.A., Banerjee, S.K., Solheid, P.A., Frechen, M., 1998. High resolution proxies of climate variability  
2745 in the Alaskan loess record. In: Busacca, A.J. (Ed.), *Dust Aerosols, Loess Soils and Global Change*.  
2746 Washington State University College of Agriculture and Home Economics, Miscellaneous Publication No.  
2747 MISC0190, Pullman, pp. 167–170.
- 2748 Owczarek, P., Opała-Owczarek, M., Rahmonov, O., Razzokov, A., Jary, Z., Niedźwiedź, T., 2017.  
2749 Relationships between loess and the Silk Road reflected by environmental change and its implications  
2750 for human societies in the area of ancient Panjikent, Central Asia. *Quaternary Research* (in press).  
2751 <https://doi.org/10.1017/qua.2017.69>
- 2752 Owen, L.A., Dortch, J.M., 2014. Nature and timing of Quaternary glaciation in the Himalayan–Tibetan  
2753 orogen. *Quaternary Science Reviews* 88, 14-54.
- 2754 Paepe, R., 1966. Comparative stratigraphy of Würm loess deposits in Belgium and Austria. *Bulletin de la*  
2755 *Société Belgique de Géologie*, 75, 203-216.
- 2756 Paepe, R., Sommé, J., 1970. Les loess et la stratigraphiedu Pleistocène récent dans le nord de la France  
2757 et en Belgique. *Annales Société Géologique du Nord* 90, 191-201.
- 2758 Palmer, A.S., Pillans B.J. 1996. Record of climatic fluctuations from ca. 500 ka loess deposits and  
2759 paleosols near Wanganui, New Zealand. *Quaternary International* 34-36, 155-162.

- 2760 Parés, J. M., 2015. Sixty years of anisotropy of magnetic susceptibility in deformed sedimentary rocks.  
2761 *Frontiers in Earth Science*, 3, 4.
- 2762 Pécsi, M., 1966. Löss und lössartige Sedimente im Karpatenbecken und ihre lithostratigraphischen  
2763 Gliederung. *Petermanns Geographische Mitteilungen* 110: 3-4, 176-189, 241-252.
- 2764 Pécsi, M., 1985. Chronostratigraphy of Hungarian loesses and the underlying subaerial formation. *Loess*  
2765 *and the Quaternary: Chinese and Hungarian Case Studies. Studies in Geography in Hungary* 18, 33-49.
- 2766 Peterse, F., Martínez-García, A., Zhou, B., Beets, C.J., Prins, M.A., Zheng, H., Eglinton, T.I., 2014.  
2767 Molecular records of continental air temperature and monsoon precipitation variability in East Asia  
2768 spanning the past 130,000 years. *Quaternary Science Reviews* 83, 76-82.
- 2769 Péwé, T.L., 1955. Origin of the upland silt near Fairbanks, Alaska: *Geological Society of America Bulletin*,  
2770 v. 66, p. 699-724.
- 2771 Péwé, T.L., 1975. Quaternary geology of Alaska. *U.S. Geological Survey Professional Paper* 835, 145 pp.
- 2772 Péwé, T.L., Berger, G.W., Westgate, J.A., Brown, P.M., and Leavitt, S.W., 1997, Eva Interglaciation Forest  
2773 Bed, Unglaciaded East-Central Alaska: Global Warming 125,000 Years Ago: *Geological Society of America*  
2774 *Special Paper* 319, 54 pp.
- 2775 Pfannenstiel, M., 1950. *Die Quartärgeschichte des Donaudeltas. Bonner Geographische Abhandlungen*,  
2776 Bonn.
- 2777 Pickering, R., Jacobs, Z., Herries, A.I.R., Karkanis, P., Bar-Matthews, M., Woodhead, J.D., Kappen, P.,  
2778 Fisher, E., Marean, C.W., 2013. Paleoanthropologically significant South African sea caves dated to 1.1–  
2779 1.0 million years using a combination of U–Pb, TT-OSL and palaeomagnetism. *Quaternary Science*  
2780 *Reviews* 65, 39-52.
- 2781 Pigati, J.S., Rech, J.A., Nekola, J.C., 2010. Radiocarbon dating of small terrestrial gastropod shells in North  
2782 America. *Quaternary Geochronology* 5, 519-532.

- 2783 Pigati, J.S., McGeehin, J.P., Muhs, D.R., Bettis, E.A., 2013. Radiocarbon dating late Quaternary loess  
2784 deposits using small terrestrial gastropod shells. *Quaternary Science Reviews* 76, 114-128.
- 2785 Pigati, J.S., McGeehin, J.P., Muhs, D.R., Grimley, D.A., Nekola, J.C., 2015. Radiocarbon dating loess  
2786 deposits in the Mississippi Valley using terrestrial gastropod shells (Polygyridae, Helicinidae, and  
2787 Discidae). *Aeolian Research* 16, 25-33.
- 2788 Porter, D., Bishop, S., 1990. Soil and lithostratigraphy below the Loveland/Sicily Island silt, Crowley's  
2789 Ridge, Arkansas. *Proceedings of the Arkansas Academy of Science* 44, 86-90.
- 2790 Porter, S.C., An, Z.S. 1995. Correlation between climate events in the North Atlantic and China during  
2791 the last glaciation. *Nature* 375, 305-308.
- 2792 Prasad, A.K., Poolton, N.R.J., Kook, M., Jain, M., 2017. Optical dating in a new light: A direct, non-  
2793 destructive probe of trapped electrons. *Scientific Reports* 7, 12097.
- 2794 Preece, S.J., Westgate, J.A., Stemper, B.A., Péwé, T.L., 1999. Tephrochronology of late Cenozoic loess at  
2795 Fairbanks, central Alaska. *Geological Society of America Bulletin* 111, 71-90.
- 2796 Prins, M.A., Vriend, M., Nugteren, G., Vandenberghe, J., Lu, H., Zheng, H., Weltje, G.J., 2007. Late  
2797 Quaternary aeolian dust input variability on the Chinese Loess Plateau: inferences from unmixing of  
2798 loess grain-size records. *Quaternary Science Reviews* 26, 230-242.
- 2799 Prud'Homme, C., Antoine, P., Moine, O., Turpin, E., Huguenard, L., Robert, V., Degeai, J.-P., 2015.  
2800 Earthworm calcite granules: a new tracker of millennial-timescale environmental changes in Last Glacial  
2801 loess deposits. *Journal of Quaternary Science* 30, 529-536.
- 2802 Pullen, A., Kapp, P., McCallister, A. T., Chang, H., Gehrels, G. E., Garzzone, C. N., Heermance, R.V., Ding,  
2803 L., 2011. Qaidam Basin and northern Tibetan Plateau as dust sources for the Chinese Loess Plateau and  
2804 paleoclimatic implications. *Geology* 39, 1031-1034.

- 2805 Pullen, A., Ibáñez-Mejía, M., Gehrels, G.E., Ibáñez-Mejía, J.C., Pecha, M., 2014. What happens when n =  
2806 1000? Creating large-*n* geochronological datasets with LA-ICP-MS for geological investigations. *Journal*  
2807 *of Analytical Atomic Spectrometry* 29, 971-980.
- 2808 Pye, K., 1995. The nature, origin and accumulation of loess. *Quaternary Science Reviews* 14, 653-667.
- 2809 Pye, K., Johnson, R. 1988. Stratigraphy, geochemistry, and thermoluminescence ages of Lower  
2810 Mississippi valley loess. *Earth Surface Processes and Landforms*, 13, 103-124.
- 2811 Pye, K., Zhou, L.P., 1989. Late Pleistocene and Holocene aeolian dust deposition in north China and the  
2812 northwest Pacific Ocean. *Palaeogeography, Palaeoclimatology, Palaeoecology* 73, 11–23,  
2813 doi:10.1016/0031-0182(89)90041-2.
- 2814 Rech, J.A., Nekola, J.C., Pigati, J.S., 2012. Radiocarbon ages of terrestrial gastropods extend duration of  
2815 ice-free conditions at the Two Creeks forest bed, Wisconsin, USA. *Quaternary Research* 77, 289-292
- 2816 Reger, R.D., Pinney, D.S., Burke, R.M., Wiltse, M.A., 1996. Catalog and initial analyses of geologic data  
2817 related to middle to late Quaternary deposits, Cook Inlet region, Alaska. *State of Alaska Division of*  
2818 *Geological and Geophysical Surveys Report of Investigations* 95-6, 188 pp.
- 2819 Renssen, H., Kasse, C., Vandenberghe, J., Lorenz, S.J., 2007. Weichselian Late Pleniglacial surface winds  
2820 over northwest and central Europe: a model-data comparison. *Journal of Quaternary Science* 22, 281-  
2821 293.
- 2822 Rex, R.W., Syers, J.K., Jackson, M.L., Clayton, R.N., 1969. Eolian origin of quartz in soils of the Hawaiian  
2823 Islands and in Pacific pelagic sediments *Science* 163, 277-279.
- 2824 Roberts, H.M., 2008. The development and application of luminescence dating to loess deposits: a  
2825 perspective on the past, present and future. *Boreas* 37, 483-507.
- 2826 Roberts, H.M., Muhs, D.R., Wintle, A.G., Duller, G.A.T., Bettis, E.A., III, 2003. Unprecedented last-glacial  
2827 mass accumulation rates determined by luminescence dating of loess from western Nebraska.  
2828 *Quaternary Research* 59, 411-419.

- 2829 Rodbell, D.T., Forman, S.L., Pierson, J., Lynn, W.C., 1997. Stratigraphy and chronology of Mississippi  
2830 Valley loess in western Tennessee. *Geological Society of America Bulletin* 109, 1134-1148.
- 2831 Roering, J.J., Almond, P., Tonkin, P., McKean, J. 2002. Soil transport driven by biological processes over  
2832 millennial time scales. *Geology* 30, 1115-1118.
- 2833 Rossignol, J., Moine, O., Rousseau, D.D. 2004. The Buzzard's Roost and Eustis mollusc sequences:  
2834 comparison between the paleoenvironments of two sites in the Wisconsinan loess of Nebraska, USA.  
2835 *Boreas* 33,145-154.
- 2836 Rousseau, D.D., 1987. Paleoclimatology of the Achenheim series (middle and upper Pleistocene, Alsace,  
2837 France). A malacological analysis. *Palaeogeography, Palaeoclimatology, Palaeoecology*. 59, 293-314.
- 2838 Rousseau, D.D., 1991. Climatic transfer function from Quaternary molluscs in European loess deposits.  
2839 *Quaternary Research* 36, 195–209.
- 2840 Rousseau, D. D. 2001. Loess biostratigraphy: new advances and approaches in mollusc studies. *Earth  
2841 Science Reviews* 54, 157–171.
- 2842 Rousseau, D.-D., Kukla, G., 1994. Late Pleistocene climate record in the Eustis loess section, Nebraska,  
2843 based on land snail assemblages and magnetic susceptibility. *Quaternary Research* 42, 176-187.
- 2844 Rousseau, D.D., Wu, N.Q., Guo, Z.T., 2000. The terrestrial mollusks as new indices of the Asian  
2845 paleomonsoons in the Chinese loess plateau. *Global and Planetary Change* 26, 199–206.
- 2846 Rousseau, D.D., Gerasimaenko N, Matvviishina Z, Kukla GJ., 2001. Late Pleistocene environments of  
2847 central Ukraine. *Quaternary Research* 56: 349–356.
- 2848 Rousseau, D.D., Antoine, P., Hatté, C., Lang, A., Zöller, L., Fontugne, M., Othman, D.B., Luck, J.M., Moine,  
2849 O., Labonne, M., Bentaleb, I., Jolly, D., 2002. Abrupt millennial climatic changes from Nussloch  
2850 (Germany) Upper Weichselian eolian records during the Last Glaciation. *Quaternary Science Reviews* 21,  
2851 1577–1582.

- 2852 Rousseau, D.-D., Sima, A., Antoine, P., Hatté, C., Lang, A., Zöller, L., 2007. Link between European and  
2853 North Atlantic abrupt climate changes over the last glaciation. *Geophysical Research Letters* 34, L22713.
- 2854 Rousseau, D.D., Wu, N., Pei, Y., Li, F., 2009. Three exceptionally strong East-Asian summer monsoon  
2855 events during glacial times in the past 470 kyr. *Climate of the Past* 5, 157–169.
- 2856 Rousseau, D.-D., Derbyshire, E., Antoine, P., Hatté, C., 2013. Loess records – Europe, In: Mock, S.A.E.J.  
2857 (Ed.), *Encyclopedia of Quaternary Science*, second ed. Elsevier, Amsterdam, pp. 606–619.
- 2858 Rousseau, D.-D., Chauvel, C., Sima, A., Hatté, C., Lacroix, F., Antoine, P., Balkanski, Y., Fuchs, M., Mellett,  
2859 C., Kageyama, M., Ramstein, G., Lang, A., 2014. European glacial dust deposits: Geochemical constraints  
2860 on atmospheric dust cycle modeling. *Geophysical Research Letters* 41, 7666-7674.
- 2861 Rousseau, D.D., Boers, N., Sima, A., Svensson, A., Bigler, M., Lacroix, F., Taylor, S., Antoine, P., 2017a.  
2862 MIS3 and 2 millennial oscillations in Greenland dust and Eurasian aeolian records - A paleosol  
2863 perspective. *Quaternary Science Reviews* 169, 99-113.
- 2864 Rousseau, D.-D., Svensson, A., Bigler, M., Sima, A., Steffensen, J. P., Boers, N., 2017b. Eurasian  
2865 contribution to the last glacial dust cycle: how are loess sequences built?, *Climate of the Past*, 13, 1181-  
2866 1197.
- 2867 Rozanski K., Araguas-Araguas L., Gonfiantini R., 1993. Isotopic patterns in modern global precipitation. In  
2868 *Climate Change in Continental Isotopic Records*, P.K. Swart et al. (Eds.), *Geophysical Monograph* 78,  
2869 American Geophysical Union, Washington, DC 20009, USA, pp. 1-37.
- 2870 Ruegg, G.H.J., 1983. Periglacial eolian evenly laminated sandy deposits in the Late Pleistocene of N.W.  
2871 Europe, a facies unrecorded in modern sedimentological handbooks. In: Brookfield, M.E., Ahlbrandt, T.S.  
2872 (Eds.), *Eolian Sediments and Processes*, Elsevier, Amsterdam, pp. 455-482.
- 2873 Ruhe, R.V., 1954. Relations of the properties of Wisconsin loess to topography in western Iowa.  
2874 *American Journal of Science* 252, 663-672.

- 2875 Ruhe, R.V., 1973. Background of model for loess-derived soils in the upper Mississippi Valley. *Soil*  
2876 *Science* 115, 250-253.
- 2877 Ruocco, M., 1989. A 3 Ma paleomagnetic record of coastal continental deposits in Argentina.  
2878 *Palaeoecology, Palaeogeography, Palaeoclimatology* 72, 105–113.
- 2879 Rutledge, E.M., Guccione, M.J., Markewich, H.W., Wysocki, D.A., Ward, L.B., 1996. Loess stratigraphy of  
2880 the Lower Mississippi Valley. *Engineering Geology* 45, 167-183.
- 2881 Rutledge, E.M., Holowaychuk, N., Hall, G.F., Wilding, L.P., 1975. Loess in Ohio in relation to several  
2882 possible source areas: I. Physical and chemical properties. *Soil Science Society of America Proceedings*  
2883 39, 1125-1132.
- 2884 Rutter, N.W., Ding, Z.L., 1993. Paleoclimates and monsoon variations interpreted from  
2885 micromorphogenic features of the Baoji paleosols, China. *Quaternary Science Reviews* 12, 853–862
- 2886 Rutter, N.W., Ding, Z.L., Evans, M.E., Liu, T.S., 1991. Baoji-type pedostratigraphic section, Loess Plateau,  
2887 north-central China. *Quaternary Science Reviews* 10, 1–22.
- 2888 Sanborn, P.T., Smith, C.A.S., Froese, D.G., Zazula, G.D., Westgate, J.A., 2006. Full-glacial paleosols in  
2889 perennially frozen loess sequences, Klondike goldfields, Yukon Territory, Canada. *Quaternary Research*  
2890 66, 147-157.
- 2891 Sarianidi V., 1992. Food-producing and other Neolithic communities in Khorasan and Transoxania:  
2892 Eastern Iran, Soviet Central Asia and Afghanistan. In: Dani, A.H., Masson (Eds.), *History of civilizations of*  
2893 *Central Asia I: The dawn of civilization: earliest times to 700 BC*. UNESCO Publishing, Paris. pp. 105 – 122.
- 2894 Sarnthein, M., Tetzlaff, G., Koopmann, B., Wolter, K., Pflaumann, U., 1981. Glacial and interglacial wind  
2895 regimes over the eastern subtropical Atlantic and North-West Africa. *Nature (London)* 293, 193-196.
- 2896 Sayago J.M., 1983. Geología de la Sierra de Ancasti-16. Geomorfología de la Sierra de Ancasti  
2897 (Argentina). *Münstersche Forschungen zur Geologie und Paläeontologie* 59, 265-284.

- 2898 Schaetzl, R.J., 1998. Lithologic discontinuities in some soils on drumlins: Theory, detection, and  
2899 application. *Soil Science* 163, 570-590.
- 2900 Schaetzl, R.J., 2008. The distribution of silty soils in the Grayling Fingers region of Michigan: Evidence for  
2901 loess deposition onto frozen ground. *Geomorphology* 102, 287-296.
- 2902 Schaetzl, R.J., Attig, J.W., 2013. The loess cover of northeastern Wisconsin. *Quaternary Research* 79,  
2903 199-214.
- 2904 Schaetzl, R.J., Hook, J., 2008. Characterizing the silty sediments of the Buckley Flats outwash plain:  
2905 Evidence for loess in NW Lower Michigan. *Physical Geography* 29, 1-18.
- 2906 Schaetzl, R.J., Loope, W.L., 2008. Evidence for an eolian origin for the silt-enriched soil mantles on the  
2907 glaciated uplands of eastern Upper Michigan, USA. *Geomorphology* 100, 285-295.
- 2908 Schaetzl, R.J., Luehmann, M.D., 2013. Coarse-textured basal zones in thin loess deposits: Products of  
2909 sediment mixing and/or paleoenvironmental change? *Geoderma* 192, 277-285.
- 2910 Schaetzl, R.J., Weisenborn, B.N., 2004. The Grayling Fingers geomorphic region of Michigan: Soils,  
2911 sedimentology, stratigraphy and geomorphic development. *Geomorphology* 61, 251-274.
- 2912 Schaetzl, R.J., Larson, P.H., Faulkner, D.J., Running, G.L., Jol, H.M., Rittenour, T.M., 2017. Eolian sand and  
2913 loess deposits indicate west-northwest paleowinds during the Late Pleistocene in Western Wisconsin,  
2914 USA. *Quaternary Research*: this issue.
- 2915 Schatz, A., Zech, M., Bugge, B., Gulyas, S., Hambach, U., Markovic, S., Sümegi, P., Scholten, T., 2011. The  
2916 late Quaternary loess record of Tokaj, Hungary: Reconstructing palaeoenvironment, vegetation and  
2917 climate using stable C and N isotopes and biomarkers. *Quaternary International* 240 (1-2), 52-61.
- 2918 Schatz, A.-K., Qi, Y., Siebel, W., Wu, J., Zöller, L., 2015. Tracking potential source areas of Central  
2919 European loess: examples from Tokaj (HU), Nussloch (D) and Grub (AT). *Open Geoscience* 7, 678–720,  
2920 DOI 10.1515/geo-2015-0048.



- 2921 Schäfer, I., Bliedtner, M., Wolf, D., Faust, D., Zech, R., 2016a. Evidence for humid conditions during the  
2922 last glacial from leaf wax patterns in the loess-paleosol sequence El Paraíso, Central Spain. *Quaternary*  
2923 *International* 407(A), 64-73.
- 2924 Schäfer, I., Lanny, V., Franke, J., Eglinton, T., Zech, M., Vysloužilová, B., Zech R., 2016b. Leaf waxes in  
2925 litter and topsoils along a European transect. *Soil* 2, 551-564.
- 2926 Scheib, A.J., Birke, M., Dinelli, E., 2013. Geochemical evidence of aeolian deposits in European soils.  
2927 *Boreas* 43, 175-192.
- 2928 Schirmer, W., 2016. Late Pleistocene loess of the lower Rhine. *Quaternary International*, 411, 44-61.
- 2929 Schreuder, L., Beets, C., Prins, M., Hatté, C., Peterese, F., 2016. Late Pleistocene climate evolution in  
2930 Southeastern Europe recorded by soil bacterial membrane lipids in Serbian loess. *Palaeogeography,*  
2931 *Palaeoclimatology, Palaeoecology* 449, 141-148.
- 2932 Scull, P., Schaetzl, R.J., 2011. Using PCA to characterize and differentiate the character of loess deposits  
2933 in Wisconsin and Upper Michigan, USA. *Geomorphology* 127, 143-155.
- 2934 Schwan, J., 1988. The structure and genesis of Weichselian to Early Holocene aeolian sand sheets in  
2935 western Europe. *Sedimentary Geology* 55, 197-232.
- 2936 Schwan, J., 1991. Palaeowetness indicators in a Weichselian Late Glacial to Holocene aeolian succession  
2937 in the southwestern Netherlands. *Zeitschrift für Geomorphologie, Suppl. Bd. 90*, 155-169.
- 2938 Semmel A., 1997. Referenzprofile des Wuerm loesses im Rhein-Main-Gebiet. *Jahresberichte der*  
2939 *Wetterauischen Gesellschaft fuer die gesamte Naturkunde* 148: 3747.
- 2940 Shackleton, N.J., An, Z., Dodonov, A.E., Gavin, J., Kukla, G.J., Ranov, V.A., Zhou, L.P., 1995. Accumulation  
2941 rate of loess in Tajikistan and China: Relationship with global ice volume cycles. *Quaternary Proceedings*  
2942 4, 1-6.

- 2943 Shang, Y., Beets, C.J., Tang, H., Prins, M., Lahaye, Y., van Elsas, R., Sukselainen, L., Kaakinen, A., 2016.  
2944 Variations in the provenance of the late Neogene Red Clay deposits in northern China. *Earth and*  
2945 *Planetary Science Letters* 439, 88-100.
- 2946 Shimek B. 1899. The Distribution of Loess Fossils. *The Journal of Geology* 7, 122-140.
- 2947 Simmons, A.H., 2011. *The Neolithic Revolution in the Near East*. University of Arizona Press, Tucson.
- 2948 Simonson, R.W., 1995. Airborne dust and its significance to soils. *Geoderma* 65, 1-43.
- 2949 Sitzia, L., Bertran, P., Bahain, J.-J., Bateman, M.D., Hernandez, M., Garon, H., de Lafontaine, G., Mercier,  
2950 N., Leroyer, C., Queffelec, A., Voinchet, P., 2015. The Quaternary coversands of southwest France.  
2951 *Quaternary Science Reviews* 124, 84-105.
- 2952 Sláma, J., Košla, J., 2012. Effects of sampling and mineral separation on accuracy of detrital zircon  
2953 studies. *Geochemistry, Geophysics, Geosystems* 13, Q05007.
- 2954 Smalley, I.J., 1968. The loess deposits and Neolithic culture of northern China. *Man (n.s.)* 3, 224-241.
- 2955 Smalley, I., 1995. Making the material: The formation of silt sized primary mineral particles for loess  
2956 deposits. *Quaternary Science Reviews* 14, 645-651.
- 2957 Smalley, I.J., Krinsley, D.H., 1978. Loess deposits associated with deserts. *Catena* 5, 53-66.
- 2958 Smalley, I.J., Leach, J.A., 1978. The origin and distribution of the loess in the Danube basin and  
2959 associated regions of East-Central Europe a review. *Sedimentary Geology* 21, 1– 26.
- 2960 Smalley, I.J., Mavlyanova, N.G., Rakhmatullaev, K.L., Shermatov, M.S., Machalet, B., O'Hara Dhand, K.,  
2961 Jefferson, I.F., 2006. The formation of loess deposits in the Tashkent region and parts of Central Asia;  
2962 and problems with irrigation, hydrocollapse and soil erosion. *Quaternary International* 152-153, 59-69.
- 2963 Smalley, I., O'Hara-Dhand, K., Wint, J., Machalet, B., Jary, Z., Jefferson, I., 2009. Rivers and loess: The  
2964 significance of long river transportation in the complex event-sequence approach to loess deposit  
2965 formation. *Quaternary International* 198, 7-18.

- 2966 Smalley, I.J., Marković, S.B., O'Hara-Dhand, K. 2010. The INQUA Loess Commission as a Central European  
2967 Enterprise. *Central European Journal of Geosciences* 2, 3-8.
- 2968 Smalley, I., O'Hara-Dhand, K., Kwong, J., 2014. China: Materials for a loess landscape. *Catena* 117, 100–  
2969 107.
- 2970 Smith, B.J., Wright, J.S., Whalley, W.B., 2002. Sources of non-glacial, loess-size quartz silt and the origins  
2971 of "desert loess". *Earth-Science Reviews* 59, 1-26.
- 2972 Smith, G.D., 1942. Illinois loess: variations in its properties and distribution. University of Illinois  
2973 Agricultural Experiment Station Bulletin 490.
- 2974 Song, Y., Hao, Q. Z., Ge, J. Y., Zhao, D. A., Zhang, Y., Li, Q., Zuo, X. X., Lü, Y.W., Wang, P., 2014.  
2975 Quantitative relationships between magnetic enhancement of modern soils and climatic variables over  
2976 the Chinese Loess Plateau. *Quaternary International*, 334, 119–131
- 2977 Song, Y., Lai, Z., Li, Y., Chen, T., Wang, Y., 2015. Comparison between luminescence and radiocarbon  
2978 dating of late Quaternary loess from the Ili Basin in Central Asia. *Quaternary Geochronology* 30, 405-  
2979 410.
- 2980 Song, Y., Guo, Z., Marković, S., Hambach, U., Deng, C., Chang, L., Wu, J., Hao, Q., 2017. Magnetic  
2981 stratigraphy of the Danube loess: a composite Titel-Stari Slankamen loess section over the last one  
2982 million years in Vojvodina, Serbia. *Journal of Asian Earth Sciences*, in press.
- 2983 Sprafke, T., Obreht, I., 2016. Loess: Rock, sediment or soil – What is missing for its definition?  
2984 *Quaternary International*, 399, 198-207.
- 2985 Stanley, K.E., Schaetzl, R.J., 2011. Characteristics and paleoenvironmental significance of a thin, dual-  
2986 sourced loess sheet, North-Central Wisconsin. *Aeolian Research* 2, 241-251.
- 2987 Stevens, T., Lu, H., Thomas D.S.G., Armitage, S.J., 2008. Optical dating of abrupt shifts in the Late  
2988 Pleistocene East Asian monsoon. *Geology* 36, 415-418.

- 2989 Stevens, T., Palk, C., Carter, A., Lu, H.Y., Clift, P.D., 2010. Assessing the provenance of loess and desert  
2990 sediments in northern China using U-Pb dating and morphology of detrital zircons. *Geological Society of*  
2991 *America Bulletin* 122, 1331-1344.
- 2992 Stevens, T., Carter, A., Watson, T.P., Vermeesch, P., Andò, S., Bird, A.F., Lu, H., Garzanti, E., Cottam,  
2993 M.A., Sevastjanova, I., 2013a. Genetic linkage between the Yellow River, the Mu Us desert and the  
2994 Chinese Loess Plateau. *Quaternary Science Reviews* 78, 355–368.
- 2995 Stevens, T., Adamiec, G., Bird, A.F., Lu, H., 2013b. An abrupt shift in dust source on the Chinese Loess  
2996 Plateau revealed through high sampling resolution OSL dating. *Quaternary Science Reviews* 82, 121-132.
- 2997 Stevens, T., Buylaert, J.-P., Lu, H., Thiel, C., Murray, A., Frechen, M., Yi, S. and Zeng, L., 2016. Mass  
2998 accumulation rate and monsoon records from Xifeng, Chinese Loess Plateau, based on a luminescence  
2999 age model. *Journal of Quaternary Science* 31, 391–405.
- 3000 Stiglitz, B.C., Banerjee, S.K., Goullan, A., Oches, E., 2006. A multi-proxy study of Argentina loess: Marine  
3001 oxygen isotope stage 4 and 5 environmental record from pedogenic hematite. *Palaeogeography,*  
3002 *Palaeoclimatology, Palaeoecology* 239, 45–62.
- 3003 Stott, L.D., 2002. The influence of diet on the  $\delta^{13}C$  of shell carbon in the pulmonate snail *Helix aspersa*.  
3004 *Earth and Planetary Science Letters* 195, 249-259.
- 3005 Stuut, J.-B., Smalley, I., O’Hara-Dhand, K., 2009. Aeolian dust in Europe: African sources and European  
3006 deposits. *Quaternary International* 198, 234-345.
- 3007 Sümegi, P., Gulyás, S., Csökmei, B., Molnár, D., Hambach, U., Stevens, T., Markovic, S.B., Almond, P.C.,  
3008 2012. Climatic fluctuations inferred for the Middle and Late Pleniglacial (MIS 2) based on high-resolution  
3009 (ca. 20 y) preliminary environmental magnetic investigation of the loess section of the Madaras  
3010 brickyard (Hungary). *Central European Geology* 55, 329–345.
- 3011 Sun, D., Bloemendal, J., Rea, D.K., Vandenberghe, J., Jiang, F., An, Z., Su, R., 2002. Grain-size distribution  
3012 function of polymodal sediments in hydraulic and aeolian environments, and numerical partitioning of  
3013 sedimentary components. *Sedimentary Geology* 152, 262-277.

- 3014 Sun, J., 2002a. Source regions and formation of the loess sediments on the high mountain regions of  
3015 northwestern China. *Quaternary Research* 58, 341-351.
- 3016 Sun, J., 2002b. Provenance of loess material and formation of loess deposits on the Chinese Loess  
3017 Plateau. *Earth and Planetary Science Letters* 203, 845-859.
- 3018 Sun, J.M., Liu, T.S., 2000. Stratigraphic evidence for the uplift of the Tibetan Plateau between ~1.1 and  
3019 ~0.9 Myr ago. *Quaternary Science Reviews* 54, 309–320.
- 3020 Sun, Y., An, Z., 2005. Late-Pliocene-Pleistocene changes in mass accumulation rates of eolian deposits on  
3021 the central Chinese Loess Plateau. *Journal of Geophysical Research* 110, D23101.
- 3022 Sun, Y., Clemens, S.C., An, Z., Yu, Z., 2006. Astronomic timescale and palaeoclimatic implication of  
3023 stacked 3.6-Myr monsoon records from the Chinese Loess Plateau. *Quaternary Science Reviews* 25, 33-  
3024 48.
- 3025 Sun, Y., Wang, X., Liu, Q., Clemens, S. C., 2010. Impacts of post-depositional processes on rapid monsoon  
3026 signals recorded by the last glacial loess deposits of northern China. *Earth and Planetary Science Letters*,  
3027 289(1), 171-179.
- 3028 Sun, Y. B., Qiang, X. K., Liu, Q. S., Bloemendal, J., and Wang, X. L., 2013. Timing and lock-in effect of the  
3029 Laschamp geomagnetic excursion in Chinese loess, *Geochemistry, Geophysics, Geosystems*, 14, 4952–  
3030 4961.
- 3031 Svirčev, Z., Marković, S.B., Stevens, T., Codd, G., Smalley, I., Simeunović, J., Obreht, I., Dulić, T., Pantelić,  
3032 D., Hambach, U., 2013. Importance of Biological Loess Crusts for Loess Formation in Semi-Arid  
3033 Environments. *Quaternary International* 296, 206-215.
- 3034 Sweeney, M.R., Mason, J.A., 2013. Mechanisms of dust emission from Pleistocene loess deposits,  
3035 Nebraska, U.S.A. *Journal of Geophysical Research-Earth Surface* 118, 1-12.

- 3036 Swinehart, J.B., Souders, V.L., De Graw, H.M., Diffendal, R.F., Jr, 1985. Cenozoic paleogeography of  
3037 western Nebraska, In: Flores, R.M., Kaplan, S.S. (Eds.), Cenozoic paleogeography of west-central United  
3038 States. Rocky Mountain Section-SEPM, Denver. Pp. 209-229.
- 3039 Taber, S., 1943. Perennially frozen ground in Alaska; its origin and history. Geological Society of America  
3040 Bulletin 54, 1433-1548.
- 3041 Taber, S., 1953. Origin of Alaska silts. *American Journal of Science* 251, 321-336.
- 3042 Taber, S., 1958. Complex origin of silts in the vicinity of Fairbanks, Alaska. Geological Society of America  
3043 Bulletin 69, 131-136.
- 3044 Tanner, S., Katra, I., Haim, A., Zaady, E., 2016. Short-term soil loss by eolian erosion in response to  
3045 different rain-fed agricultural practices. *Soil and Tillage Research* 155, 149-156.
- 3046 Tarling, D. H., Hrouda, F., 1993. *The Magnetic Anisotropy of Rocks*. Chapman & Hall, 217 pp.
- 3047 Taylor, S. N., Lacroix, F., 2015. Magnetic anisotropy reveals the depositional and postdepositional history  
3048 of a loess-paleosol sequence at Nussloch (Germany). *Journal of Geophysical Research: Solid Earth*,  
3049 120(5), 2859-2876.
- 3050 Taylor, S. N., Lacroix, F., Rousseau, D. D., Antoine, P., 2014. Mineral magnetic characterization of the  
3051 Upper Pleniglacial Nussloch loess sequence (Germany): an insight into local environmental processes.  
3052 *Geophysical Journal International*, 199(3), 1463-1480.
- 3053 Taylor, S.R., McLennan, S.M, McCulloch, M.T., 1983. Geochemistry of loess, continental crustal  
3054 composition and crustal modal ages. *Geochimica et Cosmochimica Acta* 47, 1897-1905.
- 3055 Terhorst, B., Thiel, C., Peticzka, R., Sprafke, T., Frechen, M., Fladerer, F.A., Roetzel, R., and Neugebauer-  
3056 Maresch, C., 2011. Casting new light on the chronology of the loess/paleosol sequences in Lower  
3057 Austria. *E&G Quaternary Science Journal* 60, 270–277.

- 3058 Thomas, E.K., Clemens, S.C., Sun, Y., Prell, W.L., Huang, Y., Gao, L., Loomis, S., Chen, G., Liu, Z., 2016.  
3059 Heterodynes dominate precipitation isotopes in the East Asian monsoon region, reflecting interaction of  
3060 multiple climate factors. *Earth and Planetary Science Letters* 455, 196–206.
- 3061 Thorp, J., Smith, H.T.U., 1952. Pleistocene eolian deposits of the United States, Alaska, and parts of  
3062 Canada. National Research Council Committee for the Study of Eolian Deposits. Geological Society of  
3063 America. 1:2,500,000 scale map.
- 3064 Timar-Gabor, A., Vandenberghe, D.A.G., Vasiliniuc, S., Panaitu, C.E., Panaiotu, C.G., Dimofte, D., Cosma,  
3065 C., 2011. Optical dating of Romanian loess: a comparison between silt-sized and sand-sized quartz.  
3066 *Quaternary International* 240, 62–70.
- 3067 Trask, P.D., 1932. Origin and Environment of Source Sediments of Petroleum. Gulf Publishing Co.,  
3068 Houston, TX. 67 pp.
- 3069 Tripaldi A., Zárate M., 2017. Geofomas eólicas de la cuenca del río Salado-Chadileuvú, provincia de la  
3070 Pampa Argentina. *Actas XX Congreso Geológico Argentino*, San Miguel de Tucumán, 183-185.
- 3071 Tsatskin, A., Heller, F., Hailwood, E.A., Gendler, T.S., Hus, J., Montgomery, P., Sartori, M., Virina, E.I.,  
3072 1998. Pedosedimentary division, rock magnetism and chronology of the loess/palaeosol sequence at  
3073 Rozany (Ukraine). *Palaeogeography, Palaeoclimatology, Palaeoecology* 143, 111–133.
- 3074 Tsoar, H., Pye, K., 1987. Dust transport and the question of desert loess formation. *Sedimentology* 34,  
3075 139-153.
- 3076 Tuthorn, M., Zech, M., Ruppenthal, M., Oelmann, Y., Kahmen, A., del Valle, H.F., Wilcke, W., Glaser, B.,  
3077 2014. Oxygen isotope ratios ( $^{18}\text{O}/^{16}\text{O}$ ) of hemicellulose-derived sugar biomarkers in plants, soils and  
3078 sediments as paleoclimate proxy II: Insight from a climate transect study. *Geochimica et Cosmochimica*  
3079 *Acta* 126, 624-634.
- 3080 Tuthorn, M., Zech, R., Ruppenthal, M., Oelmann, Y., Kahmen, A., del Valle, H., Eglinton, T., Rozanski, K.,  
3081 Zech, M., 2015. Coupling  $\delta^2\text{H}$  and  $\delta^{18}\text{O}$  biomarker results yields information on relative humidity and  
3082 isotopic composition of precipitation. *Biogeosciences* 12, 3913-3924.

- 3083 Újvári, G., Klötzli, U., 2015. U-Pb ages and Hf composition of zircons in Austrian last glacial loess:  
3084 constraints on heavy mineral sources and sediment transport pathways. *International Journal of Earth*  
3085 *Sciences* 104, 1365-1385.
- 3086 Újvári, G., Varga, A., Balogh-Brunstad, Z., 2008. Origin, weathering and geochemical composition of loess  
3087 in southwestern Hungary. *Quaternary Research* 69, 421-437.
- 3088 Újvári, G., Varga, A., Ramos, F.C., Kovács, J., Németh, T., Stevens, T., 2012. Evaluating the use of clay  
3089 mineralogy, Sr–Nd isotopes and zircon U–Pb ages in tracking dust provenance: An example from loess of  
3090 the Carpathian Basin. *Chemical Geology* 304, 83-96.
- 3091 Újvári, G., Klötzli, U., Kiraly, F., Ntaflos, T., 2013. Towards identifying the origin of metamorphic  
3092 components in Austrian loess: insights from detrital rutile chemistry, thermometry and U-Pb  
3093 geochronology. *Quaternary Science Reviews* 75, 132-142.
- 3094 Vandenberghe, D.A.G., Derese, C., Kasse, C., Van den haute, P., 2013. Late Weichselian (fluvio-) aeolian  
3095 sediments and Holocene drift-sands of the classic type locality in Twente (E Netherlands): a high-  
3096 resolution dating study using optically stimulated luminescence. *Quaternary Science Reviews* 68, 96–  
3097 113.
- 3098 Vandenberghe, J., 1985. Palaeoenvironment and stratigraphy during the last glacial in the Belgian-Dutch  
3099 border region. *Quaternary Research* 24, 23-38.
- 3100 Vandenberghe, J., 1991. Changing conditions of aeolian sand deposition during the last deglaciation  
3101 period. *Zeitschrift für Geomorphologie, Suppl. Bd. 90*, 193-207.
- 3102 Vandenberghe, J., 2013. Grain size of fine-grained windblown sediment: a powerful proxy for process  
3103 identification. *Earth Science Reviews* 121, 18-30.
- 3104 Vandenberghe, J., Kasse, C., 2008. Les formations sableuses en milieux périglaciaires: sables de  
3105 couverture et sables dunaires. In : Dewolf, Y., Bourrié, G. (Eds.), 'Les formations superficielles', Ellipses,  
3106 Paris, pp. 317-321.



- 3107 Vandenberghe, J., Krook, L., 1981. Stratigraphy and genesis of Pleistocene deposits at Alphen (southern  
3108 Netherlands). *Geologie en Mijnbouw* 60, 417-426.
- 3109 Vandenberghe, J., Krook, L., 1985. La stratigraphie et la genèse de dépôts Pleistocènes à Goirle (Pays-  
3110 Bas). *Bulletin Association Française d' études Quaternaires* 1985-4, 239-247.
- 3111 Vandenberghe, J., Van Huissteden, J., 1988. Fluvio-aeolian interaction in a region of continuous  
3112 permafrost. *Proceedings 5<sup>th</sup> International Permafrost Conference*, Trondheim, Norway. pp. 876-881.
- 3113 Vandenberghe, J., An, Z.S., Nugteren, G., Lu, H.Y., and Van Huissteden, K., 1997. New absolute time scale  
3114 for the Quaternary climate in the Chinese loess region by grain-size analysis. *Geology* 25, 35–38.
- 3115 Vandenberghe, J., Renssen, H., van Huissteden, K., Nugteren, G., Konert, M., Lu, H., Dodonov, A.,  
3116 Buylaert, J.-P., 2006. Penetration of Atlantic westerly winds into Central and East Asia. *Quaternary*  
3117 *Science Reviews* 25, 2380-2389.
- 3118 Vandenberghe, J., Renssen, H., Roche, D.M., Goosse, H., Velichko, A.A., Gorbunov, A., Levavasseur, G.,  
3119 2012. Eurasian permafrost instability constrained by reduced sea-ice cover. *Quaternary Science Reviews*  
3120 34, 16–23.
- 3121 Vandenberghe, J., French, H. M., Gorbunov, A., Marchenko, S., Velichko, A. A., Jin, H., Cui, Z., Zhang, T. &  
3122 Wan, X., 2014a. The Last Permafrost Maximum (LPM) map of the Northern Hemisphere: permafrost  
3123 extent and mean annual air temperatures, 25–17 ka BP. *Boreas* 43, 652–666.
- 3124 Vandenberghe, J., Markovic, S., Jovanovic, M., Hambach, U., 2014b. Site-specific variability of loess and  
3125 palaeosols (Ruma, Vojvodina, northern Serbia). *Quaternary International* 334-335, 86-93.
- 3126 Vandenberghe, J., Sun, Y., Wang, X., Abels, H.A., Liu, X., 2017. Grain-size characterization of reworked  
3127 fine-grained aeolian deposits. *Earth Science Reviews* (in press).  
3128 <https://doi.org/10.1016/j.earscirev.2017.11.005>
- 3129 Van der Hammen, Th., Maarleveld, G.C., Vogel, J., Zagwijn, W.H., 1967. Stratigraphy, climatic succession  
3130 and radiocarbon dating of the last glacial in The Netherlands. *Geologie en Mijnbouw* 46, 79-95.

- 3131 Van Huissteden, J., 1990. Tundra rivers of the last glacial: sedimentation and geomorphological  
3132 processes during the Middle Pleniglacial in Twente, eastern Netherlands. *Mededelingen Rijks Geologische*  
3133 *Dienst* 44, 1-138.
- 3134 Van Huissteden J., Vandenberghe J., Van der Hammen T., Laan W., 2000. Fluvial and eolian interaction  
3135 under permafrost conditions: Weichselian Late Pleniglacial, Twente, eastern Netherlands. *Catena* 40,  
3136 307-321.
- 3137 Velichko, A.A., 1990. Loess–paleosol formation on the Russian Plain. *Quaternary International* 7/8, 103–  
3138 114.
- 3139 Velichko, A.A., Catto, N., Kononov, Yu.M., Morozova, T.D., Novenko, E.Y., Panin, P.G., Ryskov,  
3140 Ya.G., Semenov, V.V., Timireva, S.N., Titov, V.V., Teskov, A.S., 2009. Progressively colder, drier  
3141 interglacials in southern Russia through the Quaternary: evidence from the Sea of Azov region.  
3142 *Quaternary International* 198, 204-219.
- 3143 Veres, D., Lane, C.S., Timar-Gabor, A., Hambach, U., Constantin, D., Szakács, A., Fülling, A., and Onac,  
3144 B.P., 2013. The Campanian Ignimbrite/Y5 tephra layer - A regional stratigraphic marker for Isotope Stage  
3145 3 deposits in the Lower Danube region, Romania. *Quaternary International* 293, 22-33.
- 3146 Vermeesch, P., 2004. How many grains are needed for a provenance study? *Earth and Planetary Science*  
3147 *Letters* 224, 441-451.
- 3148 Vermeesch, P., 2012. On the visualisation of detrital age distributions. *Chemical Geology* 312-313, 190-  
3149 194.
- 3150 Vermeesch, P., 2013. Multi-sample comparison of detrital age distributions. *Chemical Geology* 341, 140-  
3151 146.
- 3152 Vermeesch, P., Garzanti, E., 2015. Making geological sense of 'Big Data' in sedimentary provenance  
3153 analysis. *Chemical Geology* 409, 20-27.

- 3154 Vlamincx, S., Kehl, M., Lauer, T., Shahriari, A., Sharifi, J., Eckmeier, E., Lehndorff, E., Khormali, F.,  
3155 Frechen, M., 2016. Loess-soil sequence at Toshan (Northern Iran): Insights into late Pleistocene climate  
3156 change. *Quaternary International* 399, 122-135.
- 3157 Vriend, M., Prins, M.A., Buylaert, J.P., Vandenberghe, J., Lu, H., 2011. Contrasting dust supply patterns  
3158 across the north-western Chinese Loess Plateau during the last glacial–interglacial cycle. *Quaternary*  
3159 *International* 240, 167–180.
- 3160 Wacha, L., Rolf, C., Hambach, U., Frechen, M., Galović, L., Duchoslav, M., 2017. The Last Glacial aeolian  
3161 record of the Island of Susak (Croatia) as seen from a high-resolution grain–size and rock magnetic  
3162 analysis. *Quaternary International*, in press.
- 3163 Wang, X. L., Lu, Y. C., Wintle, A. G., 2006. Recuperated OSL dating of fine-grained quartz in Chinese loess.  
3164 *Quaternary Geochronology*, 1, 89–100.
- 3165 Wang, X., Wei, H., Taheri, M., Khormali, F., Danukalova, G., Chen, F., 2016. Early Pleistocene climate in  
3166 western arid central Asia inferred from loess-palaeosol sequences. *Scientific Reports* 6, 20560. doi:  
3167 10.1038/srep20560 (2016).
- 3168 Wang, Z., Zhao, H., Dong, G., Zhou, A., Liu, J., and Zhang, D., 2014. Reliability of radiocarbon dating on  
3169 various fractions of loess-soil sequence for Dadiwan section in the western Chinese Loess Plateau.  
3170 *Frontiers of Earth Science* 8, 540-546.
- 3171 Watson, W. 1966. *Early Civilization in China*. Thames & Hudson, London.
- 3172 Westgate, J.A., Stemper, B.A., Péwé, T.L., 1990. A 3 m.y. record of Pliocene-Pleistocene loess in interior  
3173 Alaska. *Geology* 18, 858-861.
- 3174 Wiesenberg, G., Gocke, M., 2013. Reconstruction of the late Quaternary paleoenvironments of the  
3175 Nussloch loess paleosol sequence - Comment to the paper published by Zech et al., *Quaternary*  
3176 *Research* 78 (2012), 226–235. *Quaternary Research* 79, 304-305.

- 3177 Wilding, L.P., Odell, R.T., Fehrenbacher, J.B., Beavers, A.H., 1963. Source and distribution of sodium in  
3178 Solonchic soils in Illinois. *Soil Science Society of America Proceedings* 27, 432-438.
- 3179 Williams, J.R., 1962. Geologic reconnaissance of the Yukon Flats district, Alaska. U.S. Geological Survey  
3180 Bulletin 1111-H, p. H289–H331.
- 3181 Willmes, C., 2015. LGM sea level change (HiRes), CRC806-Database. Collaborative Research Centre 806,  
3182 Cologne.
- 3183 Wintle, A.G., Adamiec, G., 2017. Optically stimulated luminescence signals from quartz: A review.  
3184 *Radiation Measurements* 98, 10-33.
- 3185 Wright, J.S., 2001. "Desert" loess versus "glacial" loess: quartz silt formation, source areas and sediment  
3186 pathways in the formation of loess deposits. *Geomorphology* 36, 231-256.
- 3187 Wu, B., Wu, N.Q., 2011. Terrestrial mollusk records from Xifeng and Luochuan L9 loess strata and their  
3188 implications for paleoclimatic evolution in the Chinese Loess Plateau during marine Oxygen Isotope  
3189 Stages 24-22. *Climate of the Past* 7, 349–359.
- 3190 Wünnemann, B., Mischke, S., Chen, F.H., 2006. A Holocene sedimentary record from Bosten Lake, China.  
3191 *Palaeogeography, Palaeoclimatology, Palaeoecology* 234, 223–238.
- 3192 Xiao, G., Zong, K., Li, G., Hu, Z., Dupont-Nivet, G., Peng, S., Zhang, K., 2012. Spatial and glacial-interglacial  
3193 variations in provenance of the Chinese Loess Plateau. *Geophysical Research Letters* 39, L20715.
- 3194 Yaalon, D.H., 1969. Origin of desert loess, *Etudes sur le Quaternaire dans le Monde*, Vol. 2. Association  
3195 Francaise pour l'Etude du Quaternaire (AFEQ), Paris, France, p. 755.
- 3196 Yaalon, D.H., Dan, J., 1974. Accumulation and distribution of loess-derived deposits in the semi-desert  
3197 and desert fringe areas of Israel. *Zeitschrift für Geomorphologie Supplementband* 20, 91-105.
- 3198 Yaalon, D.H., Ganor, E., 1973. The influence of dust on soils during the Quaternary. *Soil Science* 116, 146-  
3199 155.

- 3200 Yaalon, D.H., Ganor, E., 1979. East Mediterranean trajectories of dust-carrying storms from the Sahara  
3201 and Sinai, In: Morales, C. (Ed.), *Saharan Dust*. John Wiley and Sons, pp. 187-193.
- 3202 Yanes, Y., 2015. Stable isotope ecology of land snails from a high-latitude site near Fairbanks, interior  
3203 Alaska, USA. *Quaternary Res* 83, 588-595.
- 3204 Yanes, Y., Romanek, C.S., Delgado, A., Brant, H.A., Noakes, J.E., Alonso, M.R., Ibáñez, M., 2009. Oxygen  
3205 and carbon stable isotopes of modern land snail shells as environmental indicators from a low-latitude  
3206 oceanic island. *Geochimica et Cosmochimica Acta* 73, 4077–4099.
- 3207 Yanes, Y., Gutierrez-Zugasti, I., Delgado, A., 2012. Late-glacial to Holocene transition in northern Spain  
3208 deduced from land-snail shelly accumulations. *Quaternary Research* 78, 373-385.
- 3209 Yang, S., Ding, Z., 2006. Winter–spring precipitation as the principal control on predominance of C3  
3210 plants in Central Asia over the past 1.77 Myr: Evidence from  $\delta^{13}\text{C}$  of loess organic matter in Tajikistan.  
3211 *Palaeogeography, Palaeoclimatology, Palaeoecology* 235, 330-339.
- 3212 Yang, S., Ding, Z., 2008. Advance-retreat history of the East-Asian summer monsoon rainfall belt over  
3213 northern China during the last two glacial-interglacial cycles. *Earth and Planetary Science Letters* 274,  
3214 499–510.
- 3215 Yang, S., Ding, Z., 2010. Drastic climatic shift at  $\sim 2.8$  Ma as recorded in eolian deposits of China and its  
3216 implications for redefining the Pliocene-Pleistocene boundary. *Quaternary International* 219, 37–44.
- 3217 Yang, S., Ding, Z., 2014. A 249 kyr stack of eight loess grain size records from northern China  
3218 documenting millennial-scale climate variability. *Geochemistry, Geophysics, Geosystems* 15, 798-814.
- 3219 Yang, S., Ding, F., Ding, Z., 2006. Pleistocene chemical weathering history of Asian arid and semi-arid  
3220 regions recorded in loess deposits of China and Tajikistan. *Geochimica et Cosmochimica Acta* 70, 1695-  
3221 1709.

- 3222 Yang, S., Ding, Z., Wang, X., Tang, Z., Gu, Z., 2012. Negative  $\delta^{18}\text{O}$ - $\delta^{13}\text{C}$  relationship of pedogenic  
3223 carbonate from northern China indicates a strong response of  $\text{C}_3/\text{C}_4$  biomass to the seasonality of Asian  
3224 monsoon precipitation. *Palaeogeography, Palaeoclimatology, Palaeoecology* 317-318, 32–40.
- 3225 Yang, S., Ding, Z., Li, Y., Wang, X., Jiang, W., Huang, X., 2015. Warming-induced northwestward migration  
3226 of the East Asian monsoon rain belt from the Last Glacial Maximum to the mid-Holocene. *Proceedings of*  
3227 *the National Academy of Sciences of the United States of America* 112, 13178–13183.
- 3228 Yang, Y., Mason, J.A., Zhang, H., Lu, H., Ji, J., Chen, J., Liu, L., 2017. Provenance of loess in the central  
3229 Great Plains, U.S.A., based on Nd-Sr isotopic composition, and paleoenvironmental implications.  
3230 *Quaternary Science Reviews* 173, 114-123.
- 3231 Yapp, C.J., 1979. Oxygen and carbon isotope measurements of land snail shell carbonate. *Geochimica et*  
3232 *Cosmochimica Acta* 43, 629-635.
- 3233 Yin, J., Su, Y., Fang, X., 2016. Climate change and social vicissitudes in China over the past two millennia.  
3234 *Quaternary Research* 86: 133-143.
- 3235 Youn, J.H., Seong, Y.B., Choi, J.H., Abdrakhmatov, K., Ormukov, C., 2014. Loess deposits in the northern  
3236 Kyrgyz Tien Shan: Implications for the paleoclimate reconstruction during the Late Quaternary. *Catena*  
3237 117, 81-93.
- 3238 Yong M., Sun Y., 1994. The western regions under the Hsiung-Nu and the Han. In: Harmatta, J., Puri,  
3239 B.N., Etemadi, G.F. (Eds.), *History of civilizations of Central Asia: The development of sedentary and*  
3240 *nomadic civilizations: 700 B.C. to A.D. 250*. UNESCO Publishing, Paris. pp. 219 – 238.
- 3241 Zárte, M., 2003. Loess of southern South America. *Quaternary Science Reviews* 22, 1987-2006.
- 3242 Zárte M., Blasi A., 1993. Late Pleistocene–Holocene eolian deposits of the southern Buenos Aires  
3243 Province, Argentina: a preliminary model. *Quaternary International* 17, 15–20.
- 3244 Zárte M., Tripaldi A., 2012. The aeolian system of central Argentina. *Aeolian Research* 3, 401-417.

- 3245 Zech, M., Glaser, B., 2009. Compound-specific  $\delta^{18}\text{O}$  analyses of neutral sugars in soils using GC-Py-IRMS:  
3246 problems, possible solutions and a first application. *Rapid Communications in Mass Spectrometry* 23,  
3247 3522-3532.
- 3248 Zech, M., Zech, R., Glaser, B., 2007. A 240,000-year stable carbon and nitrogen isotope record from a  
3249 loess-like palaeosol sequence in the Tumara Valley, Northeast Siberia. *Chemical Geology* 242, 307-318.
- 3250 Zech, M., Buggle, B., Leiber, K., Markovic, S., Glaser, B., Hambach, U., Huwe, B., Stevens, T., Sümegi, P.,  
3251 Wiesenberg, G., Zöller, L., 2009. Reconstructing Quaternary vegetation history in the Carpathian Basin,  
3252 SE Europe, using n-alkane biomarkers as molecular fossils: problems and possible solutions, potential  
3253 and limitations. - *Eiszeitalter und Gegenwart - Quaternary Science Journal* 85(2), 150-157.
- 3254 Zech, M., Zech, R., Buggle, B., Zöller, L., 2011. Novel methodological approaches in loess research –  
3255 interrogating biomarkers and compound-specific stable isotopes. *Eiszeitalter & Gegenwart – Quaternary*  
3256 *Science Journal* 60 (1), 170-187.
- 3257 Zech, M., Rass, S., Buggle, B., Löscher, M., Zöller, L., 2012. Reconstruction of the late Quaternary  
3258 paleoenvironment of the Nussloch loess paleosol sequence, Germany, using n-alkane biomarkers.  
3259 *Quaternary Research* 78, 326-335.
- 3260 Zech, M., Krause, T., Meszner, S., Faust, D., 2013a. Incorrect when uncorrected: Reconstructing  
3261 vegetation history using n-alkane biomarkers in loess-paleosol sequences – A case study from the  
3262 Saxonian loess region, Germany. *Quaternary International* 296, 108-116.
- 3263 Zech, M., Rass, S., Buggle, B., Löscher, M., Zöller, L., 2013b. Reconstruction of the late Quaternary  
3264 paleoenvironments of the Nussloch loess paleosol -- Response to the comments by G. Wiesenberg and  
3265 M. Gocke. *Quaternary Research* 79(2), 306-307.
- 3266 Zech, M., Tuthorn, M., Detsch, F., Rozanski, K., Zech, R., Zöller, L., Zech, W., Glaser, B., 2013c. A 220 ka  
3267 terrestrial  $\delta^{18}\text{O}$  and deuterium excess biomarker record from an eolian permafrost paleosol sequence,  
3268 NE-Siberia. *Chemical Geology* 360-361, 220-230.

- 3269 Zech, M., Tuthorn, M., Zech, R., Schlütz, F., Zech, W., Glaser, B., 2014. A 16-ka  $\delta^{18}\text{O}$  record of lacustrine  
3270 sugar biomarkers from the High Himalaya reflects Indian Summer Monsoon variability. *Journal of*  
3271 *Paleolimnology* 51, 241-251.
- 3272 Zech, M., Zech, R., Rozanski, K., Gleixner, G., Zech, W., 2015. Do n-alkane biomarkers in soils/sediments  
3273 reflect the  $\delta^2\text{H}$  isotopic composition of precipitation? A case study from Mt. Kilimanjaro and implications  
3274 for paleoaltimetry and paleoclimate research. *Isotopes in Environmental and Health Studies* 51(4), 508-  
3275 524.
- 3276 Zech, M., Kreutzer, S., Zech, R., Goslar, T., Meszner, S., McIntyre, C., Häggi, C., Eglinton, T., Faust D.,  
3277 Fuchs, M., 2017. Comparative  $^{14}\text{C}$  and OSL dating of loess-paleosol sequences to evaluate post-  
3278 depositional contamination of n-alkane biomarkers. *Quaternary Research* 87, 180-189.
- 3279 Zech, R., Gao, L., Tarozo, R., Huang, Y., 2012. Branched glycerol dialkyl glycerol tetraethers in Pleistocene  
3280 loess-paleosol sequences: Three case studies. *Organic Geochemistry* 53, 38-44.
- 3281 Zech, R., Zech, M., Marković, S., Hambach, U., Huang, Y., 2013. Humid glacials, arid interglacials? Critical  
3282 thoughts on pedogenesis and paleoclimate based on multi-proxy analyses of the loess-paleosol  
3283 sequence Crvenka, Northern Serbia. *Palaeogeography, Palaeoclimatology, Palaeoecology* 387, 165-175.
- 3284 Zeeberg, J.J., 1998. The European sand belt in eastern Europe - a comparison of Late Glacial dune  
3285 orientation with G.C.M. simulation results. *Boreas* 27, 127-139.
- 3286 Zeeden, C., Kels, H., Hambach, U., Schulte, P., Protze, J., Eckmeier, E., Marković, S.B., Klasen, N.,  
3287 Lehmkuhl, F., 2016. Three climatic cycles recorded in a loess-palaeosol sequence at Semlac (Romania) –  
3288 implications for dust accumulation in south-eastern Europe. *Quaternary Science Reviews* 154, 130–154.
- 3289 Zeeden, C., Hambach, U., Veres, D., Fitzsimmons, K., Obrecht, I., Böskén, J., Lehmkuhl, F., in press.  
3290 Millennial scale climate oscillations recorded in the Lower Danube loess over the last glacial period.  
3291 *Palaeogeography, Palaeoclimatology, Palaeoecology*.



- 3292 Zhang, H., Lu, H., Xu, X., Liu, X., Yang, T., Stevens, T., Bird, A., Xu, Z., Zhang, T., Lei, F., Feng, H., 2016.  
3293 Quantitative estimation of the contribution of dust sources to Chinese Loess using detrital zircon U-Pb  
3294 age patterns. *Journal of Geophysical Research: Earth Surface* F003936.
- 3295 Zhang, N., Yamada, K., Suzuki, N., Yoshida, N., 2014. Factors controlling shell carbon isotopic  
3296 composition of land snail *Acusta despecta sieboldiana* estimated from laboratory culturing experiment.  
3297 *Biogeosciences* 11, 5335-5348.
- 3298 Zhang, X.Y., Arimoto, R., An, Z., 1999. Glacial and interglacial patterns for Asian dust transport.  
3299 *Quaternary Science Reviews* 18, 811-819.
- 3300 Zhang, Z., Zhao, M., Eglinton, G., Lu, H., Huang, C., 2006. Leaf wax lipids as paleovegetational and  
3301 paleoenvironmental proxies for the Chinese Loess Plateau over the last 170 kyr. *Quaternary Science*  
3302 *Reviews* 20, 575-594.
- 3303 Zhao, H., Qiang, X., Sun, Y., 2014. Apparent timing and duration of the Matuyama-Brunhes geomagnetic  
3304 reversal in Chinese loess, *Geochemistry, Geophysics, Geosystems*, 15, 4468–4480.
- 3305 Zheng, H., Chen, H., Cao, J., 2002. Palaeoenvironmental implication of the Plio-Pleistocene loess deposits  
3306 in southern Tarim Basin. *Chinese Science Bulletin* 47, 700-704.
- 3307 Zheng, H., Powell, C.M., Butcher, K., Cao, J., 2003. Late Neogene loess deposition in southern Tarim  
3308 Basin: tectonic and palaeoenvironmental implications. *Tectonophysics* 375, 49-59.
- 3309 Zhou, L. P., Shackleton, N. J., 1999. Misleading positions of geomagnetic reversal boundaries in Eurasian  
3310 loess and implications for correlation between continental and marine sedimentary sequences, *Earth*  
3311 *and Planetary Science Letters*, 168, 117–130.
- 3312 Zhu, R., Liu, Q., Jackson, M. J., 2004. Paleoenvironmental significance of the magnetic fabrics in Chinese  
3313 loess-paleosols since the last interglacial (<130 ka). *Earth and Planetary Science Letters*, 221, 55-69.
- 3314 Zöller, L., Semmel, A., 2001. 175 years of loess research in Germany – long records and  
3315 “unconformities”. *Earth-Science Reviews* 54, 19-28.

- 3316 Zykin, V.S., Zykina, V.S., 2015. The Middle and Late Pleistocene loess-soil record in the Iskitim area of  
3317 Novosibirsk Priobie, south-eastern West Siberia. *Quaternary International* 365, 15-25.
- 3318 Zykina, V., Zykin, V., 2012. Loess-soil sequence and environment and climate evolution of West Sibiria in  
3319 Pleistocene (in Russian). Novosibirsk Academic Publishing House "GEO", Novosibirsk, Russia.
- 3320

3321 Figure 1:

3322

3323

3324

3325

3326

3327

3328

3329



3330 Figure 2:

3331

3332

3333

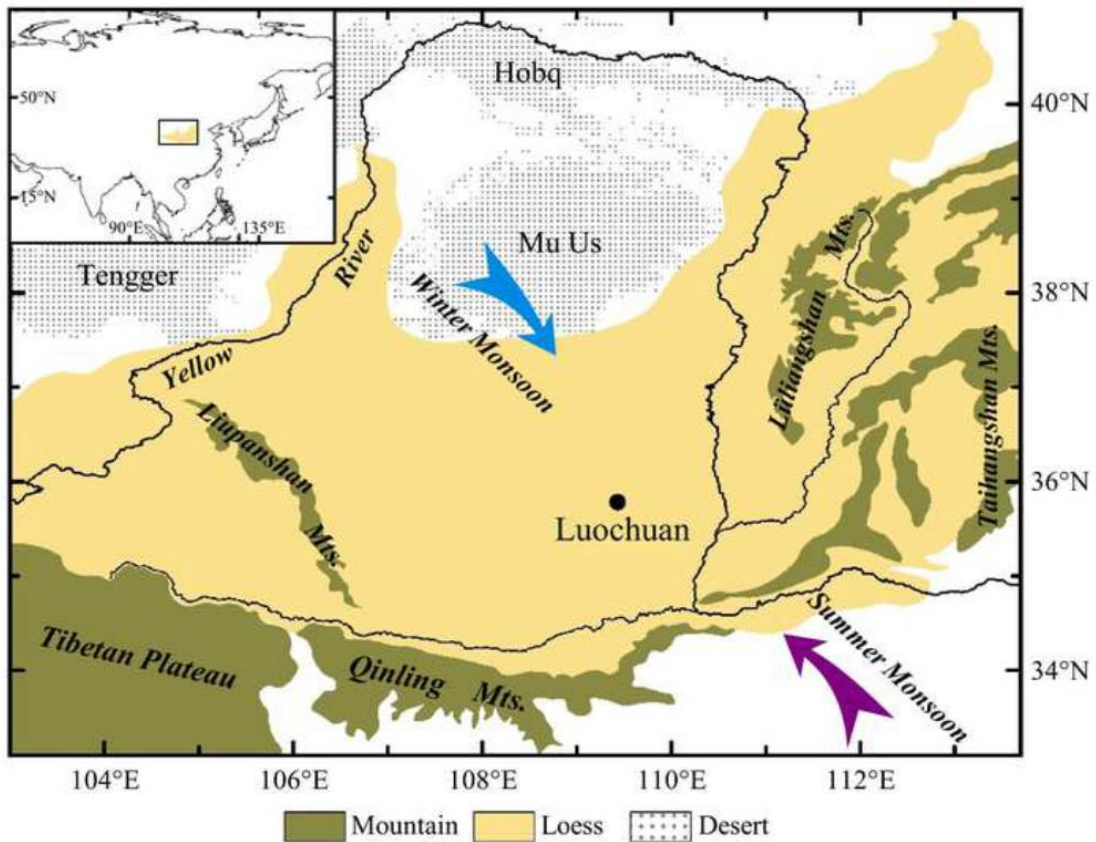
3334

3335

3336

3337

3338





3339

3340 Figure 3:



3341

3342

3343 Figure 4:

3344

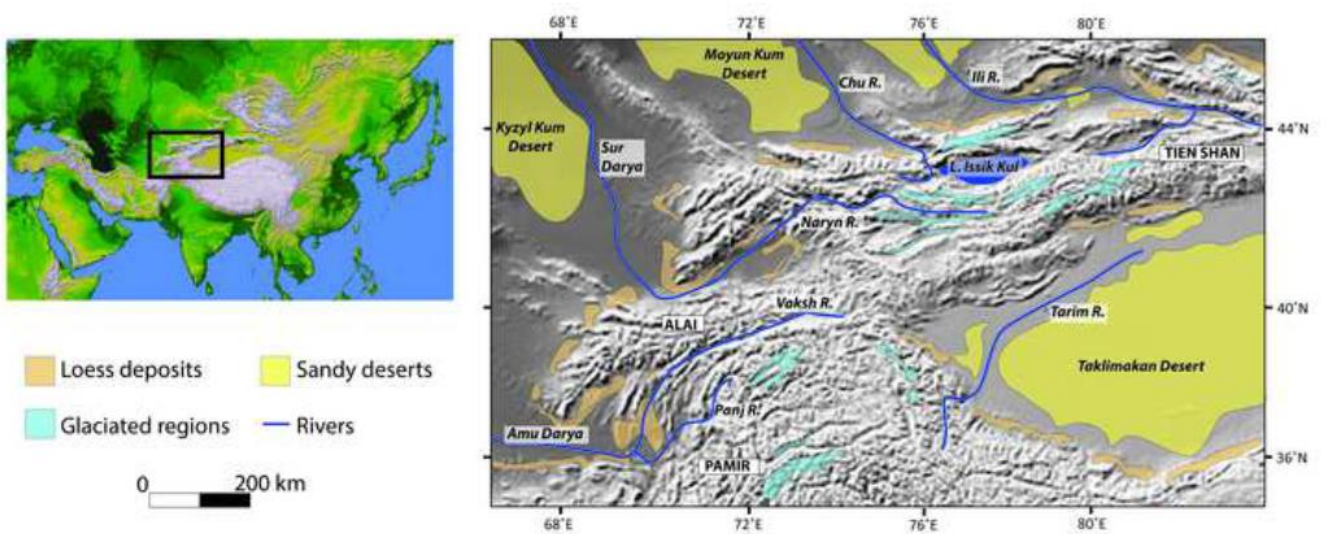
3345

3346

3347

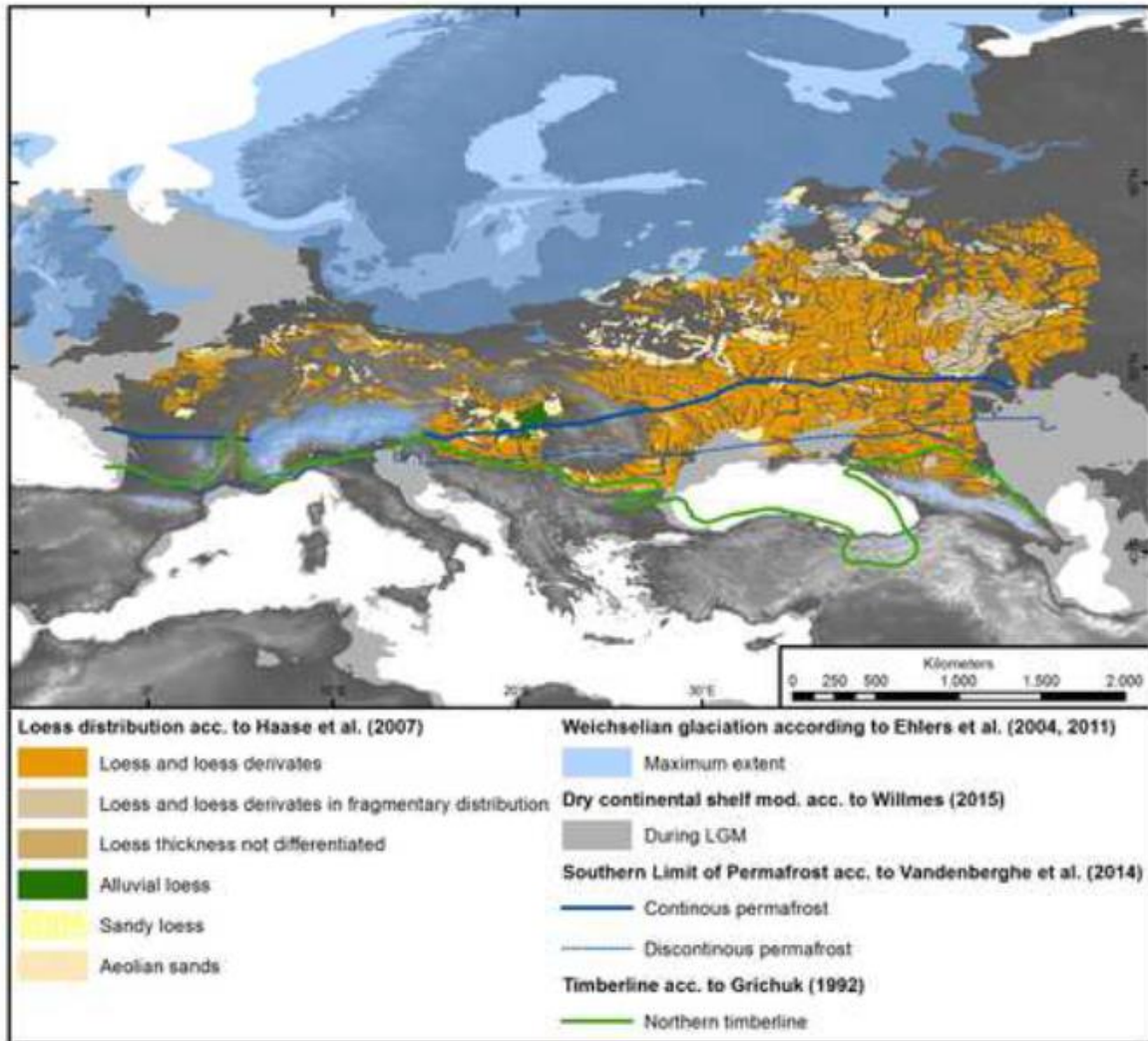
3348

3349



3350

3351 Figure 5:



3352

3353

3354

3355

3356



3357

3358 Figure 6:

3359

3360

3361

3362

3363

3364

3365



3366 Figure 7:

3367

3368

3369

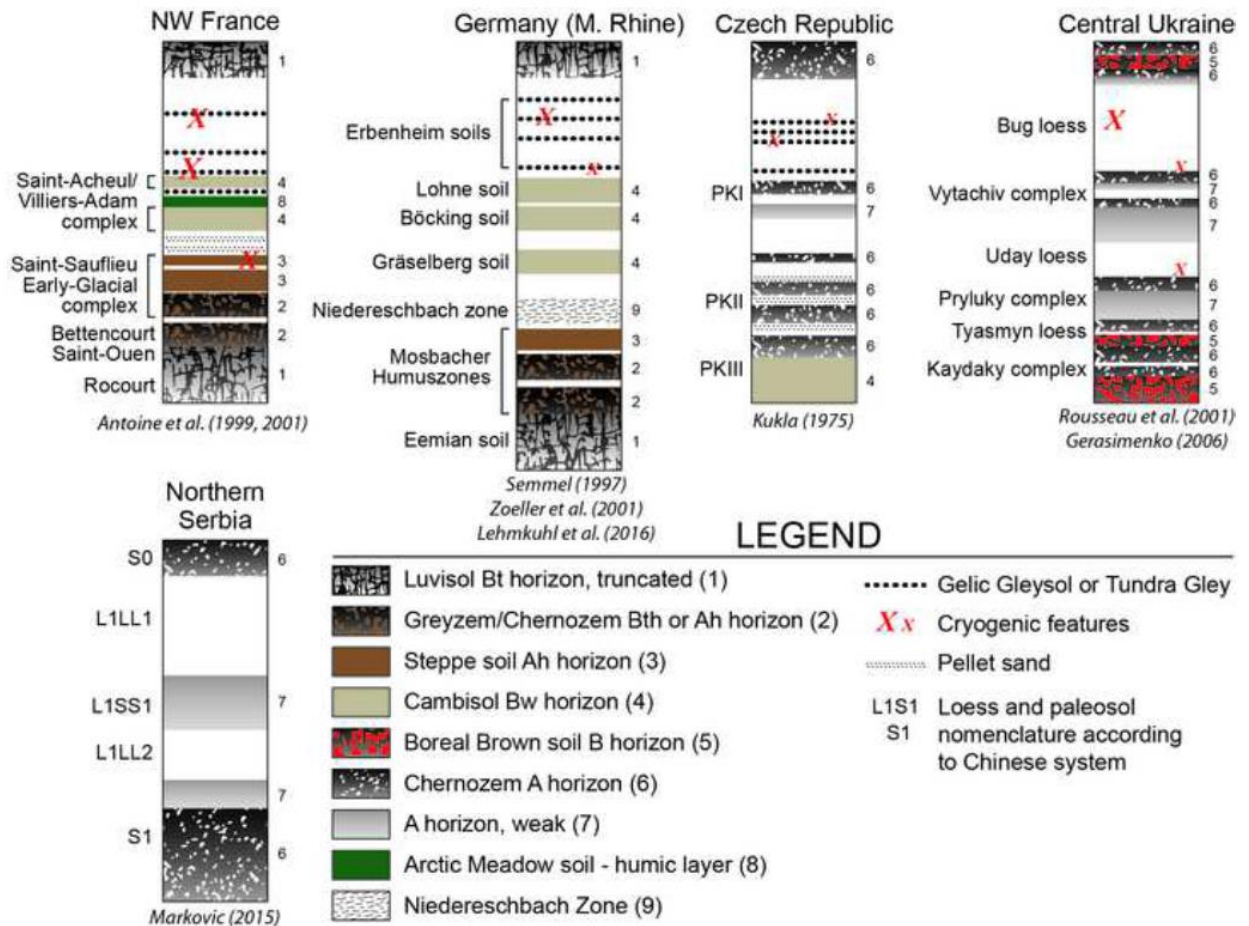
3370

3371

3372

3373

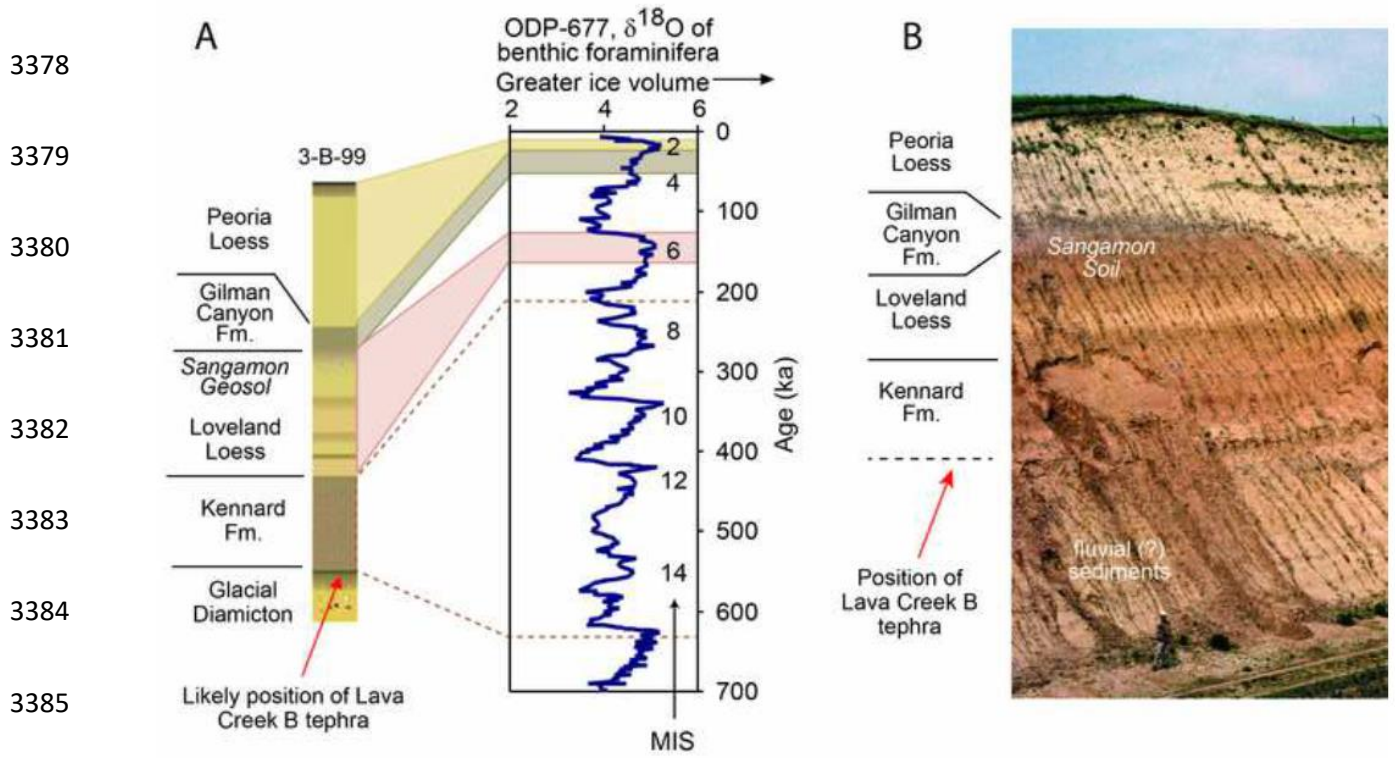
3374



3375

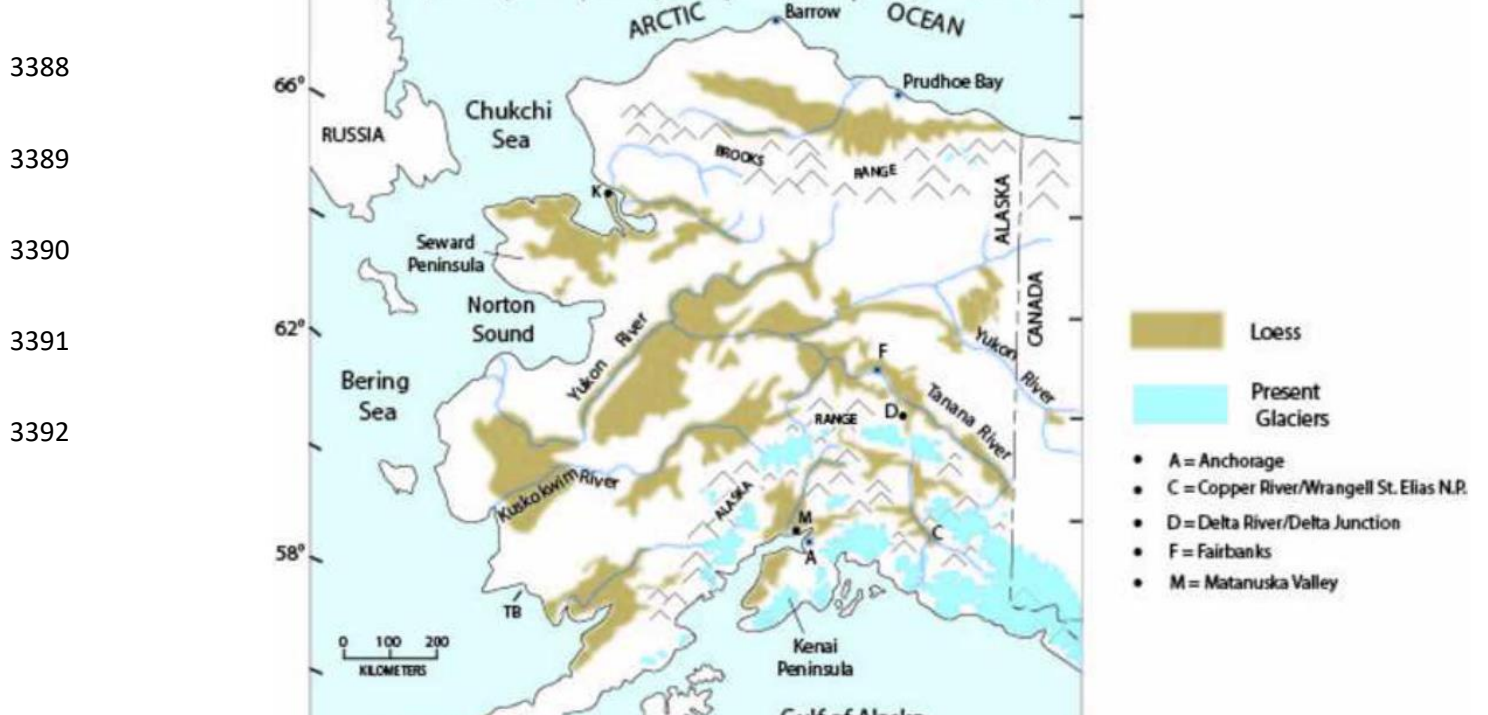
3376

3377 Figure 8:



3386

3387 Figure 9:





3393

3394

3395

3396 Figure 10:

3397

3398

3399

3400

3401

3402

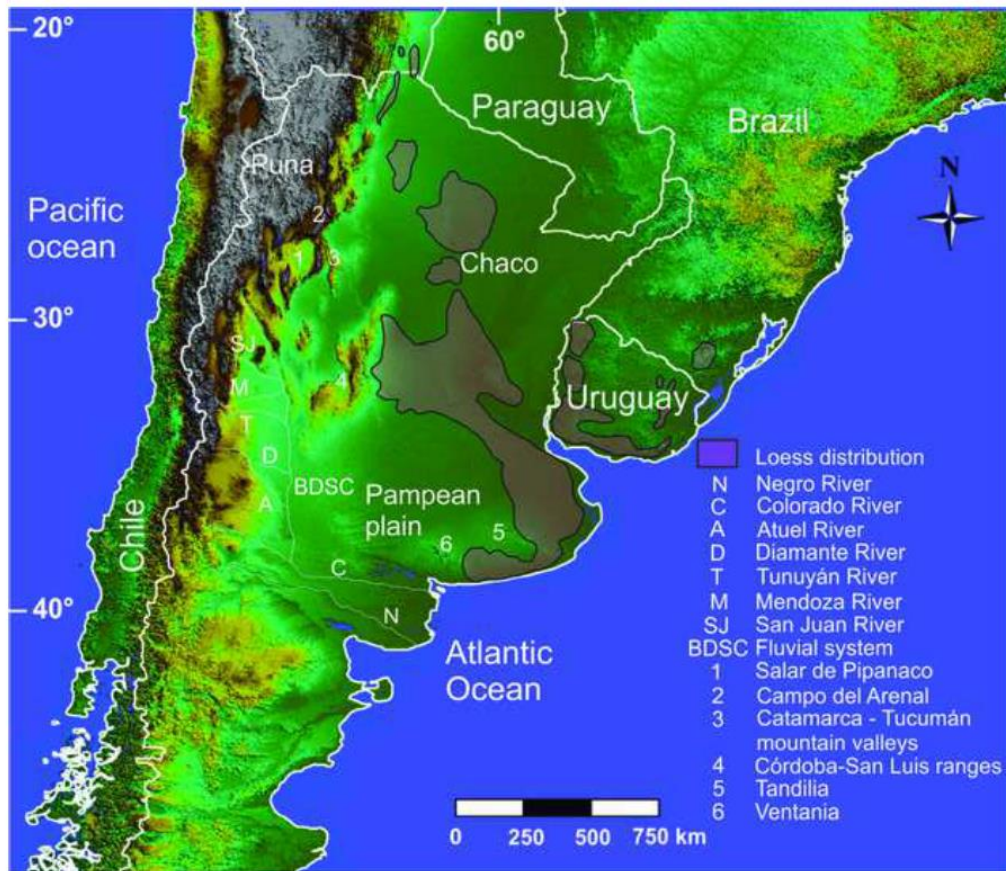
3403

3404

3405

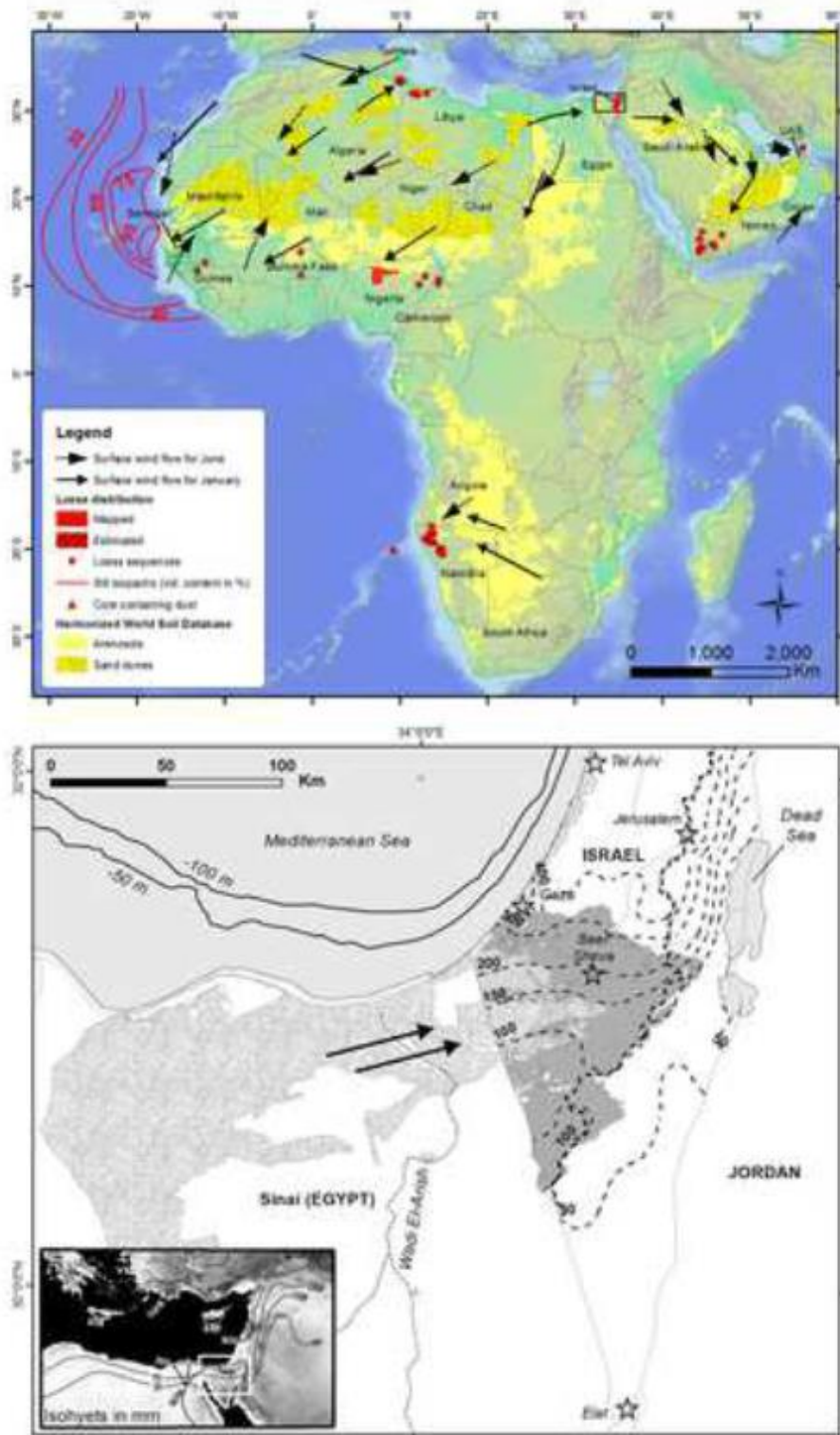
3406

3407

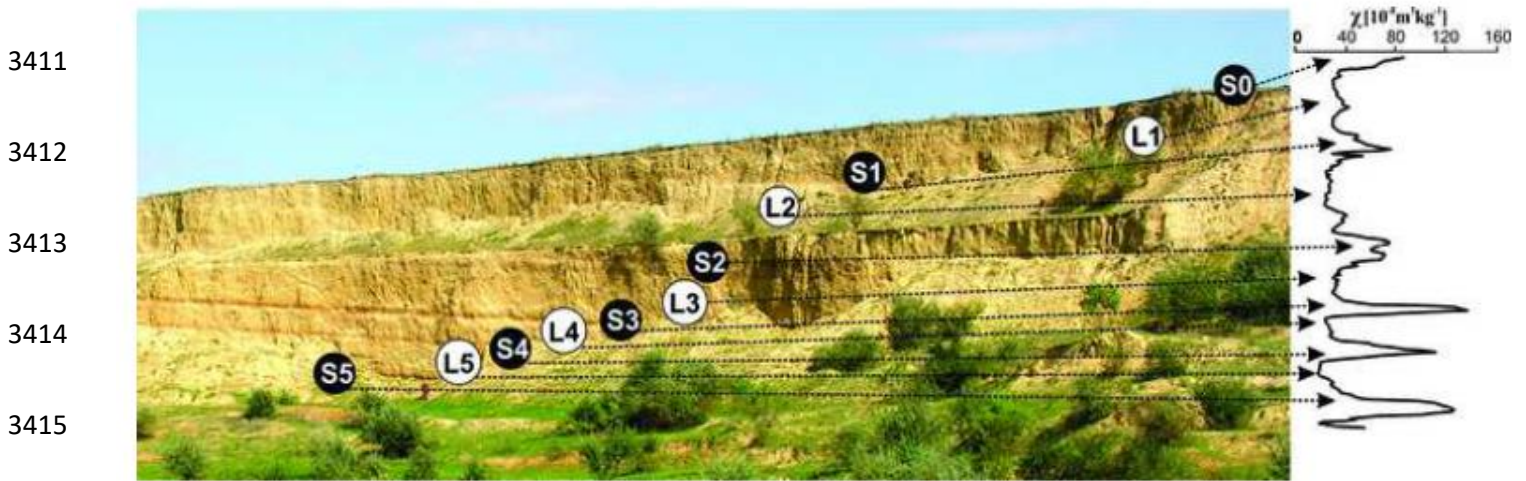




3408 Figure 11:

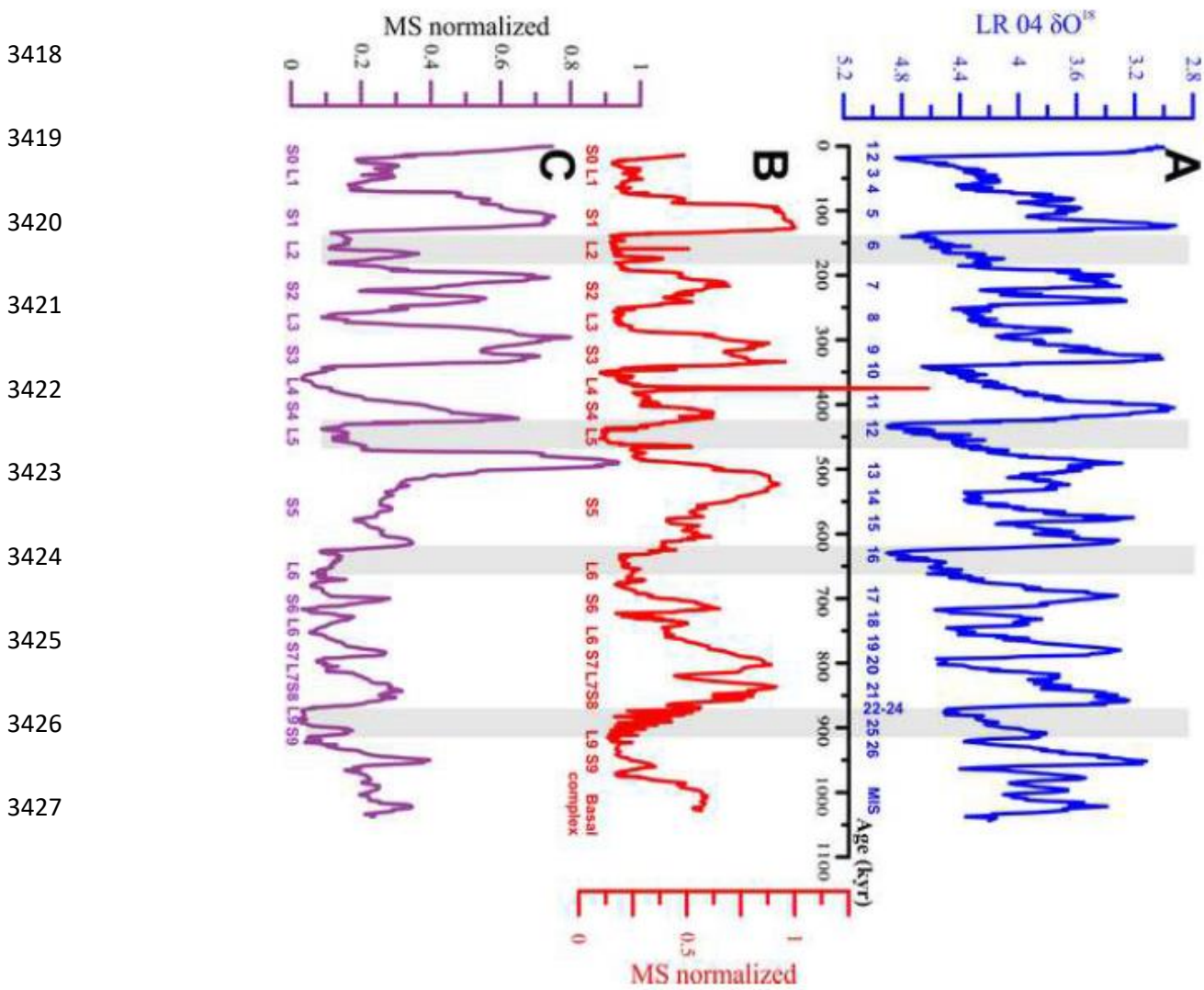


3410 Figure 12:



3416

3417 Figure 13:



3428

3429 Figure 14:

3430

3431

3432

3433

3434

3435

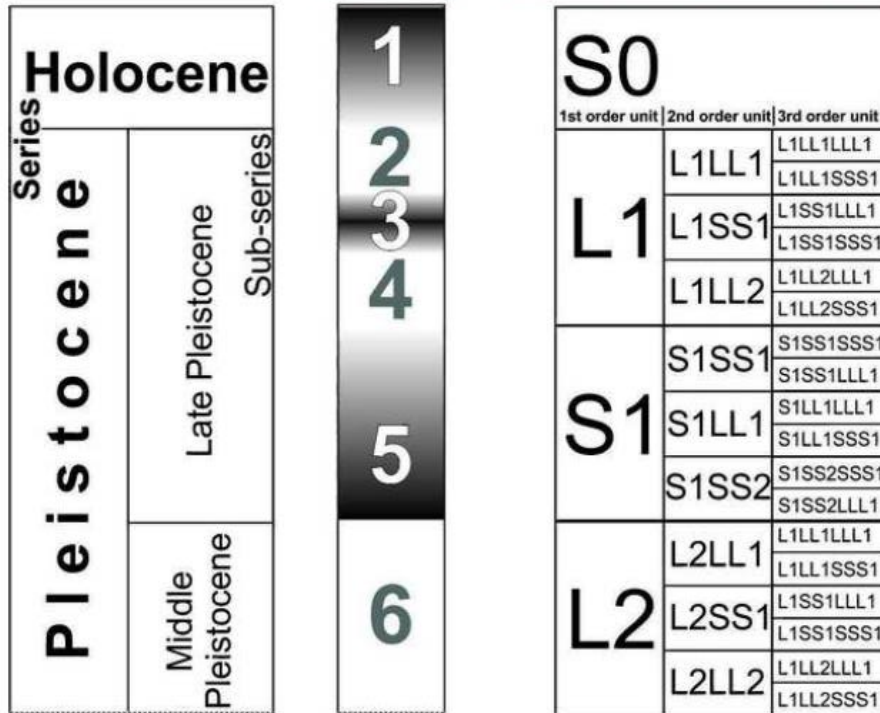
3436

3437

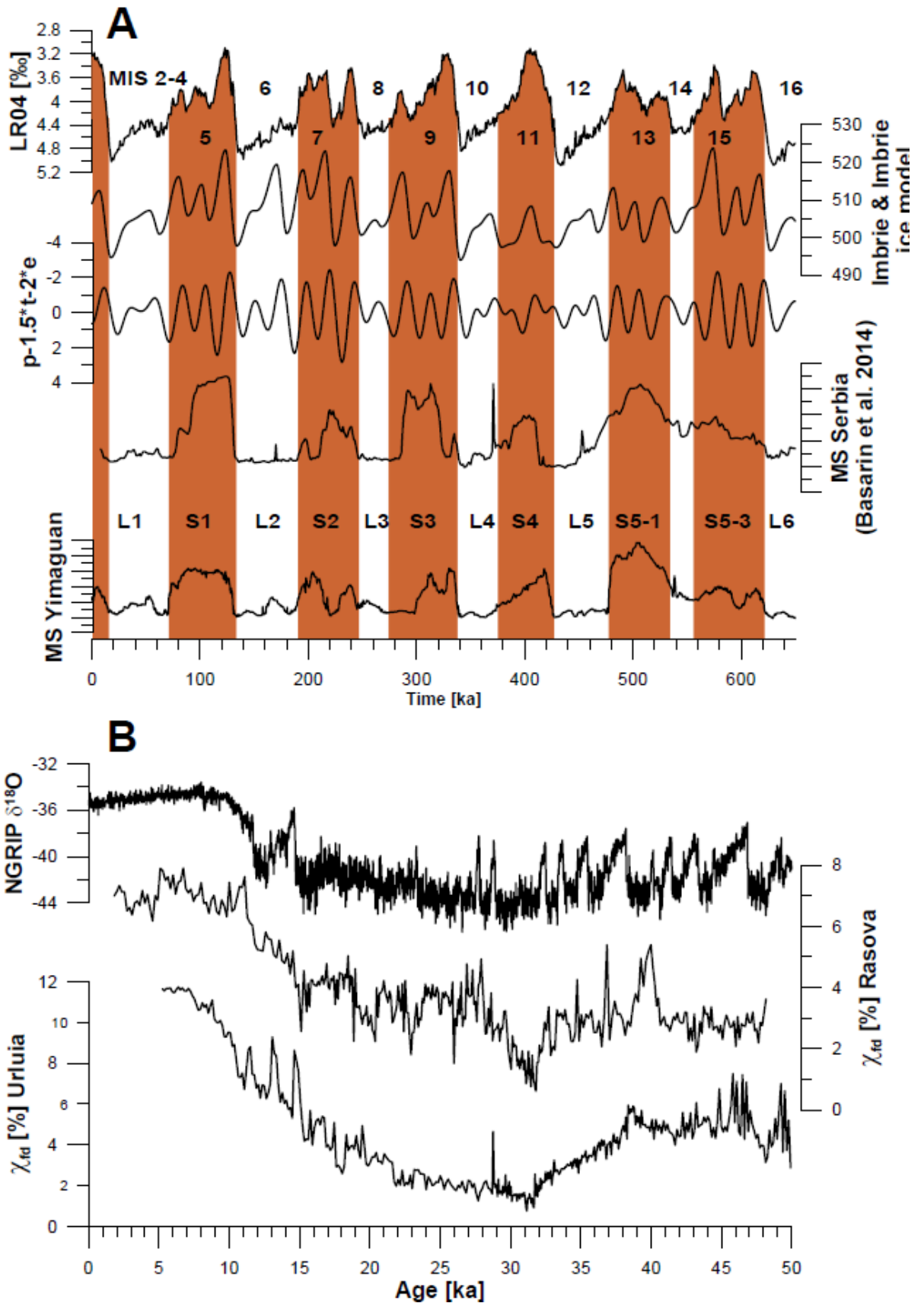
3438

3439

## MIS L&S scheme



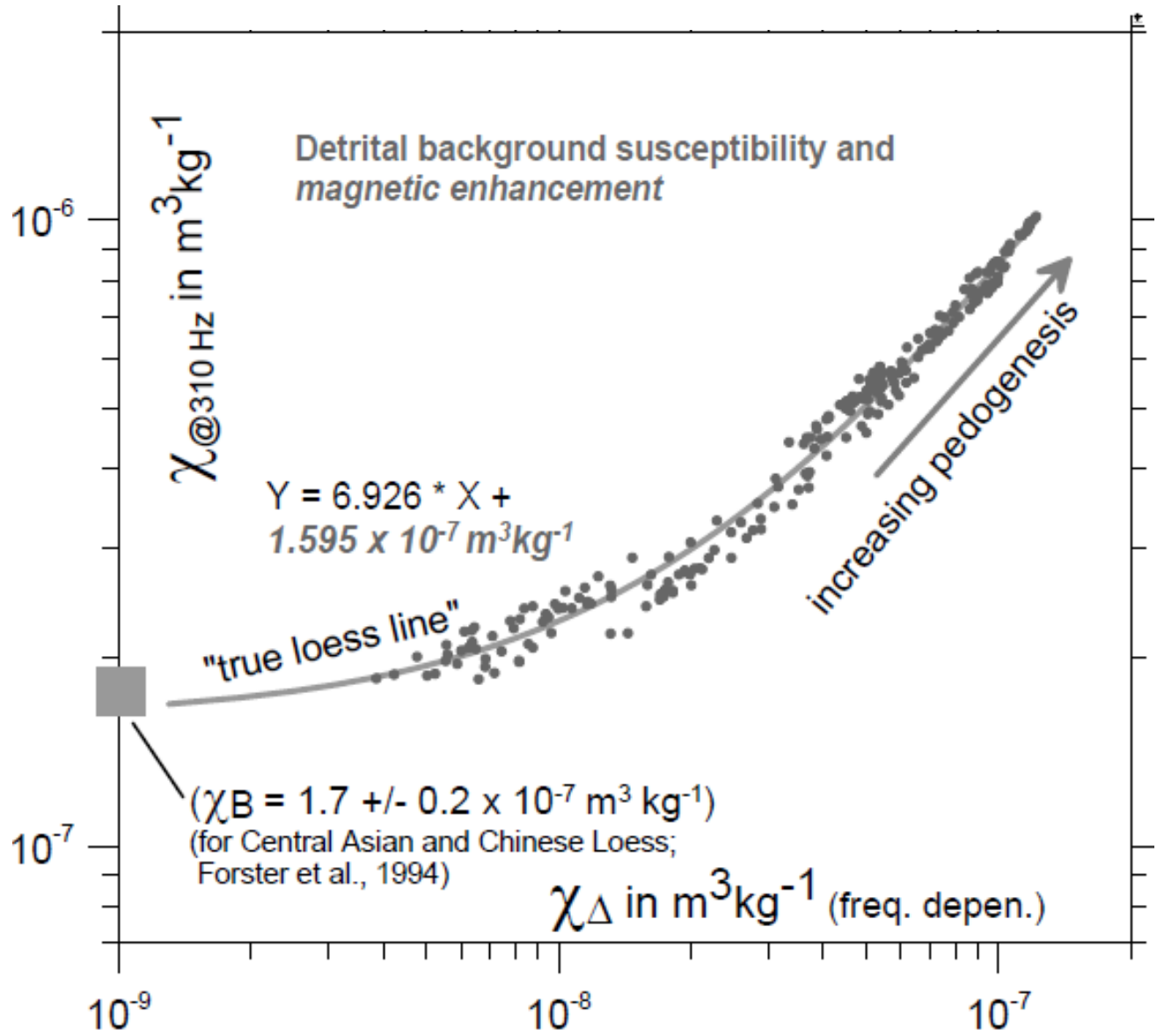
3440 Figure 15:





3458

3459 Figure 16:

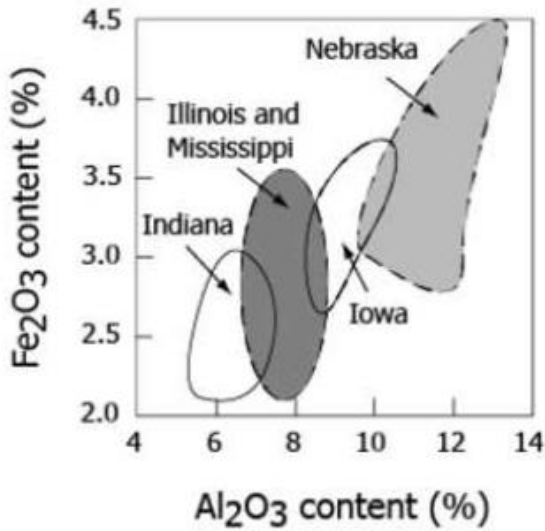


3460

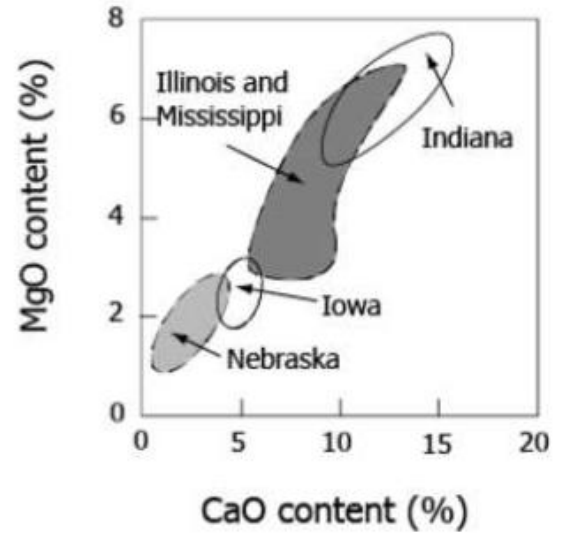
3461

3462

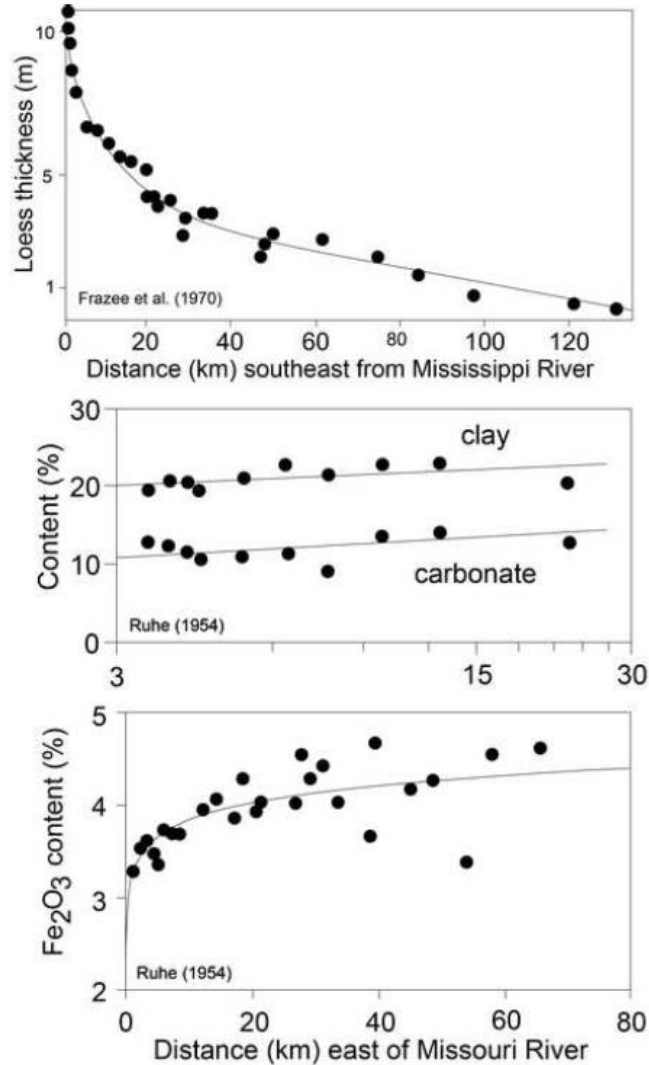
3463 Figure 17: (A)



(B)

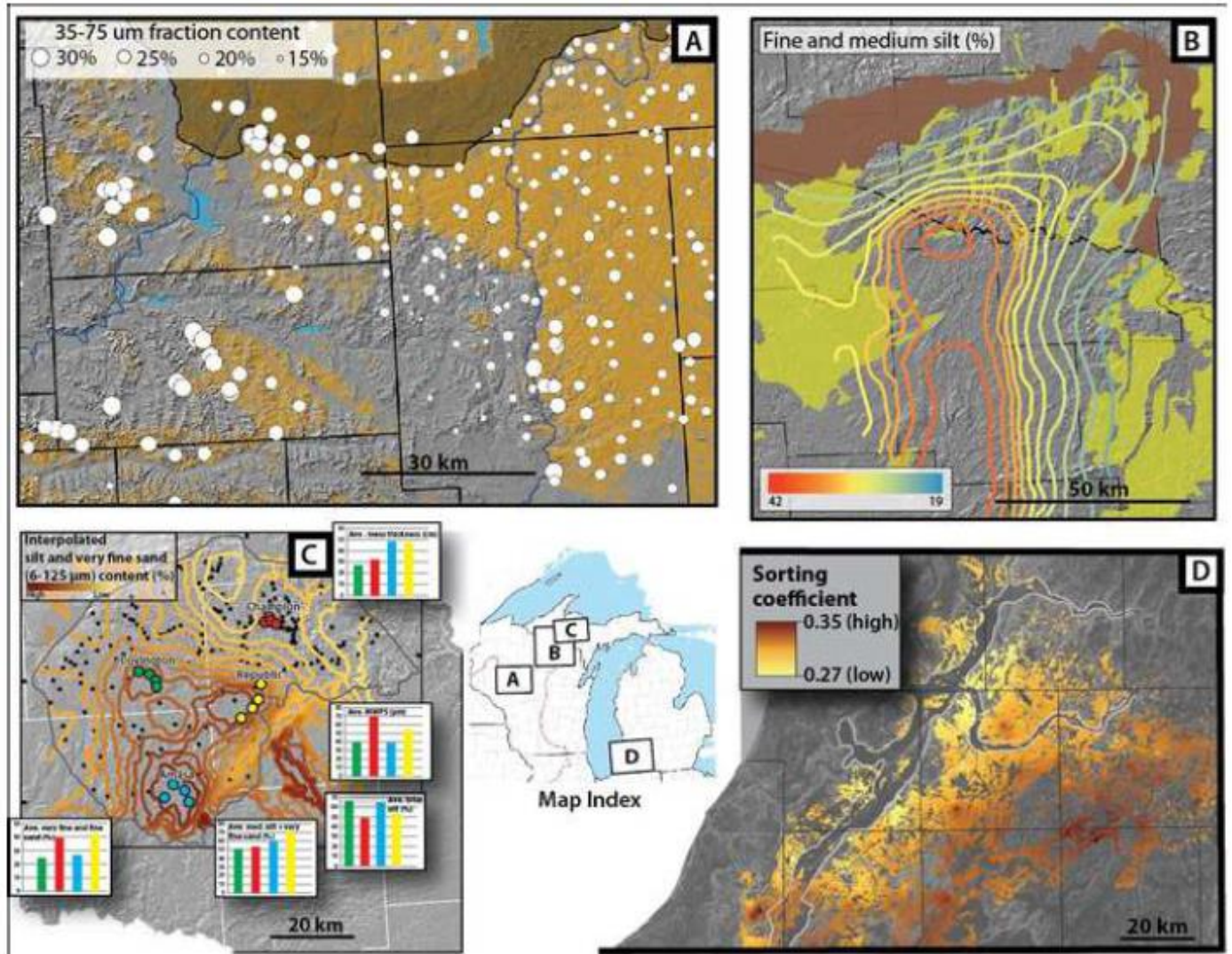


3471 Figure 18:



3481

3482 Figure 19:

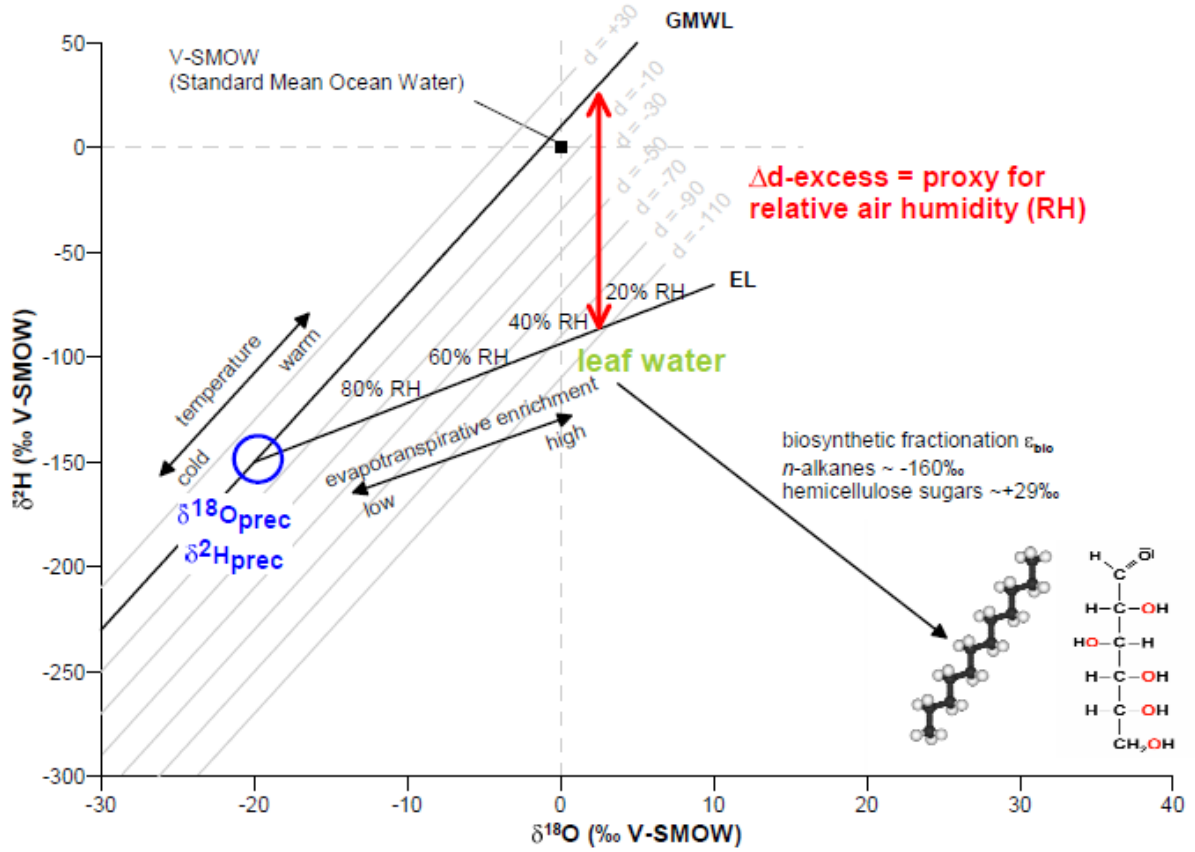


3483

3484

3485

3486 Figure 20:



3487

3488

3489



3490 Figure 21:

3491

3492

3493

3494

3495

3496

3497

3498

3499

3500

3501

3502

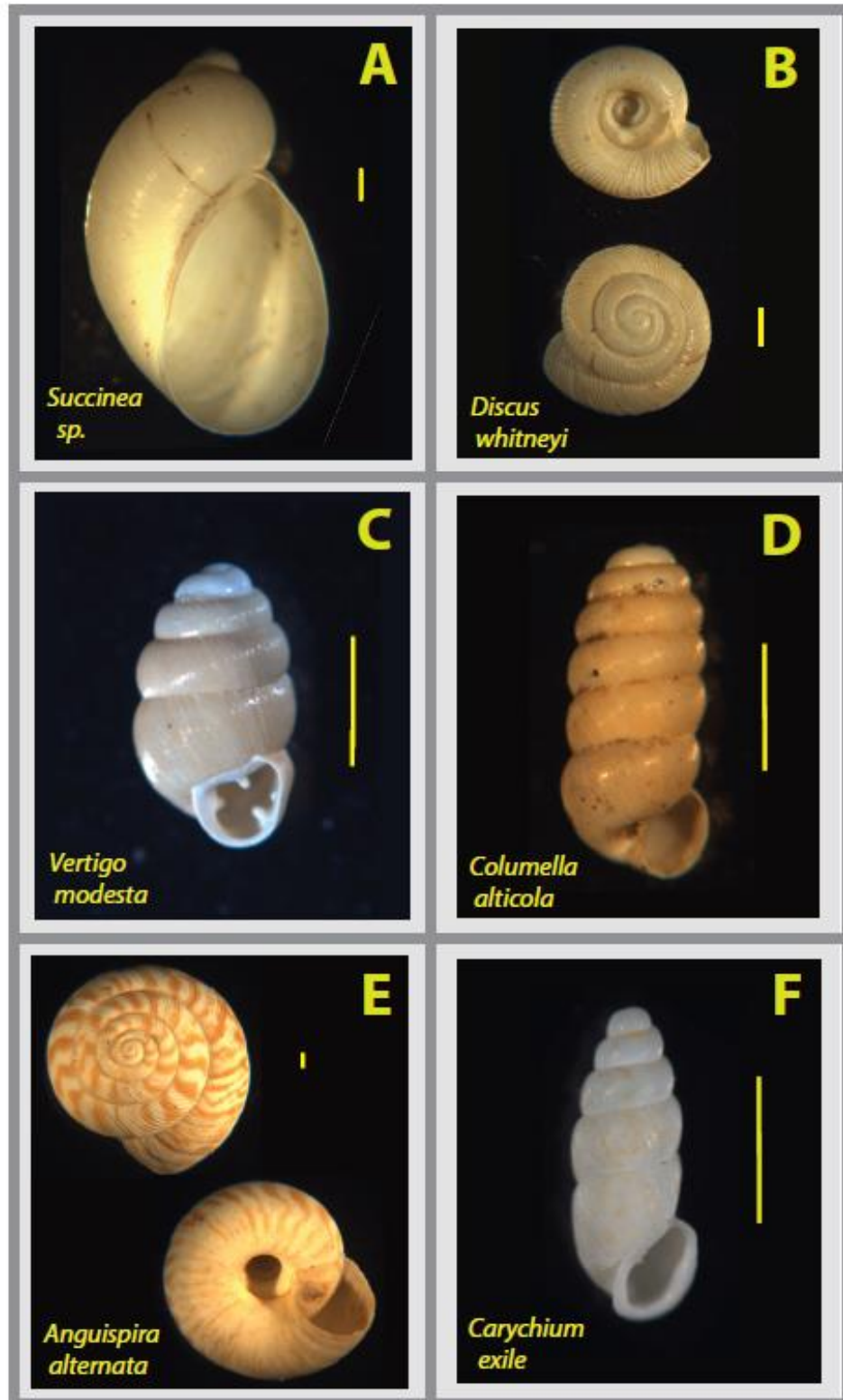
3503

3504

3505

3506

3507



3508

3509 Figure 22:

3510

3511

3512

3513

3514

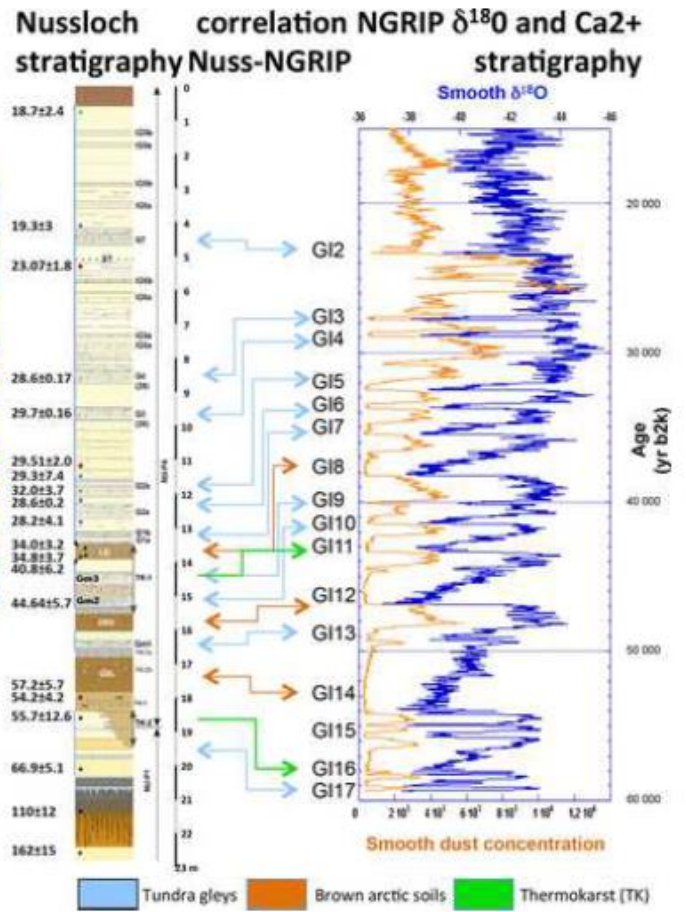
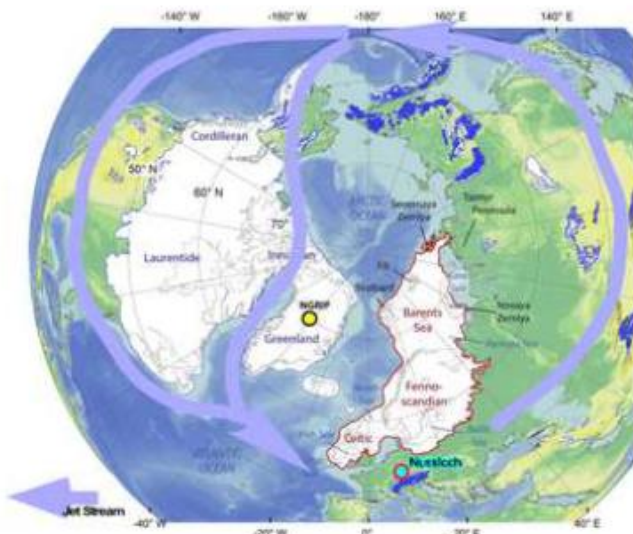
3515

3516

3517

3518

3519



3520 Figure 23:

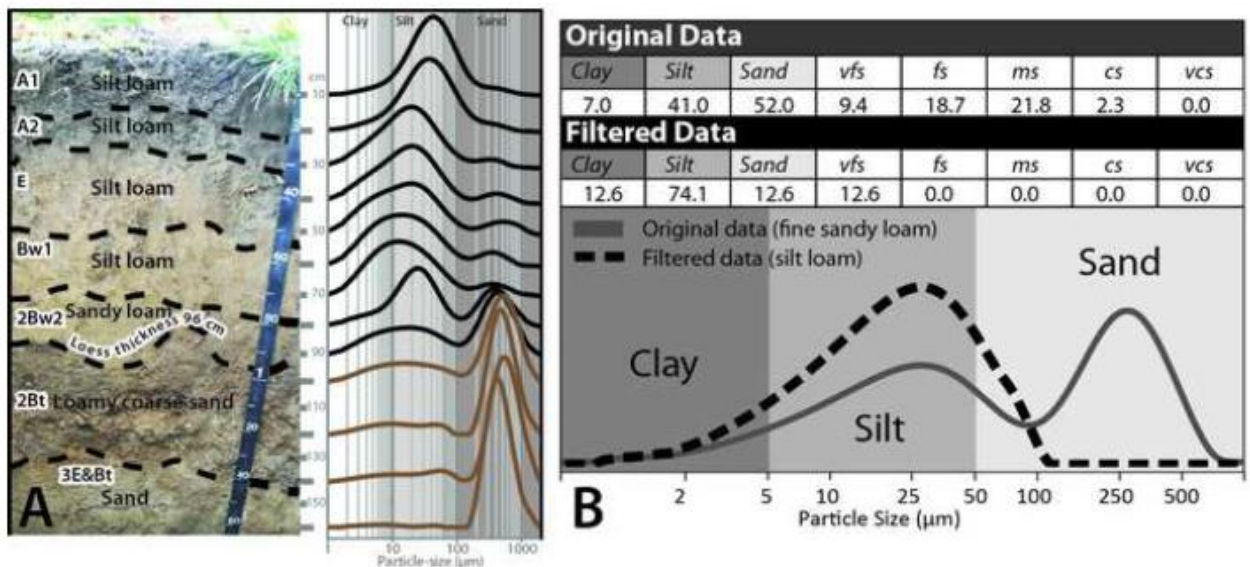
3521

3522

3523

3524

3525



3526

3527

3528 Figure 24a:

3529

3530

3531

3532

3533

3534

3535

3536

3537



3538



3539 Figure 24b:

3540

3541

3542

3543

3544

3545

3546

3547

3548

3549

3550

3551

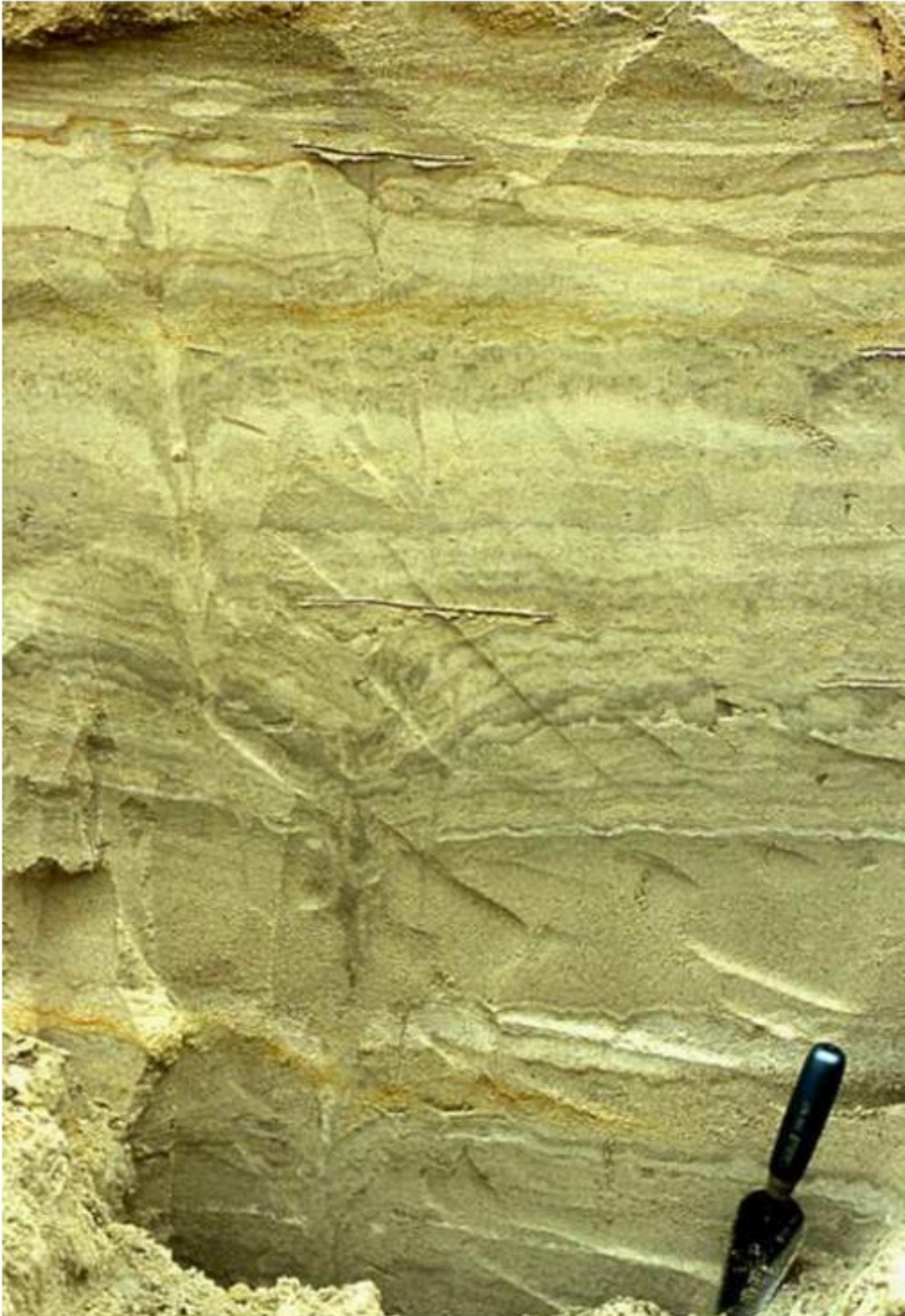
3552

3553

3554

3555

3556





3557

3558 Figure 24c:

3559

3560

3561

3562

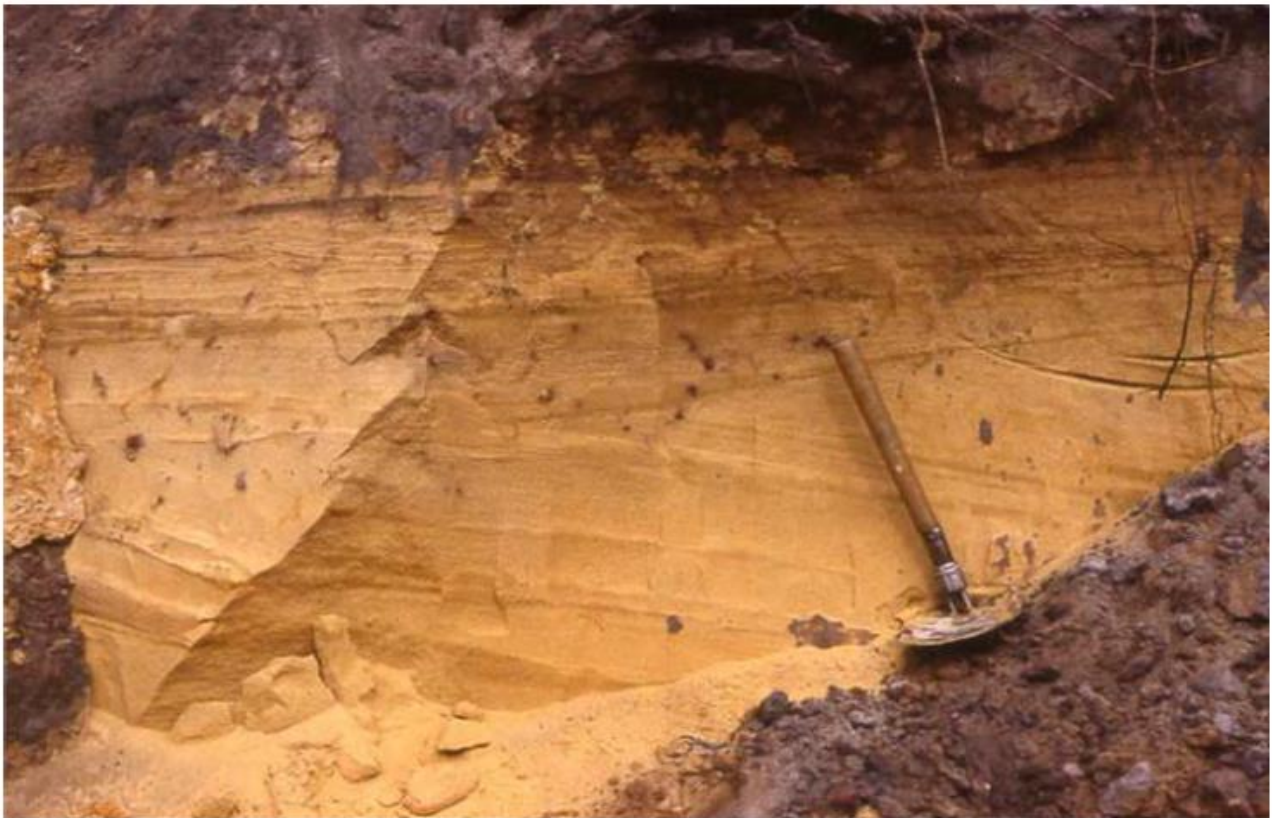
3563

3564

3565

3566

3567



3568

3569 Figure 25:

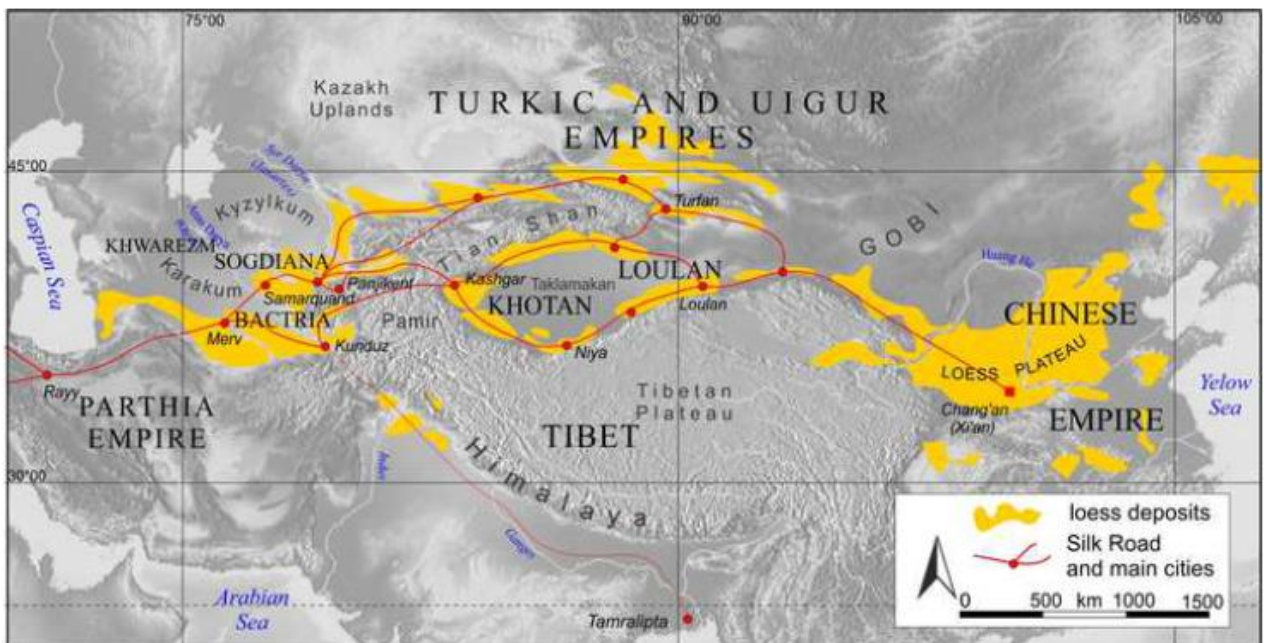
3570

3571

3572

3573

3574



3575

3576

3577 Figure 26:

